

Documentation of Risvollan Urban Hydrological Research Field, 2011

Trondheim, Norway

A master's thesis

submitted to the Department of Hydraulic and Environmental Engineering

at the Norwegian University of Science and Technology

in fulfillment of the requirements for the degree of

Master of Science in Civil and Environmental Engineering

by Christian Sveen

2012

Acknowledgements

This report is the result of a new documentation of Risvollan Urban Hydrological Research Field (RUHRF). The documentation was completed and submitted in February 2012 to the Department of Hydraulic and Environmental Engineering at the Norwegian University of Science and Technology. The subject of this thesis is to give a thorough documentation of the current conditions in the research field. The research field includes a separate wastewater system, a field catchment, an urban hydrological station and a rain garden.

The main supervisor Professor Sveinung Sægrov and PhD student Kim Aleksander Haukeland Paus have been supportive throughout the phase of the thesis. I would like to thank them for their commitment, inspiration, guidance and professional advice.

I would like to thank civil engineer Hans Vebjørn Kristoffersen at COWI for sharing his time and expertise regarding development of runoff models.

I would also like to thank Professor Karl Yngve Frøyen at the department of urban design and planning (NTNU) for his expertise regarding handling of ArcGIS software, and Master of Science student Torstein Dalen for supporting the estimation of water balance equations.

The staff at Trondheim municipality, the Norwegian water resources and energy directorate (NVE), the Norwegian geological research institute (NGU), and the Norwegian meteorological institute (DNMI) have been very helpful during the project. Special thanks go to senior engineers Harald Viken (NVE), Sveinn Taksdal (NVE), Olav Nilssen (Trondheim Municipality) and Harald Sveian (NGU).

The main initiative behind the development of Risvollan Urban Hydrological Research Field came from associate Professor Sveinn Torfi Thorolfsson. The report would never have been written if it weren't for his commitment. Therefore I would like to give him a special thank for giving me the opportunity to complete a thesis like this.

I hope that this thesis can be of benefit to the Department of Water and Environmental Engineering, and otherwise generally to foreign and domestic students.

This thesis meets the requirements and guidelines for master theses at NTNU.

Trondheim, 06. February 2012

Christian Sveen

Abstract

Risvollan urban hydrology research field is a field laboratory located in Trondheim city, Sør-Trøndelag County in Norway. The field includes a main catchment, and an urban hydrological station. The field has also a small rain garden recently added nearby the main catchment in 2010. The station is located downstream at the end of the main catchment. It is capable of measuring parameters such as storm water- and wastewater flow, short duration precipitations, snowmelt intensity, air- and ground temperature, air humidity, short wave radiation and wind speed/direction. Since 1986, the field has worked as a research laboratory for dozens of projects such as several semester, master and PhD thesis, as well as scientific articles and reports. To mention a few of their topics, sometimes focused on flooding analysis, pollution control, bio retention, urban runoff modeling, LID solutions, open storm water management, surface analysis, anthropogenic effect on snow melting, climate change and uncertainty of rainfall- and urban modeling. Almost from the beginning of the operational time, Risvollan station has been able to collect qualified data on central parameters necessary to complete a hydrologic balance model for the catchment. Recently (2010 and 2011), the station has been upgraded by installations of new instruments together with new data transmission system. The main catchment has during the autumn of 2011 been developed by the construction of 27 new apartments at the downstream end nearby the station. It was not expected that these changes would give significant impact on the amount of surface runoff. However, it was necessary to carry out an updated description of the catchment and to investigate how the properties may affect the hydrological conditions. It was also important to perform a detailed documentation of the current measurement equipments, along with their capacities/limitations. Detailed analyses and discussions of recently measured data would be carried out to control the performance of the new instruments, and to investigate the trends in rainfall/runoff characteristics of the catchment. The documentation of the research field would comprise preparation for model analyses, and a presentation of the outcome of this. The purpose with this thesis was to carry out these tasks so that it would be possible to get a clear picture of the current status and function of the research field.

The thesis provided a clear overview of the current conditions of the research field. However, it also revealed how uncertain some of the catchment properties could be, and the degree of validity for some of the instruments at the station. There were also uncertainties surrounding some of the pipe dimensions of the storm water network. In detail, the most important findings were:

- The hand drawn outer field boundary was considered to be partially valid. The watershed analyses performed in ArcMap generated catchments that were very similar to it.
- The comparison between the precipitation gauges showed that the newly installed Geonor gauge didn't provide realistic precipitation data between May and November 2011.
- The main catchment's total infiltration capacity was estimated to be approximately 5 mm.
- The statistical calculations of historical precipitation data showed that the annual amount of precipitation had slightly increased since 1986 (1.6 – 2.7 %).
- The determination of surface characteristics by the use of geo referred satellite images in ArcMap was considered to be valid.
- The runoff model developed in PCSWMM was considered to be realistic. It was easy to calibrate it, and it had almost the same appearance as the runoff model developed by DHI.

Table of contents

1. Introduction	1
1.1 Project background and purpose	1
1.2 Objectives	5
1.3 Project outline	6
2. Methodology	7
2.1 Catchment characterization	7
2.1.1 Field observations	7
2.1.2 Digitalization	7
2.1.3 Watershed delineation analyses	10
2.1.4 Visualization and verification	15
2.1.5 Pipe network, importing and editing	16
2.1.6 Slope calculations	17
2.1.7 New buildings	18
2.1.8 Inhabitants	19
2.2 Verification of RUHS rain gauges	20
2.2.1 Precipitation, total amounts	21
2.2.2 Precipitation, single events	22
2.2.3 Precipitation, historical data	22
2.3 Water balance equation	23
2.3.1 Evaporation	24
2.3.2 Infiltration	27
2.4 PCSWMM	30
2.4.1 Pipe network	31
2.4.2 The catchment	33
2.4.3 Rainfall events	35
2.5 Calibration	42
3. Risvollan Urban Hydrological Research Field	44
3.1 Area and topography	44
3.2 Storm water system	52
3.2.1 Manholes	52
3.2.2 Pipe network	54
3.3 Surface characteristics and sub catchments	58

3.3.1	Surface characteristics	58
3.3.2	Sub catchments	62
3.4	RUHS Instrumentation	71
3.4.1	Geonor	72
3.4.2	Lambrecht	73
3.4.3	Plumatic	74
3.4.4	V – notch weir	75
3.4.5	Other instruments	82
3.5	RUHS Transmission System	88
4.	Precipitation gauges	91
4.1	Comparison between instruments	91
4.1.1	Monthly precipitation	91
4.1.2	Weekly precipitation	95
4.1.3	Rainfall events	98
4.2	Previous precipitation records	101
4.3	Water balance	105
4.3.1	Water balance representing 02.June	105
4.3.2	Water balance representing 16.Aug.	106
5.	Runoff model	108
5.1	Model appearance	108
5.2	Calibration results	112
5.2.1	Calibration of 02. June rain event	112
5.2.2	Calibration of 16. August rain event	117
5.2.3	Peak flow profiles	124
6.	Conclusions	127
6.2	Future studies	128
	References	130
	Appendices	133
	Appendix A: Some RUHRF/RUHS thesis	133
	Later storm water projects:	133
	Earlier projects from IVM RUHS, 2011	134
	Appendix B	137
	Geo referred satellite picture on TIN – model	137
	Appendix C: Presentation V – notch weir	138

List of Figures

1. Sør-Trøndelag County, Norway
2. Location of RUHRF, Trondheim
3. RUHRF between Utleirvegen and Blaklivegen
4. Construction of 27 new apartments at RUHRF
5. First drawn outer field boundary
6. Start drawing polygon of playground
7. Playground polygon finished
8. An example of a DEM – model
9. The main catchment with sub catchments from earlier documentation in 1994
10. Connected manholes located at the downstream border of its respectable sub catchment
11. An illustration of how the watershed analysis works
12. Added pipe- and virtual manhole downstream the station
13. Drawing a 3D interpolation line before generating length profile
14. JPG – file of newly arriving buildings
15. Collecting 8 registrations for statistical precipitation analyses
16. Annual amount of evaporation
17. Map illustrating the soil properties at Risvollan
18. The principles behind Horton’s method in PCSWMM
19. The outfall and its bottom elevation
20. Manhole principle used in PCSWMM
21. Flow length estimation in ArcMap
22. Flow length inserted in PCSWMM
23. Rainfall event 02. June, scatter chart with straight lines
24. Rainfall event 02. June, clustered column chart
25. Rainfall event 02. June, cumulative amount
26. Rainfall event 16. August, scatter chart with straight lines
27. Rainfall event 16. August, clustered column chart
28. Rainfall event 16. August, cumulative amount
29. 02. June. Rainfall input following principle 1
30. 02. June. Rainfall input following principle 2
31. 02. June. Rainfall input following principle 3
32. 16. August. Rainfall input following principle 1
33. 16. August. Rainfall input following principle 1, imported after conversion into intensity
34. Hand drawn boundary compared with watershed delineation analysis
35. Connected buildings located outside the watershed generated boundary
36. Final outer field boundary
37. Elevation distribution in the field based on the contour map
38. Highest and lowest area in the field
39. Pictures taken during inspections
40. Another picture taken from inspection

41. TIN – model of RUHRF with surrounding areas (color scale = elevation range)
42. DEM of RUHRF, resolution 1 x 1 meter
43. Slope map
44. Comparison between ArcScene spatial model and tilted air photo
45. Manhole principal similar to the manholes at Risvollan
46. Location of replaced manholes
47. Map location of replaced manholes
48. Count of manhole installations before data editing
49. Count of manhole installations after data editing
50. Dimension distribution in the network before data editing
51. Dimension- and volume distribution in the network after data editing
52. Storm water system before data editing
53. Storm water system after data editing
54. Complete overview of surface characteristics
55. WMS service used for verification of surface characteristics
56. Population distribution in the field
57. Distribution of rooftops larger than 40 m²
58. Modifications of sub catchments
59. Red Thiessen polygons, TIN – model beneath
60. Runoff- and wastewater model of RUHRF, developed by DHI
61. The area distribution of sub catchments, DHI runoff model
62. Pipe network statistics, DHI runoff model
63. Location of sub catchments
64. Area distribution of the sub catchments
65. Future buildings in sub catchment 2, 3, 44, 45, 46 and 55
66. Construction of 27 new apartments
67. Final spatial model in ArcScene
68. Picture of RUHS
69. Geonor T200 – B gauge
70. Geonor T200 – B gauge opened
71. The old pluviograph
72. Associate Professor Sveinn T. Thorolfsson explains about the Lambrecht gauge
73. The top of the Lambrecht gauge
74. The Plumatic gauge
75. The top of the Plumatic gauge
76. The V – notch weir
77. The V – notch weir from another angle
78. V – notch weir sketch, theoretical maximum height calculated from the angle
79. Contraction coefficients in relation to the angle
80. Empirical diagram developed by NVE and NTNU
81. Assessment of the combination of failures
82. Stilling well
83. Runoff diagram downloaded from NVE's website
84. Shuttle logger
85. Shuttle ultrasonic sensor

86. Meter stick
87. Wire and line with scale
88. The creek Fredlybekken is marked blue, the connection with RUHRF is marked green
89. Temperature- and humidity sensor
90. Thermometer and sensor
91. Young instrument for measurement of wind speed and wind direction
92. Definition of different types of radiation
93. The short wave instrument
94. Location of ground temperature sensor
95. The PB – flume
96. Principle sketch of the PB – flume
97. Snow lysimeter
98. The snowmelt container
99. Principle sketch of the snow lysimeter
100. Paper roll storm water
101. Paper roll wastewater
102. Old transmission system
103. New transmission system
104. The CR1000 connection board
105. Current data displayed on the PC screen
106. Monthly precipitation from NTNU
107. Monthly precipitation including Geonor hour intervals data
108. Percentage of deviation from NVE's average registrations
109. Cumulative developments per month
110. Weekly precipitation in 2011
111. Weekly precipitation in 2011 including Geonor hour intervals data
112. Percentage of deviation from NVE
113. Cumulative developments per week
114. Precipitation data from CR1000 and Sutron, 02. June
115. Precipitation data from CR1000 and Sutron, 16. Aug
116. Average linear growth from 1987 and 1990
117. Monthly variations in mm
118. Monthly development in relation to the years
119. Runoff quantity continuity (02.June) from PCSWMM after simulation
120. Outfall loadings (02.June) from the "Status" bar in PCSWMM after simulation
121. The water balance distribution representing 02.June
122. Runoff quantity continuity (16.Aug.) from PCSWMM after simulation
123. Outfall loadings (16.Aug.) from the "Status" bar in PCSWMM after simulation
124. The water balance distribution representing 16.Aug
125. Initial plan overview of the runoff model (un-scaled)
126. Model displayed on satellite pictures via Google Earth
127. System flow rate before calibration, 02. June
128. System volume before calibration, 02. June
129. Flow rate results after first calibration of pipe roughness (K), 02. June
130. Total volume results after first calibration of pipe roughness (K), 02. June

131. Flow rate results after final calibration, 02. June
132. Volume results after final calibration, 02. June
133. Comparison between rainfall inputs following principle 1, 2 and 3
134. System flow rate before calibration, 16. August
135. System volume before calibration, 16. August
136. Flow rate after first calibration of pipe roughness (K), 16. August
137. Total volume after first calibration, pipe roughness (K), 16. August
138. Flow rate after calibration part 2, infiltration changed, 16. August
139. Total volume after calibration part 2, infiltration changed, 16. August
140. Flow rate after final calibration, 16. August
141. Total volume after final calibration, 16. August
142. Runoff quantity continuity for 16. August
143. Maximum flow rate by the end of the system before calibration of 02. June
144. Maximum flow rate by the end of the system after calibration of 02. June
145. Maximum flow rate by the end of the system before calibration of 16. August
146. Maximum flow rate by the end of the system after calibration of 16. August

List of Tables

1. RUHS instruments in operation
2. Size and summarizations of sub catchment properties
3. Runoff coefficients chosen for amount of impervious surfaces
4. Downloaded data for usage in this thesis
5. Soil characteristics from User's guide to SWMM5
6. Suggestions for Horton's infiltration parameters in PCSWMM
7. Roughness suggestions from PH – Consults
8. Total count of manholes before data editing
9. Total count of manholes after data editing
10. Pipe dimensions and their total lengths before data editing
11. Pipe dimensions and their total lengths and volume after data editing
12. Area distribution and characteristics
13. The size and slope of the sub catchments
14. Replacements of terrain- and past developed areas
15. List of all available instruments and installations (new and old)
16. Percentage of deviation based on water level
17. Monthly precipitation from May to December
18. Weekly precipitation in 2011
19. Precipitation data from CR1000 (Lambrecht) and Sutron (Lambrecht and Plumatic), 02. June
20. Intensity and duration of rainfall event from 02. June
21. Precipitation data from CR1000 (Lambrecht) and Sutron (Lambrecht and Plumatic), 16. Aug
22. Intensity and duration of rainfall event from 16. August
23. Monthly precipitation at RUHS since 1986
24. Summary made of the runoff quantity continuity for 02.June
25. Summary made of the runoff quantity continuity for 16.Aug
26. Surface properties before calibration
27. Infiltration properties before calibration
28. Calibration results after first reduction of pipe roughness, 02. June
29. Final calibration results, 02. June
30. Change of parameters during the calibration, 02. June
31. Initial conditions before calibration, 16. Aug
32. Results from calibration part 1, 16. August
33. Parameters changed during calibration part 1, 16. August
34. Results from calibration part 2, 16. August
35. Parameters changed during calibration part 2, 16. August
36. Results after final calibration, 16. August
37. Parameters changed during the calibration steps, 16. August

Nomenclature

RUHRF – Risvollan Urban Hydrological Research Field

RUHS – Risvollan Urban Hydrological Station

Ha – Hectare: $0.01 \text{ km}^2 = 1 \text{ ha} = 10 \text{ da (decare)} = 10\,000 \text{ m}^2$

IVM - Department of Hydraulic and Environmental Engineering

IVM, NTNU - The Department of Hydraulic and Environmental Engineering at the Norwegian University of Science and Technology

WGS – World Geodetic System

NVE - Norwegian water resources and energy directorate

LID – Low Impact Development

SWMM - Storm Water Management Model

ESRI - Environmental Systems Research Institute

WMS – Web Map Service

OPC – Open Geospatial Consortium

1. Introduction

1.1 Project background and purpose

Risvollan urban hydrology research field (RUHRF) is a field laboratory located in Trondheim city, Sør-Trøndelag County in Norway. Its exact location is approximately 4 km southeast from the city center. The field itself includes a catchment, and an urban hydrological station (RUHS). RUHS is located downstream the end of the catchment, in the northwest corner. In addition, a small rain garden (≈ 40 m²) has recently been added nearby the catchment, and it was included into the RUHRF in 2010, (MSc student Torstein Dalen, 2011, IVM NTNU). The size of the catchment is more or less 21 hectares, and it stretches about 1 km southeast from the road Utleirvegen to the road Blaklivegen. Today approximately 1500 persons live in the area. Mostly they live in terraced residents, but also in suburban residents (Thorolfsson & Høgeli, 1994). All residents are connected to a separate wastewater system, which transport the storm water and the wastewater by each pipe through the RUHS downstream the catchment. The RUHS are capable of measuring parameters such as storm water- and wastewater flow, short duration precipitations, snowmelt intensity, air- and ground temperature, air humidity, short wave radiation and wind speed/direction. See Table 1 page 5 to overview the available instrumentation today. The figure below shows which county in Norway RUHRF is located.

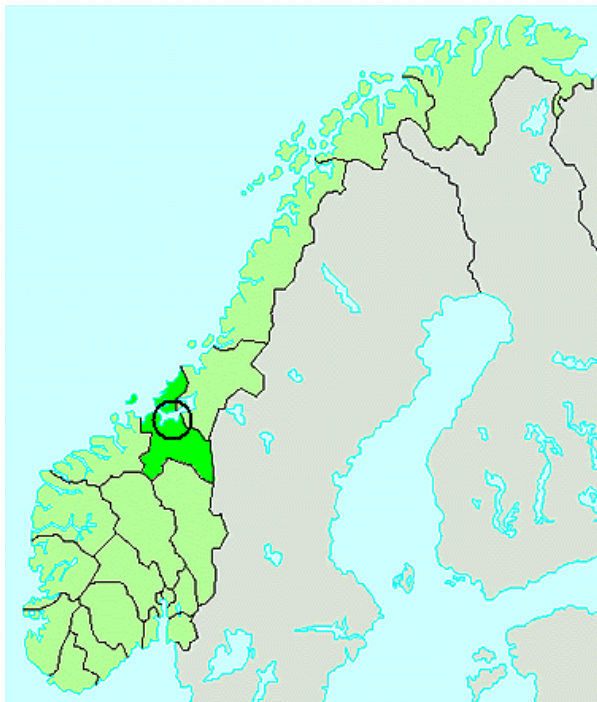


Figure 1: Sør-Trøndelag County, Norway. Trondheim encircled, (Store Norske Leksikon, 2011)

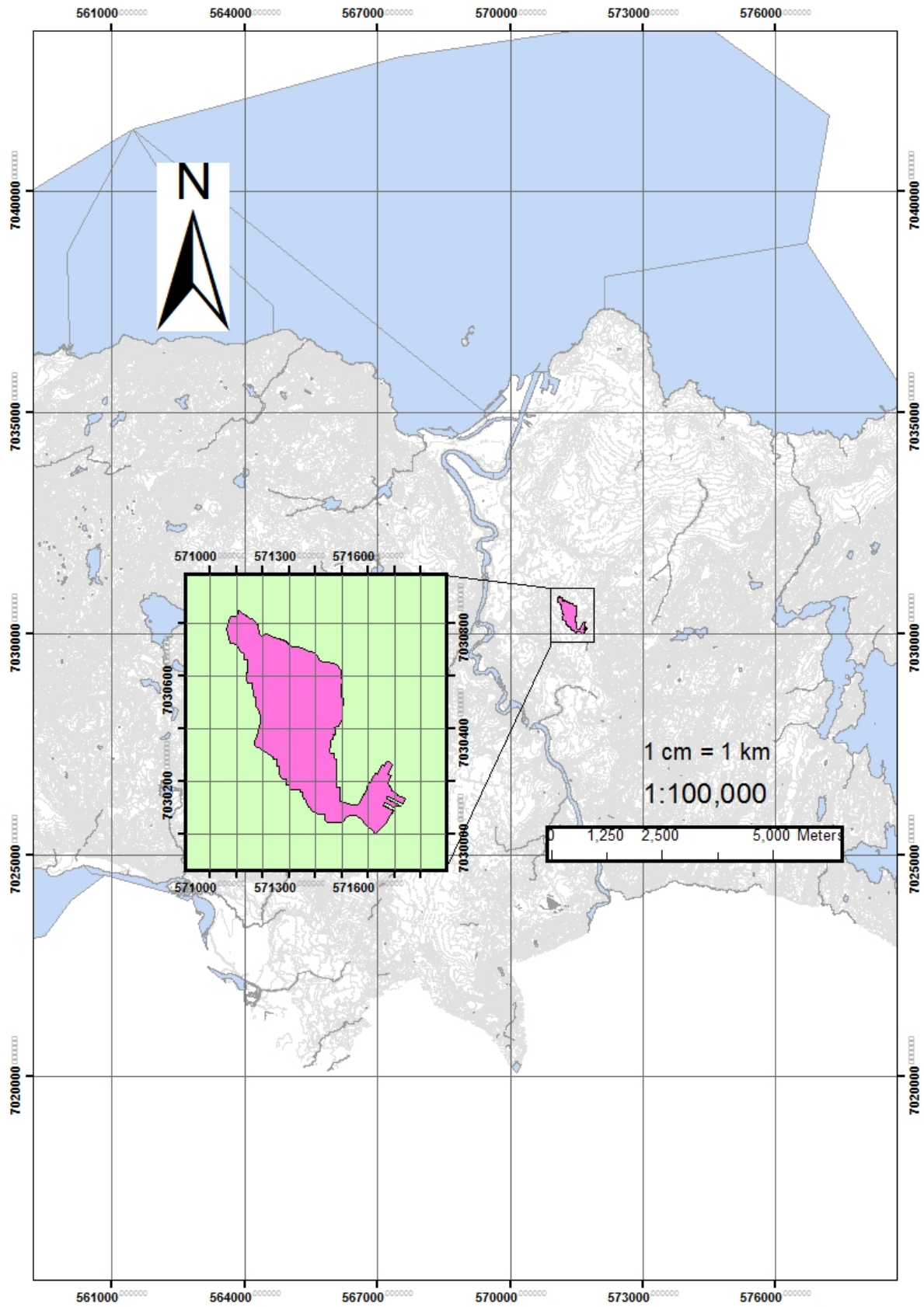


Figure 2: Location of RUHRF, Trondheim (coordinate system: wgs84 utm32N, field center at coordinate N: 571321.630m E: 7030479.864m)

Documentation of Risvollan Urban Hydrological Research Field, 2011

By cooperation between The Department of Hydraulic and Environmental Engineering at the Norwegian University of Science and Technology (IVM, NTNU), Trondheim Municipality and the Norwegian water resources and energy directorate (NVE), the RUHS was built and put into operation in 1986. Associate professor Sveinn T. Thorolfsson led the project. Since then, RUHS has worked as a research laboratory for dozens of projects such as several semester, master and PhD thesis, as well as scientific articles and reports. Some of these theses had virtually the same purpose and objectives. However, many of them differ from each other. To mention a few of their topics, some theses focused on flooding analysis, pollution control, bio retention, urban runoff modeling, LID solutions, open storm water management, surface analysis, anthropogenic effect on snow melting, climate change and the uncertainty of rainfall- and urban modeling (IVM RUHS, 2011). For more information about some of the theses, see Appendix A.

Almost from the beginning of the operational time, RUHS has been able to collect qualified data on central parameters that were necessary to complete a hydrologic balance model for the catchment. Recently (2010 and 2011), the station has been upgraded by installations of new instruments together with a new system of data transmission. As earlier mentioned, a rain garden has also been established. In addition, the main catchment itself has during autumn 2011 been developed by the construction of 27 new apartments (each from 77 – 115 m²) near the downstream end. See Figure 3 below to view the location of RUHS and the rain garden.



Figure 3: RUHS between Utleirvegen and Blaklivegen, RUHS location red circled and rain garden location yellow circled

Documentation of Risvollan Urban Hydrological Research Field, 2011

Some minor modifications inside the catchment have been made during the 25 years of measurement period. It is not expected that these changes will give significant impact on the amount of surface runoff. However, it was necessary to carry out an updated description of the catchment and to investigate how the properties may affect the hydrologic balance. It was also important to perform a detailed documentation of the current measurement equipments, along with their capacities/limitations.

Detailed analysis and discussion of recently measured data should be carried out to control the performance of the new instruments and to investigate trends in rainfall/runoff characteristics of the catchment.

The documentation of RHURF should comprise preparation for model analysis and a presentation of the outcome of this.

The purpose with this thesis was to carry out these requests, so that it is possible to get a clear picture of the RUHRF's current status and function.

See figure 4 below to view the poster about the construction of new apartments, and table 1 page 5 for an overview of instruments at RUHS.



Figure 4: Construction of 27 new apartments at RUHRF

Table 1: RUHS instruments in operation

Parameters	Units	Fabrication	Model
Rainfall intensity	Gauge 1	Geonor	T-200B
	Gauge 2	Lambrecht	Tipping gauge
	Gauge 3	Plumatic	Tipping gauge
Storm water flow	Snow lysimeter	#	#
	V - notch weir	#	#
Air temperature	Air.temp. sensor	Vaisala	HMP45
Snowmelt intensity	Snow lysimeter	#	#
Ground temperature	Ground temp. sensor	Campbell	107
Relative air humidity	Humidity probe	Vaisala	HMP45
Short wave radiation	Radiation balance	Klipp & Zonen	CMP 11
Wind speed	Anemometer	Young	85004
Wind direction	Anemometer	Young	85004
waste water flow	PB - flume	#	#
	Logger 1 NVE	Sutron	#
	Logger 2 NVE	Shuttle	#
	Logger new, NTNU	Campbell	CR1000

1.2 Objectives

The specified tasks to complete the documentation and analyzes in this thesis:

1. Describe properties (total catchment area, paved area, sub-catchments, slope and surface characteristics) of RUHRF
2. Describe new instrumentation and data transmission system and its intended use and capacity.
3. Present recent data on precipitation, runoff, temperature, wind, and discuss their reliability and accuracy. Analyze measurement consistency between old and new instruments.
4. Discuss trends in precipitation by comparing with data from previous periods
5. Set up a rainfall/runoff model based on SWMM and calibrate the hydrological part of it. Discuss calibration parameters.

1.3 Project outline

Chapter 2 explains about the methodologies used to complete the thesis. It describes how the catchment was characterized and how the field observations were conducted. That includes the handling of useful tools such as ArcMap/ArcView (ArcGIS Desktop 10.0), and the choices behind the calculation of the water balance equation. It also describes the procedure behind the comparison between instruments, their current data and previous data. The chapter will finally describe how the runoff model was developed and calibrated.

Chapter 3 describes the actual characteristics of the RUHRF, and about the RUHS instruments. At first the area and topography of the whole catchment will be presented and discussed, including a description of the pipe network. The description of sub catchments characteristics will then be presented, and how their boundaries are defined. Further a complete list of all RUHS instrumentation will be given, followed by the description of the short duration precipitation gauges. A study of the V – notch weir will also be presented. A short description of the rest of the instruments will also be given. At the end of the chapter, a brief presentation of the data transmission system along with the explanation about the distribution of responsibilities will be provided.

Chapter 4 focuses on the degree of validation of the new precipitation instrumentation, to investigate if it can be verified after comparison with measured data from NVE. Weekly and monthly precipitation will be compared, along with a couple of chosen rainfall events. Comparison with previous records will also be given, followed by the estimation of water balance equations. At the end of the chapter, some of the results will be discussed. Chapter 5 will present the results from the runoff model of the field catchment. The calibrations steps are also presented and discussed. Conclusions and recommendations for future work are given in Chapter 6.

2. Methodology

2.1 Catchment characterization

In this thesis, characterizations of the main catchment were performed by eight operations:

1. Field observations
2. Digitalization
3. Watershed delineation analyses
4. Visualization and verification
5. Pipe network, importing and editing
6. Slope calculations
7. New buildings
8. Inhabitants

2.1.1 Field observations

Field observations were performed by several inspections of the main catchment, mapping it by hand and taking pictures. At first, the inspections focused mainly on the outer boundary, especially in areas where there was doubt regarding the runoff direction. Storm water connections to the residents were also taken into account, by using a printed pipe network map received from the municipality. The pictures were important to use later on, both for digitalization and to catch up local appearances before the assessment of pervious/impervious properties, see Appendix CD.1 on CD for pictures. During the first inspections, an outer field boundary was drawn. Mapping by hand was then finished. Further inspections were necessary, especially to observe the runoff direction in some areas during heavy rainfall events.

2.1.2 Digitalization

Next step in the process was to digitalize the field. The outer boundary, along with the field's various internal properties (buildings, roads, parking lots, driveways and playgrounds), had to be characterized through digitalization. For this, the software ArcGIS Desktop 10.0 was used. ArcGIS software is an internationally well known design- and planning tool used by many agencies. It is developed by the U.S. company ESRI (Environmental Systems Research Institute), founded in 1969, and currently has its headquarters in Redlands, California (ESRI Website, 2011). The software is able to handle, combine, import or export almost any type of file formats. In this thesis, shape files are mostly used, as both basis and resulting files (filename.shp). ArcGIS Desktop 10.0 is a software

package which includes three main applications: ArcView, ArcEditor and ArcInfo. Through the thesis, these main packages were combined for both digitalization and visualization.

Trondheim Municipality supported with basis files of Trondheim city. These contained areas representing buildings, roads, properties, contour maps and elevation top points. In addition, they supported with shape files containing pipe network, in this case for the entire catchment of Fredlybekken. Fredlybekken is a creek located downstream the RUHRF, which today receive both storm water and wastewater from a combined system.

The basis files were received with coordinate system EUREF89 UTM 32N (R. Høseggen, 2010. Trondheim Municipality). After these files were collected and stored into a geodatabase, they were ready for editing. A geodatabase works as a central data storage, for any types of files involved in the project. It will keep all files at one place before, during and after editing (Professor Karl Yngve Frøyen, 2011).

Using ArcMap 10 as an editing tool, the outer field boundary was drawn as a polygon. The boundary was based on the field inspections, see Figure 5 on next page. By creating polygons, areas were made available for analyses. The only two types of areas that already were made of polygons, were roads and rooftops. Other types of areas such as parking lots, driveways and playgrounds, had to be made manually. The reason for creating polygons from these additional areas is to get more accurate information about the area distribution of different surfaces in the field.

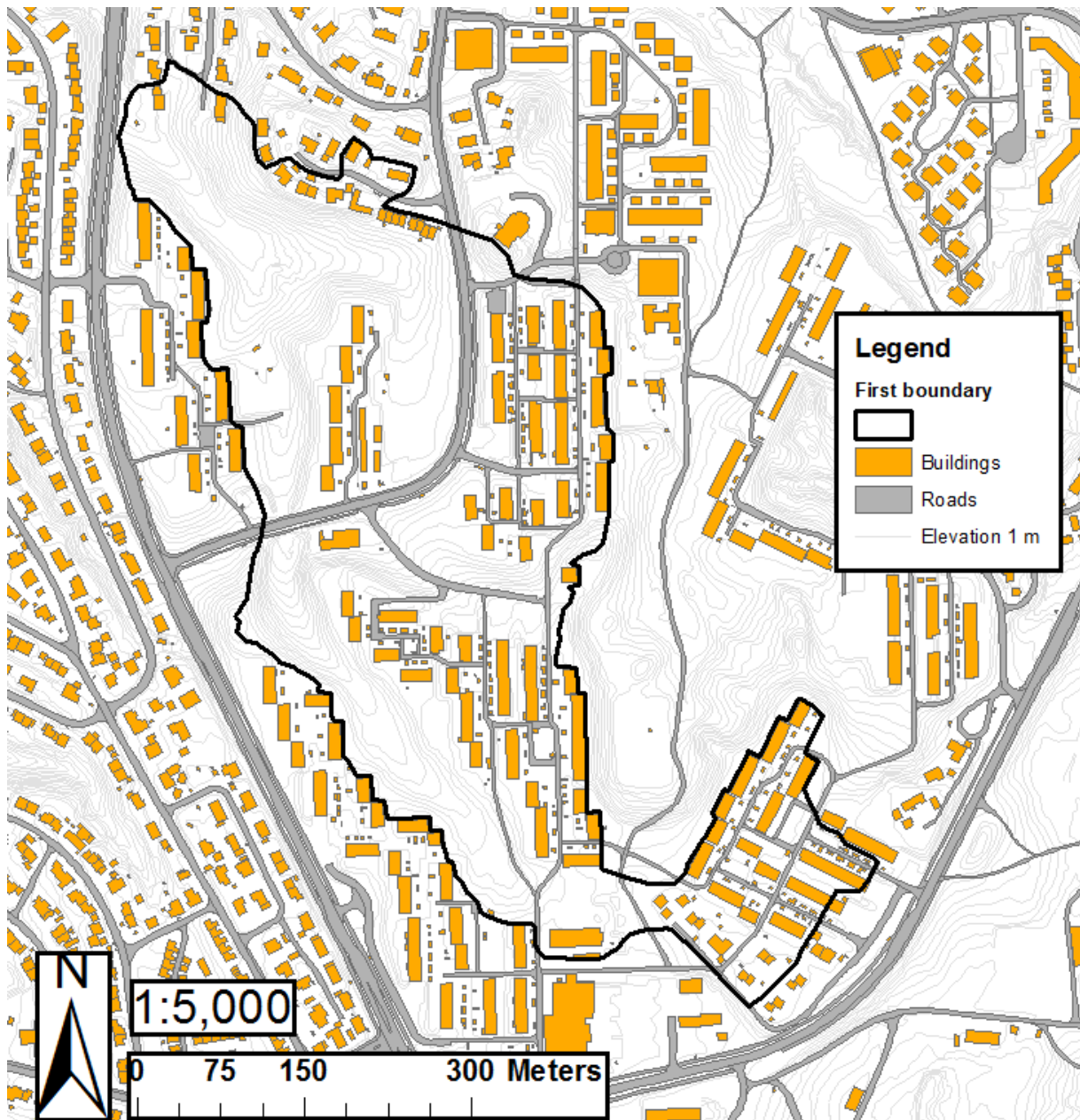


Figure 5: First drawn outer field boundary, displayed together with polygon files of roads and rooftops

There are several ways of digitalizing different types of areas; the easiest way is to put a geo referred satellite image into ArcMap. It's important that the image itself is correctly referred and visually clear. Geo referred images means that the images are fitted in both scale and coordinates, so that it corresponds to the features inside ArcMap. The purpose of adding a satellite image is to make it easier to draw polygons by following the real edges of the respected areas displayed on it, see Figure 6 and 7 next on page. It is also possible to create polygons by following the fragmented lines inside shape file layers such as "Other areas". Other areas include sometimes parking lots, driveways, traffic islands etcetera. Unfortunately these lines can sometimes be very inaccurate. The satellite image will therefore become a more reliable tool. In addition to the use of satellite image, pictures from the inspections were used as support, in case doubt about local appearances emerged along the way.

These were especially useful when shadows appeared on the satellite image, blocking the view at the exact locations where the edges go.



Figure 6: Start drawing polygon of playground Figure 7: Playground polygon finished

The best way to get a good visual and correctly geo referred satellite image into ArcMap, is to use the Web Map Service (WMS). The service has its origin within the organization Open Geospatial Consortium (OGC). The satellite image only works as a raster image, but it also automatically geo refer itself within the respective coordinate system (WMS, 2011. ESRI). A trick that was used during the creation of polygons was to adjust the polygon transparency from 100% to 50%, making it possible to see the satellite image beneath it. This made it easier to control the edges, look at the playgrounds on Figure 7.

2.1.3 Watershed delineation analyses

After parking lots, driveways and playgrounds were digitalized, it was necessary to verify the outer boundary. Knowing the hand drawn boundary could very well be wrong, it was necessary to control its credibility by performing watershed delineation analyses. The Watershed Delineation Tool is an application which is basically unavailable in the ArcToolbox menu, but it's possible to add it after downloading the package from ESRI's website (Watershed Delineation Tools, 2011). The tool produce four different results after finishing the analyses: flow accumulation, flow direction, location of streams and their respective catchments. The purpose of the analyses is to compare the generated catchments in ArcMap with the hand drawn boundary. In addition, sub catchments within the field will be generated at the same time. This is essential because it helps to decide how the final outer limit should look like. It also helps to determine the amount of sub catchments within the main catchment, and how they are arranged before importing it into PCSWMM Professional 2011 for runoff model development.

Before the watershed analyses could be performed, it was necessary to create a Digital Elevation Model (DEM) from a 3 – dimensional terrain model. Creating 3D – models using ArcMap is a simple process, but it's important to make sure the basis files for this operation are carefully chosen.

The contour map with highest resolution (1 meter elevation curves) combined with the elevation top points and the road area maps were used to create the 3D – model. The model itself is called Triangular Irregular Model (TIN – model). That means the terrain is defined by small triangles formed between points with known heights from the data base. A TIN model describes the terrain in an accurate and efficient manner because it can use many triangles in a broken terrain and fewer larger triangles in a simple terrain. However, the accuracy of the model itself depends of the accuracy inherent in the incoming data before creating it. Triangles are used because three points will always describe a flat surface in a room without uneven contour lines (Terrain- and raster analysis, Prof. K. Y. Frøyen, 2011). Before creating the TIN – model, unnecessary elevation data within the basis files had to be deleted, such as contour lines containing values equal to -999, and 0 etcetera. Figure 41 in chapter 3 illustrates the final result after creating the model.

Next part of the process was to create a DEM model. The difference between a TIN - model and a DEM model is that the resolution of the DEM consists of square elevation grids, working as average elevation top points, (Exploring digital elevation models ESRI, 2011). It is possible to decide the resolution of the grid before creating the DEM. In this case the resolution was set to the highest value possible, 1 x 1 meter. Figure 8 below shows an example of a DEM model.

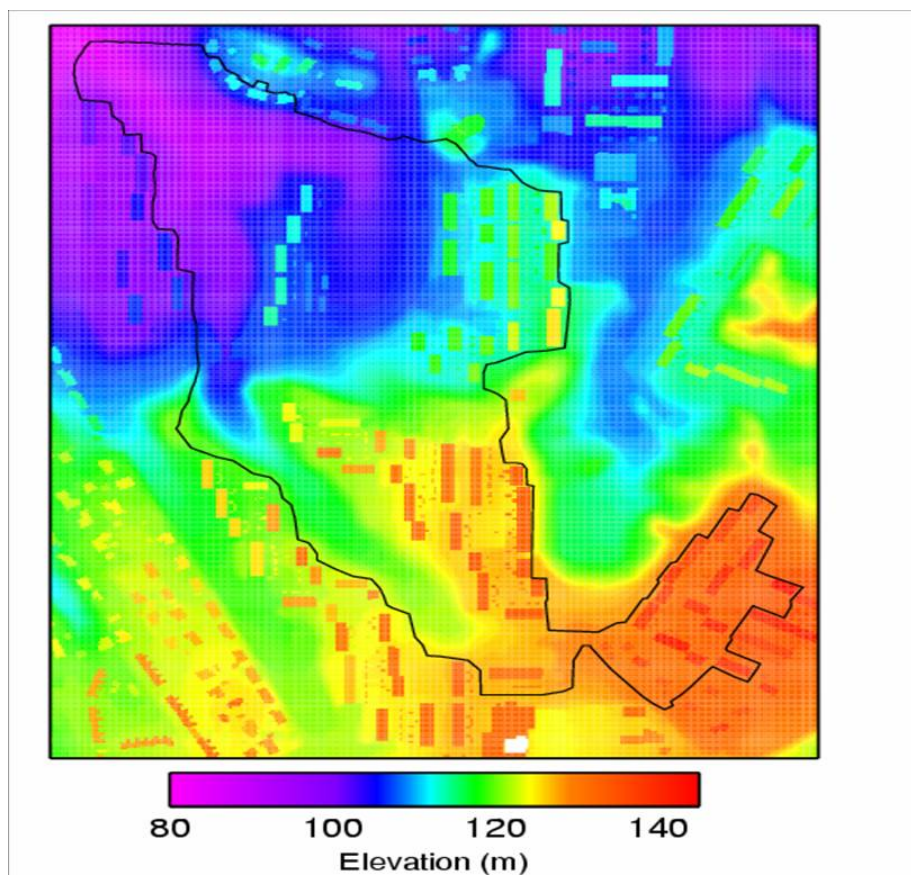


Figure 8: An example of a DEM – model, resolution: 2 x 2 meter (IVM, RUHS 2011)

Finally, watershed delineation analyses were ready to be performed. As earlier mentioned, these analyses generated four types of results. Two of them were essential in this thesis; the location of the streams and their belonging catchments. The streams are based on the flow accumulation analyses, which detect or trace the flow directions, along with the increase or decrease of flows. Every stream is connected to a catchment or sub catchment, (How watershed works 2011, ESRI).

However, before starting the watershed analyses, it was necessary to determine the minimum size of sub catchments.

An earlier documentation of RUHS from 1994, made by associate professor Sveinn T. Thorolfsson and MSc student Stephen Høgeli, included information about the main catchment as well. In their documentation the catchment was divided into 21 sub catchments, see figure 9 and table 2 for more information.

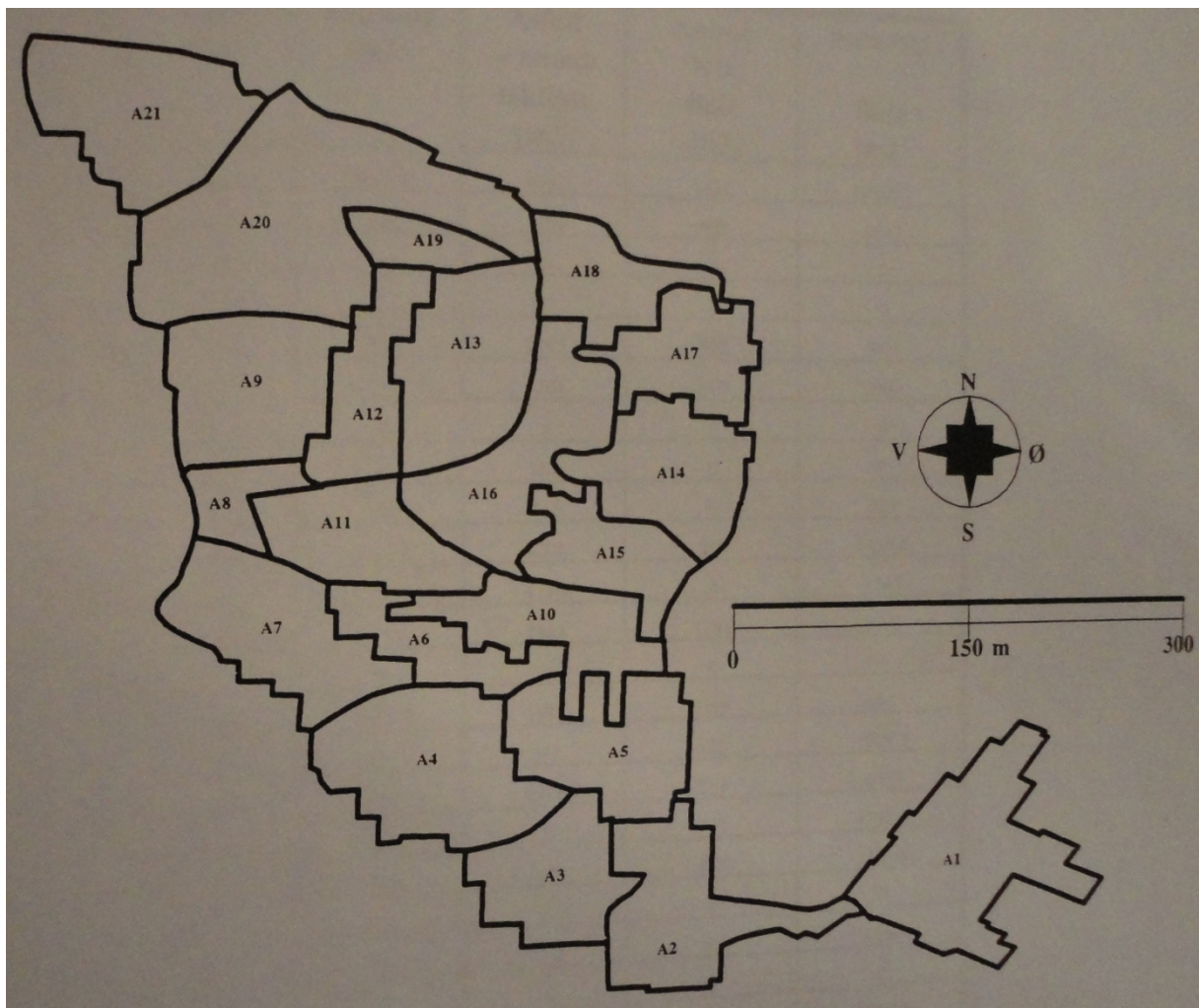


Figure 9: The main catchment with sub catchments from earlier documentation in 1994

Table 2: Size and summarizations of sub catchment properties, from earlier documentation in 1994

Felt	Areal (ha)	Takflate (m ²)	Asfalt + annen takflate (m ²)	Annen tett flate (m ²)	Sum tett flate (m ²)
A1	1,516	4336.2	4057	1916	10309.2
A2	1,005	2078	1407	567	4052
A3	0,81	0	0	0	0
A4	1,308	0	0	0	0
A5	1,004	2464	2265	950	5679
A6	0,555	1248	1201	550	2999
A7	1,118	0	0	0	0
A8	0,364	0	367.	0	367
A9	0,935	0	813	0	813
A10	0,864	2252.8	3202	983	6437.8
A11	0,768	0	1740	0	1740
A12	0,672	1711	2454	1244	5409
A13	1,166	0	0	0	0
A14	1,004	2522.3	1821	1101	5444.3
A15	0,68	958.5	541	430	1929.5
A16	1,143	495	3338	215	4048
A17	0,743	2158.2	1836.3	942	4936.5
A18	0,616	809.6	2229	353	3391.6
A19	0,309	0	0	0	0
A20	2,313	780	370	0	1150
A21	1,204	0	0	0	0
SUM	20,097	21813.6	27641.3	9251	58705.9

A decision had to be made, how many sub catchments are sensible to use in this thesis? A discussion with civil engineer Hans Vebjørn Kristoffersen (COWI employee and former MSc student at IVM, also known as the creator of the designed rainfall “Kristoffersen – regnet”), gave some perspective around the choice of the total amount. According to him, the ideal amount should be between 15 to 50 sub catchments for such an area. By decreasing or increasing the amount beyond that range could perhaps lead to increased uncertainty regarding the runoff model results. The final amount of sub catchments will further be discussed in chapter 3.

Following the given recommendations, several watershed analyses were performed by using different criteria. In this case, analyses were performed by using minimum sub catchment areas equal to 0.05, 0.1, 0.2, 0.3, 0.5 and 1.0 hectare. It's important to add that the watershed analyses only take into account the terrain- and the road surface. In other words the location of the streams could very well "pass through" the buildings on the map as a result, and the analyses are totally independent from the pipe network. The sub catchments must therefore be edited and adapted to the local conditions after the analyses, the storm water connections to the residents also had to be taken into account. It was necessary to determine which manholes were to be connected with which sub catchments. Following the principle used in this thesis, the manhole located by the downstream border of the sub catchment was to be connected with it. This operation was essential before importing the sub catchments into PCSWMM. See figure below for illustration of the manhole connections.



Figure 10: Connected manholes located at the downstream border of its respectable sub catchment

Another operation was to determine the degree of pervious- or imperviousness within the sub catchments. In ArcMap, a function called intersection was used to calculate the amount of different surface characteristics within each sub catchment. After the procedure was done, the results were imported into excel. A complete overview of surface characteristics was then available, but further measures were necessary to complete. Different areas contribute to different runoff patterns. Trying to determine these properties, a downloaded table containing various runoff coefficients was used to give suggestions regarding pervious/impervious properties. These coefficients adjusted the amount of impervious areas regarding surfaces such as rooftops, parking lots, roads, playgrounds and driveways. The purpose was to provide "default values" for the runoff model, before it eventually had to be calibrated if necessary. The table on the next page lists the coefficients used.

Table 3: Runoff coefficients chosen for amount of impervious surfaces (Hydraulic Design Manual, 2009)

Surface	Coefficient	Category	Range
Roofs	0.95	Roofs	0.75 - 0.95
Roads	0.85	Asphaltic	0.85 - 0.95
Parkinglots	0.85	Asphaltic	0.85 - 0.95
Driveways	0.75	Paving bricks	0.70 - 0.85
Playgrounds	0.30	Playgrounds	0.30 - 0.40
Terrain	0.25	Heavy soil, steep 7%	0.25 - 0.35

Most of the roof surfaces belonged to terraced residents. These had flat roofs with surfaces layers made of bitumen. The roads showed signs of age, a lot of them had cracks along the roadside. The parking lots were in better condition, with some exceptions. The driveways were made of both paving bricks and asphalt. The playground surfaces consisted of sand (Appendix CD.1). The coefficient chosen for the terrain was based on the estimated soil type and the overall average terrain slope.

The figure below illustrates how the watershed analysis works.

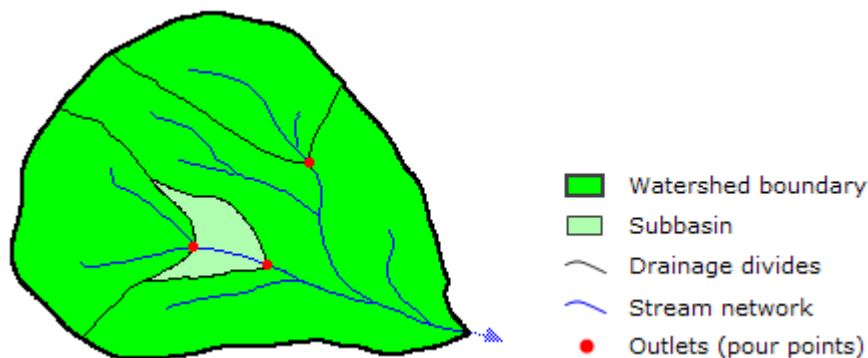


Figure 11: An illustration of how the watershed analysis works, subbasin = sub catchment (How watershed works, 2011)

After the watershed analyses were completed, the generated sub catchments were counted and statistical calculations were carried out. After the best suited watershed analysis was chosen and edited, the hand drawn field boundary and the generated field boundary were compared with each other, before a final field boundary was created. This is presented and discussed in chapter 3.

2.1.4 Visualization and verification

As a final measure to verify the physical properties of the main field and its sub catchments, 3 – dimensional visualization was carried out. ArcScene was the application used to visualize it, along with some of the surrounding areas. For this, the TIN – model and all the polygon shape files were used.

The purpose of this task was to investigate the credibility of the terrain model, by comparing it with the real world. This was done by looking at the model together with tilted air photos, obtained from map – supported internet places for example “<http://kart.gulesider.no/>”.

The pictures from the field inspections were used as well. A satellite picture from Google Earth was geo referred and attached to the TIN – surface, just to confirm that the different surfaces were on the same place. However, the WMS service was the best tool for this operation. See Appendix B to view the geo referred satellite picture on the TIN – model.

Except from visualizing the terrain, buildings were also established as 3D – objects. The rest of the layers were attached to the TIN – surface. The reason for making 3D – buildings was to make the model appear more realistic, and to give the reader an impression of the size of the field.

Creating an ArcScene model is basically a quick process. Except from uploading the needed files, adding symbologies, conversion from 2D to 3D – buildings, obtaining surface heights on remaining polygon shape files, the 3D – model was practically ready for presentation. Most of these operations were done by entering the layer properties from the table of contents (TOC). Useful functions inside the layer properties: base heights, extrusion and rendering. The visualization is presented in chapter 3.

2.1.5 Pipe network, importing and editing

As mentioned earlier, Trondheim municipality supported with shape files containing pipe network for the catchment belonging to Fredlybekken. That included the network within RUHRF. To remove the redundant elements, the network outside the field was cut away, using the outer boundary as “scissor” in ArcMap. In addition, the waste water network was also removed. In this thesis, the storm water system was the prioritized network to work on.

To start with, tables and figures of both pipes and manholes were created after exporting the attributes from the shape files inside ArcMap. The attributes contained main properties such as dimension, construction year, material, lengths, along with other data. Trondheim Municipality is responsible for the information inside the attribute tables, the same information is stored inside their database called Gemini.

By studying the attribute tables, it was clear that a lot of data was missing, especially data such as manhole diameters, terrain- and manhole bottom elevation. Pipe lengths along with other information such as material, dimensions and construction year were partly intact. To complete the missing data, an earlier field documentation written by E. Aasnes in 1985 was studied. Aasnes had a complete documentation of the storm water network, done by manual registrations in the field. Aasnes carried this out as a part of his master thesis at the time.

Before completing the missing data, two steps were taken. First, it was necessary to investigate the credibility of Aasnes work by doing some manual registrations in the field, independently from his work. The depth of seven randomly chosen manholes were measured, and the surface elevation were controlled by using the TIN – model.

After verifying the network, the next step was to simplify it by removing the pipe dimensions up to 200 mm. These removed dimensions represented the connection pipes with the residents.

The reason for doing this was the same as the reason for the decision about the amount of sub catchments, to avoid increased uncertainty inside the runoff model. As for the sub catchments, the pipe network will be imported into PCSWMM after finished editing inside ArcMap. After completing the missing data, new tables and figures were created. As a final adjustment, a pipe- and a virtual manhole were added downstream the station, to make sure that the entire capacity of the field was included into the runoff model. See Figure 12 below to overview the pipe and the virtual manhole. The manhole at the end would be converted into an outfall inside the runoff model. The slope and dimension of the ending pipe are genuine, since the pipe is extracted from the network system outside the main catchment. The ending manhole on the other hand, is not, but the bottom elevation of it is true due to the interpolation made between the station and the real manhole across the street.



Figure 12: Added pipe- and virtual manhole downstream the station

2.1.6 Slope calculations

One important parameter that was necessary to analyze and collect before importing the sub catchments and the pipe network into PCSWMM, was the slope in every sub catchment. A slope map was created in ArcGIS, illustrating the slope variations. Based on this map, slopes had to be estimated by a color scale. This method seemed to give to rough estimations. The most important thing was to obtain the exact values.

This was done by generating length profiles in ArcMap, drawing one or several 3D – interpolate lines above every catchment. This operation was performed by using the 3D analyst tool. The profiles were then exported as text files before importing them into excel.

The average slope was calculated for each sub catchment. See Appendix CD.2 for spreadsheet calculations and generated length profiles. See Figure 13 below to view the process of creating length profiles.



Figure 13: Drawing a 3D interpolation line before generating length profile

2.1.7 New buildings

During late summer and autumn of 2011, 27 new apartments were constructed by the contractor Skanska Norge AS. These apartments are today located inside three of the field's sub catchments, built as 3 continuous terraced houses. Unfortunately, digital data of these apartments was unavailable during the start- up phase of this thesis. However, the map service located at Trondheim municipality's website illustrated their location. The map with this overview was saved as a JPG – file before it was later uploaded and geo referred into ArcMap, see Figure 14 on the next page. Then, it was possible to digitalize the apartments by creating new polygons along their edges. The JPG – file also revealed another location inside the field where construction of a new building is going to take place. Further three sub catchments will then be developed.

Both the storm water and the wastewater from the recently established apartments are connected to a system outside the research field (Olav Nilssen, 2011). However, in return the apartments contribute to a decrease of terrain surface and some developed areas. That was taken into account before the sub catchments were imported into PCSWMM.



Figure 14: JPG – file of newly arriving buildings (green symbology) (Trondheim municipality website, 2011)

2.1.8 Inhabitants

As an excluded operation without any effects on the desired results of this thesis, the population distribution in the field was also analyzed. Files were received from Professor Karl Yngve Frøyen, an employee from the Department of Urban Design and Planning at NTNU. These contained information about the amount of population within divided sectors of Trondheim city, representing the year 2002 and 2005. A map displaying the population distribution from the year 2005 was made. This was done by using a dot – density function, located in the symbology menu. The purpose of this was to display the population distribution and to see how it relates with the distribution of urban areas, this with respect to any later discussions about further developments in the field.

2.2 Verification of RUHS rain gauges

By verifying the rain gauges at the station, comparison between them and others by using statistical approaches was necessary. In this thesis, the comparison mainly focused on two different approaches between 4 separated gauges. The approaches are as follows:

1. Precipitation, total amounts
2. Precipitation , rainfall events

The approaches follow some of the basic principles found in a report written by Wiel Wauben (Precipitation amount and intensity measurements with the Ott Pluvio). See Appendix CD.3 to view the report.

It was necessary to create an overview of all available instruments at RUHS, along with additional information and descriptions such as principles, capacities and limitations. The rain gauges and the V – notch weir was the main focus in this thesis. Next part was to create a couple of sketches, which displayed how the instruments were connected to the loggers both in the past and present. This was followed by a brief explanation about the capacities of loggers. In addition, an explanation about the distribution of responsibilities regarding the station was given. The final task was to collect data from the instruments, and compare these with each other followed by the principles mentioned above. Other parameters will also be presented, such as temperature, runoff and wind speed. In addition, historical data from the station would be obtained and analyzed separately from the comparison between the instruments.

To compare the gauges, credible precipitation data had to be obtained. The higher resolution of the time steps within the dataset, the more credible it was. In this thesis, precipitation data was obtained by either receiving or downloading it from The Metrological Institute of Norway (DNMI) or the NVE. The most preferable time step intervals would be 1 to 10 minutes, but depending on the availability and the age of the desired dataset, the intervals varied. Table 4 on next page displays the type of dataset for which parameters that were used in this thesis. The table also includes the source the datasets were obtained from, as well as the stations and the instruments that produced them. As mentioned earlier, four separate gauges were compared; meaning that one external gauge outside RUHS was included. This will further be discussed in the coming sub chapter 2.2.1.

During the thesis phase, it was essential to collect precipitation- and runoff data continuously, mainly for two reasons. One was to compare precipitation data from old instruments with a recently installed instrument, to verify its credibility. The second purpose was to study both the precipitation- and the runoff data, before extracting a couple of rain- and runoff events that could help calibrating the runoff model. In addition, other parameters such as air temperature, air humidity, short wave radiation and wind speed were used to calculate estimations of the evaporation in the field. In this case, Penman Monteith and Penman Shuttleworth equations were used. The calculation of evaporation was supported by MSc student Torstein Dalen, who wrote the project thesis “Hydrologic performance of rain garden in cold climate conditions”. The evaporation results were intended to support the development of the main catchment’s hydraulic balance equation, by inserting them into the runoff model.

Table 4: Downloaded data for usage in this thesis, historical data located at the bottom

Source	Station	Logger	Instrument	Period	Parameter	Intervals
NTNU	RUHS	CR1000	Geonor	11.05.2011 - 01.11.2011	Precipitation mm	2 minutes
NTNU	RUHS	CR1000	Lambrecht	11.05.2011 - 01.11.2011	Precipitation mm	2 minutes
NTNU	RUHS	CR1000	Geonor	11.05.2011 - 01.11.2011	Precipitation mm	1 hour
NTNU	RUHS	CR1000	Lambrecht	11.05.2011 - 01.11.2011	Precipitation mm	1 hour
NTNU	RUHS	CR1000	Lambrecht	11.05.2011 - 01.11.2011	Precipitation mm	1 hour
NVE	RUHS	Sutron	Lambrecht	01.05.2011 - 04.12.2011	Precipitation mm	Obs.Breakvalues
NVE	RUHS	Sutron	Plumatic	01.05.2011 - 04.12.2011	Precipitation mm	Obs.Breakvalues
NTNU	RUHS	CR1000	Young	11.05.2011 - 01.11.2011	Wind speed m/s	1 minute
NTNU	RUHS	CR1000	Young	11.05.2011 - 01.11.2011	Wind speed m/s	10 minutes
NTNU	RUHS	CR1000	Vaisala	11.05.2011 - 01.11.2011	Rel. air humidity %	2 minutes
NTNU	RUHS	CR1000	Vaisala	11.05.2011 - 01.11.2011	Rel. air humidity %	1 hour
NTNU	RUHS	CR1000	Klipp & Zonen	11.05.2011 - 01.11.2011	Radiation W/m2	1 hour
NTNU	RUHS	CR1000	Klipp & Zonen	11.05.2011 - 01.11.2011	Radiation W/m2	2 minutes
NTNU	RUHS	CR1000	Vaisala	11.05.2011 - 01.11.2011	Air temperature °C	1 hour
NTNU	RUHS	CR1000	Vaisala	11.05.2011 - 01.11.2011	Air temperature °C	2 minutes
NVE	RUHS	Sutron	V - notch weir	01.06.2011 - 01.10.2011	Runoff m3/s	1 minute
NVE	RUHS	Sutron	V - notch weir	14.11.2011 - 04.12.2011	Runoff m3/s	1 minute
NVE	RUHS	Sutron	V - notch weir	01.09.2011 - 14.11.2011	Runoff m3/s	15 minutes
DNMI (eKlima.no)	Voll	#	Plumatic	15.04.2011 - 01.12.2011	Precipitation mm	Obs.Breakvalues
DNMI (yr.no)	Voll	#	Plumatic	01.12.2010 - 04.12.2011	Precipitation mm	Day values
DNMI (yr.no)	Voll	#	#	01.12.2010 - 04.12.2011	Air temperature °C	Day values
DNMI (yr.no)	Voll	#	#	01.12.2010 - 04.12.2011	Wind speed m/s	Day values
NVE	RUHS	Sutron	Plu./Lam.	01.01.1988 - 19.09.2011	Precipitation mm	1 hour

2.2.1 Precipitation, total amounts

The precipitation data between 01.05.2011 – 04.12.2012 were aggregated into weekly and monthly summarizations. Differences in percentage between the gauges were also calculated, along with the cumulative amounts. This was done by using the excel tool Pivot table. The operation included data from 4 different gauges based on 8 different registrations, see figure 15 below.

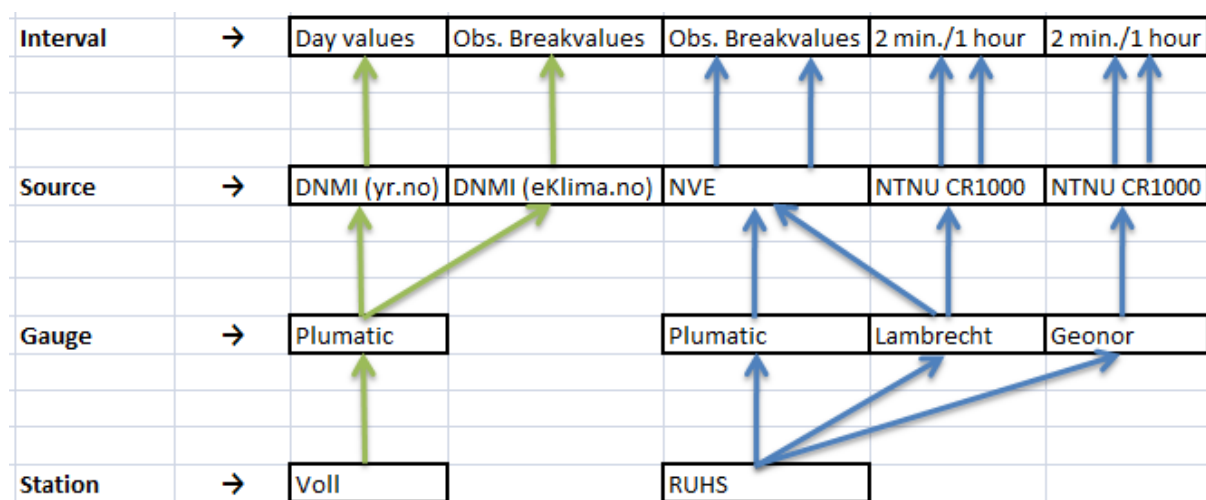


Figure 15: Collecting 8 registrations for statistical precipitation analyses

Two of the registrations were obtained from a pluviometric gauge at Voll, a weather station located approximately 2 km northeast of RUHS. Datasets from Voll worked as an external basis for comparison.

For practical use, several registrations were obtained to secure the quality of the datasets. If one of the datasets would by any chance be incomplete, then it was easy to replace it with another.

The purpose with the statistical comparisons was mainly to try to verify the Geonor gauge, which was installed at RUHS in early May 2011. Nevertheless, the other gauges were also a relevant concern for verification.

2.2.2 Precipitation, single events

A couple of independent rainfall- and runoff events were needed to calibrate the runoff model. The basic principle was to pick out a normal event and an extreme event. The normal event was chosen based on the overall average of the measured precipitation data. The overall average covers the period from 01.05.2011 – 04.12.2011, using the weekly summarizations as basis. The extreme event was chosen within the same period, by selecting it from the day with most precipitation.

Both rainfalls represent short duration precipitation, which means the duration lasts between a few minutes to a few hours, similar to the behavior of convective precipitation. (Norsk Vann rapport 162, 2008). The normal event was selected from 02. June, the duration was about 2 hours and 20 minutes. The extreme event was selected from 16. August, the duration was about 12 hours. See chapter 4 for more details.

Through these events, the gauges were compared both in relative and cumulative amounts.

2.2.3 Precipitation, historical data

Historical data from RUHS was received from NVE, covering the entire period from 01.01.1986 – 19.09.2011 using day intervals. Through various statistical analyses, these parameters were appropriate to present:

- Annual rainfall 1986 - 2011
- Monthly relationships (max, min, average) 1986 – 2011
- Monthly developments 1986 – 2011
- Percentage of average linear growth for 1987 – 2011 and 1990 – 2011

The purpose of these statistical analyses was to get a good overview of the developments for the past 25 years. In essence, the focus was on the increase of precipitation due to climate change.

2.3 Water balance equation

The complete water balance can be complex in its forms depending on the location and its climate conditions, but usually the equation is generally expressed by follows:

$$Q = P - E - \text{Inf.} - \text{Int.} - \text{Po} - \text{Others} + (\Delta S) \quad (\text{mm})$$

Where:

Q = Surface runoff.

P = Precipitation, rainfall.

E = Evaporation.

Inf. = Infiltration into the ground, as long as the type of soil allows it to.

Int. = Interception (amount of precipitation that doesn't reach the soil, in example precipitation hindered by leaves, branches, plants, and forest floors).

Po = Ponding, water that accumulates on the surface when local infiltration capacity has exceeded due to > 100 % saturation of the soil. Local conditions make it impossible for the water to be transported away, which leads to pond formation. The pond will eventually evaporate away over time.

Others = could be for example nearby lava activity which leads to increased evaporation, or an underground river that leads to more rapid ponding in soil with great infiltration potential.

ΔS = Snowmelt amount. Usually an added amount during the spring when the temperature rises and the sun radiation increases, melting the snow before surface runoff. The snow melt contributes to surface runoff due to frozen soil. The snow amount subtracted from the precipitation happens as a result of the exact opposite situation, when the snow settles on the surface without melting, (S.Lawrence Dingman, 2008. Physical Hydrology).

By simulating the two chosen rainfall events in PCSWMM, it was possible to provide suggestions on how the water balance is distributed in the field. Every parameter is expressed by the unit mm. In this thesis, the water balance equation was simplified by excluding a few of the parameters. The equation was then expressed by follows:

$$Q = P - E - \text{Inf.} \quad (\text{mm})$$

2.3.1 Evaporation

It was possible to give an estimation of the infiltration in the field by using the PCSWMM manual, but the field evaporation had to be calculated in advance before the results were applied into the runoff model.

For this, the Penman equation was used. The equation is expressed in two different ways: the Penman Monteith- and the Penman Shuttleworth version.

Penman Shuttleworth:

$$E_{mass} = \frac{mR_n + \gamma * 6.43 (1 + 0.536 * U_2) \delta e}{\lambda_v (m + \gamma)}$$

Where:

- Emass = Evaporation rate (mm day-1)
- m = Slope of saturation vapor pressure curve (kPa K-1)
- U2 = wind speed (m s-1)
- δe = vapor pressure deficit (kPa)
- λv = latent heat of vaporization (MJ kg-1)
- Rn = Net irradiance (MJ m-2 day-1)
- γ = psychrometric constant = (kPa K-1)

Penman Monteith:

$$E_{mass} = \frac{mR_n + \rho_a c_p (\delta e) g_a}{\lambda_v (m + \gamma)}$$

Where:

- m = Slope of saturation vapor pressure curve (Pa K-1)
- Rn = Net irradiance (W m-2)
- ρa = density of air (kg m-3)
- δe = vapor pressure deficit (Pa)
- λv = latent heat of vaporization (J kg-1)
- γ = psychrometric constant =

$$\frac{0.0016286 * P_{kPa}}{\lambda_v} \quad (\text{Pa K-1})$$

- cp = heat capacity, air (J kg-1 K-1)
- ga = momentum surface aerodynamic conductance (m s-1)

Relationships for both equations:

$$m = \Delta = \frac{de_s}{dT_a} = \frac{5336}{T_a^2} e^{\left(21.07 - \frac{5336}{T_a}\right)}$$

Where:

ea = vapor pressure of air.

es, mmHg = $\exp(21.07 - 5336/T_a)$

$\delta e = (e_s - e_a) = (1 - \text{relative humidity})e_s$

es = saturated vapor pressure air, inside plant stoma.

(S.Lawrence Dingman, 2008. Physical Hydrology).

At first a climate map from a report written by the Norwegian Climate Center was obtained. It showed the annual average evaporation of Norway, and gave a reasonable indication of the total amount of evaporation per year ($\approx >500$ mm). See climate map on next page, Figure 16. See Appendix CD.4 to view the Climate Center report.

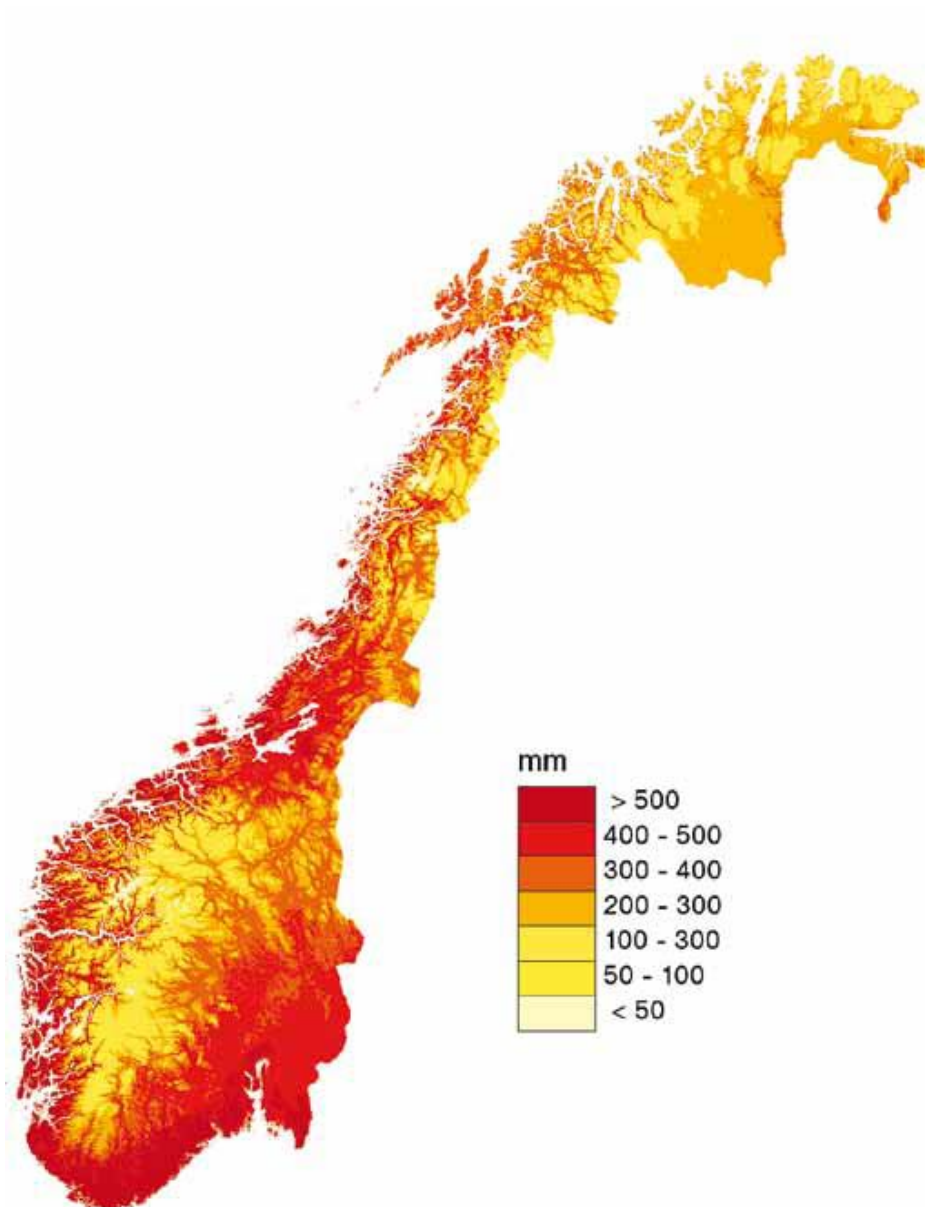


Figure 16: Annual amount of evaporation (based on statistics from 1961 – 1990), (Norwegian Climate Center, 2009)

The rainfall events chosen for simulation were extracted from June and August. Calculation of evaporation for these two months was therefore prioritized. To carry this out, data from solar radiation, air humidity, air temperature, and wind speed were obtained from NTNU's CR1000 logger at RUHS.

The Penman Shuttleworth equation seemed to generate large evaporation values (average between 5 – 8 mm/day). The reason for that was because the Shuttleworth equation was based on evaporation from open surfaces. The estimation of evaporation was then performed by using the Penman Monteith equation. This equation was based on evaporation from vegetated surfaces. However, the results were almost the same, until the final adjustments by using certain factors were performed. Some factors describing different terrain properties had to be accounted for. One factor named C-leaf had a great impact on the final results.

The factor described the amount of pore openings on leafs present in the field, (MSc student Torstein Dalen, 2011. IVM NTNU), (S.Lawrence Dingman, 2008. Physical Hydrology).

The final average evaporation was estimated to be 2.1 mm/day in June and 1.5 mm/day in August.

For more details about the calculation steps, see spreadsheets in Appendix CD.5

2.3.2 Infiltration

To estimate the infiltration capacity, a choice between different principles had to be made. PCSWMM were able to calculate the infiltration capacity by using three different models:

- Green Ampt method
- Horton's method
- SCS Curve number method

To investigate which one of them was the better approach to use, the type of soil in the field had to be determined. A map displaying the soil properties was obtained from The Norwegian Geological Research Institute (NGU). It shows that thick marine soil covers the entire field, meaning that most of it consists of clay. For RUHRF the clay was covered by a thin topsoil layer (20 – 30 cm), originally cultural soil. The layer was a result of earlier agricultural activities about 40 – 50 years ago (Harald Sveian, 2011. NGU). Figure 17 below illustrates the soil properties of the RUHRF.

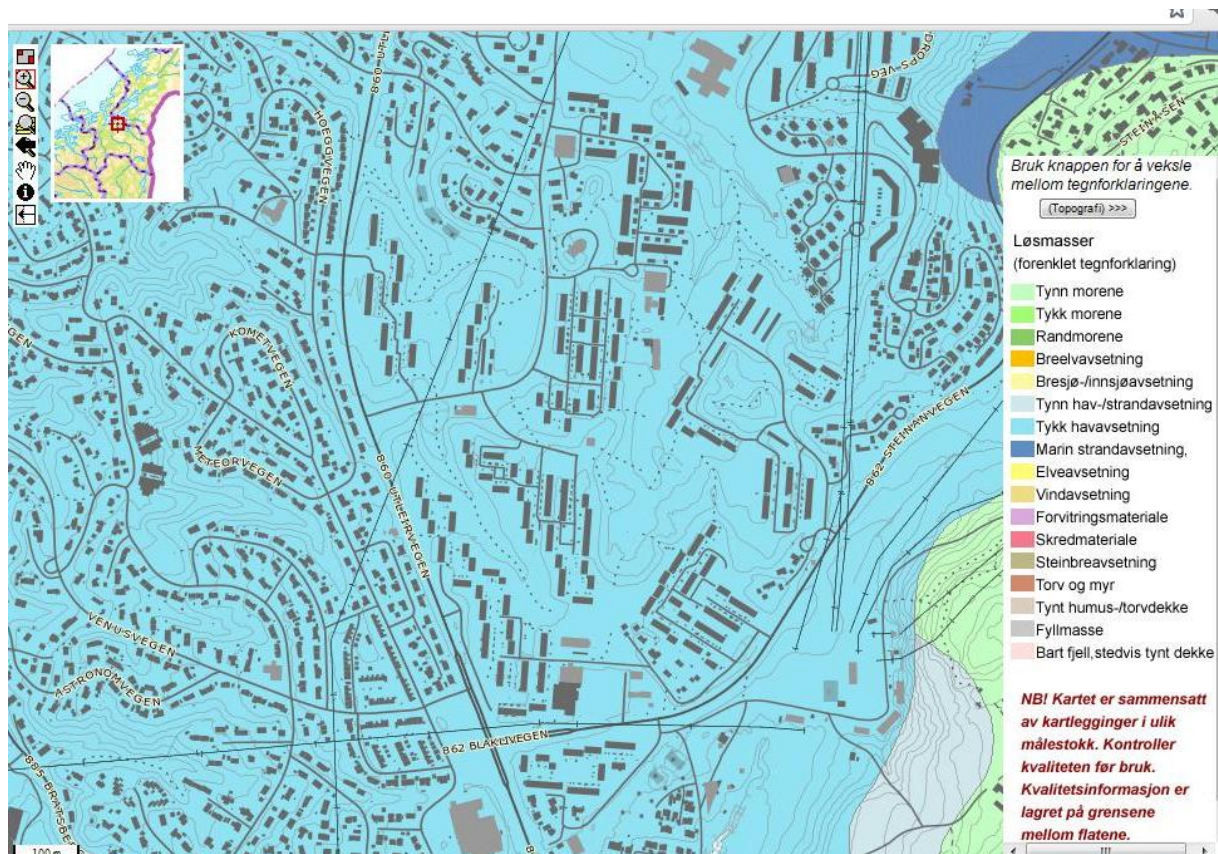


Figure 17: Map illustrating the soil properties at Risvollan (NGU, 2011)

The Green Ampt equation requires specific parameters such as suction head (Ψ), water content (θ), hydraulic conductivity (K), and initial infiltrated volume (F). To get adequate data on these parameters, the best way is to obtain soil samples extracted from the field. The alternative was to use data from another soil sample, assuming that it contains the same properties. The manual "User's guide to SWMM5" written by William James, Lewis E. Rossman et.al, offered typical values from a table containing soil characteristics. However, there was limited information about the soil classes displayed in it, see table 5 below.

Green Ampt equation:

$$\int_0^{F(t)} \frac{F}{F + \psi \Delta\theta} dF = \int_0^t K dt$$

Table 5: Soil characteristics from User's guide to SWMM5

Soil Texture Class	K	Ψ	ϕ	FC	WP
Sand	4.74	1.93	0.437	0.062	0.024
Loamy Sand	1.18	2.40	0.437	0.105	0.047
Sandy Loam	0.43	4.33	0.453	0.190	0.085
Loam	0.13	3.50	0.463	0.232	0.116
Silt Loam	0.26	6.69	0.501	0.284	0.135
Sandy Clay Loam	0.06	8.66	0.398	0.244	0.136
Clay Loam	0.04	8.27	0.464	0.310	0.187
Silty Clay Loam	0.04	10.63	0.471	0.342	0.210
Sandy Clay	0.02	9.45	0.430	0.321	0.221
Silty Clay	0.02	11.42	0.479	0.371	0.251
Clay	0.01	12.60	0.475	0.378	0.265

The Horton's equation also requires specific parameters just like the Green Ampt method, but the description of different soil classes along with which parameters to use on them were more extensive. Horton's method made it easier to determine the infiltration capacity. First of all it separated between sandy soils, loam soils and clay soils. Second it also separated between dry soils and moist soils, both with and without vegetation.

The topsoil at RUHRF was considered to be relatively moist, due to the relatively frequent rate of rainfall at any season. The moist soil was divided into three different categories: soils which have drained but not dried out, soils close to saturation, and soils which have partially dried out. In this thesis, the first category was chosen, reasoned that the topsoil layer never gets a chance to dry out completely, (S.Lawrence Dingman, 2008. Physical Hydrology).

Horton's equation:

$$f_t = f_c + (f_0 - f_c)e^{-kt}$$

Where:

f_t = infiltration rate at time t .

f_0 = initial infiltration rate or maximum infiltration rate.

f_c = constant or equilibrium infiltration rate after the soil has been saturated or minimum infiltration rate.

k = the decay constant specific to the soil.

See Figure 18 and Table 6 to view the principle behind the Horton's method in PCSWMM and the values chosen for each infiltration parameter.

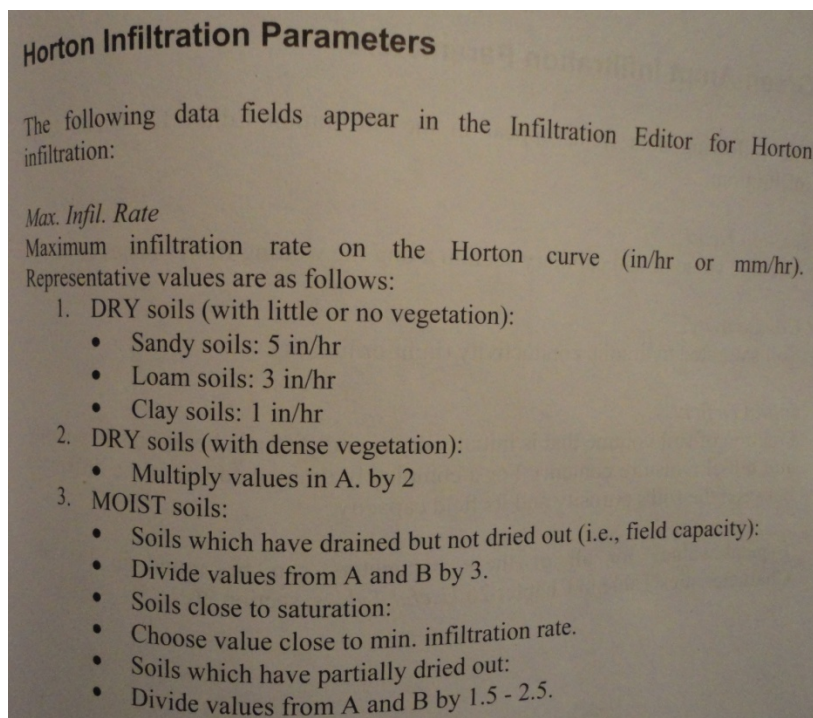


Figure 18: The principles behind Horton's method in PCSWMM (User's guide to SWMM5, 2008)

Table 6: Suggestions for Horton's infiltration parameters in PCSWMM

☐ Infiltration : Horton	
Max. Infil. Rate (mm/hr)	1
Min. Infil. Rate (mm/hr)	0.1
Decay Constant (1/hr)	3
Drying Time (days)	7
Max. Volume (mm)	2

SCS Curve number method, or the runoff curve, is an empirical parameter used for estimation of direct runoff or infiltration during a rainfall event. The curves are developed based on empirical data for soil conditions and the degree of urbanized areas. The SCS method does not offer any assessment of individual parameters, and was therefore considered irrelevant for this task (Hans Vebjørn Kristoffersen, 2010)

2.4 PCSWMM

The runoff simulations were performed by using PCSWMM Professional 2011, developed by Computational Hydraulics International (CHI) in Canada. The application is supported by the mathematical software Storm Water Management Model (SWMM), which is developed by United States Environmental Protection Agency (US EPA). It is the most widely used software for computational runoff modeling today. PCSWMM provides a graphical user interface of the mathematical software SWMM. PCSWMM includes an application which supports GIS – software that makes it possible to import map- and pipe network data from GIS – systems. Many agencies use SWMM products (CHI, 2011).

The choice of calculation method used for simulation in this thesis was to include non – stationary flow by applying dynamic wave in the routing process. Alternatively, kinematic wave or steady flow were the two other possibilities. Non – stationary flow in the pipes will give a more complex relationship between the flow rate and the water wave height inside a partially filled pipe. When the water wave is led through a pipe network it spreads out over time and the maximum flow rate will then be reduced, not to mention the wave will still be moving forward in the system. In order to simulate the flow in a realistic manner, the dynamic equation St. Venant and the continuity equation were used (Butler and Davies, 2010). The Darcy Weisbach equation was used to compute the friction losses for pressurized flow in conduits that have been assigned a circular cross section shape. SWMM used the Manning equation to express the relationship between the flow rate, cross sectional area, hydraulic radius, and the slope in all conduits during non pressurized conditions (Lewis E. Rossman, 2009). In this thesis, SI units were used.

The continuity equation:

$$v \frac{\partial A}{\partial x} + A \frac{\partial v}{\partial x} + b \frac{\partial h}{\partial t} = 0$$

The dynamic, or momentum, equation:

$$g \frac{\partial h}{\partial x} + v \frac{\partial v}{\partial x} + \frac{\partial v}{\partial t} = g(i - j)$$

Darcy Weisbach equation:

$$Q = \sqrt{\frac{8g}{f}} AR^{1/2} S^{1/2}$$

Manning equation:

$$V = \frac{k}{n} R_h^{2/3} \cdot S^{1/2}$$

The time steps used in the simulations was 5 seconds. The recommended calculation step was less than 10 seconds, or there would be trouble getting the deviation from the continuity equation below 20% in vulnerable points (Hans Vebjørn Kristoffersen, 2010).

PCSWMM is based on the SWMM routine, which means it follows the box principle. The box principle is based on the allowance of ponding, before water runs over the edge and out of the box. On pervious surfaces, some of the water will be infiltrated. The water that runs out of the box goes over to the hydraulic part of the simulation.

2.4.1 Pipe network

The pipe network was imported from ArcMap into PCSWMM, along with the elevation data. The manholes were categorized as storage units, allowing surface flooding in case the system would be overloaded. It is also important to add that as soon as the water level rises above pipe diameter inside the manhole, the flow pattern will change from channel flow to pressurized flow. This principle increases the capacity of the system, and is more realistic in relation to reality.

The manholes respective diameters were missing, but an estimated diameter equal to 1000 mm was chosen for every one of them. Trondheim Municipality confirmed that most of the manholes were 1000 mm in diameter, and some were 1200 mm. The documentation written by Aasnes did not include the manhole diameters. In this thesis, bottom elevations of the manholes were the same as the bottom elevation of the connected pipes, see figure 20.

A couple of junctions were added at locations where the pipes were either accidentally unconnected or were missing an intake, PCSWMM had some difficulties interpreting the change of direction through the bends. The measure was carried out by using linear interpolation between known manholes, or by estimation in case of placing an intake. The manholes were given the same ID's as the manholes from the documentation written by Aasnes. The pipes however, were given random ID's. To verify the pipe network inside PCSWMM, a table containing the pipe data was exported and compared with the table extracted from Aasnes documentation. Downstream at the end of the system, an outfall was added, see Figure 19 below. In addition, a couple of new manholes were added at the location of RUHS, in case there was a need to insert another storage unit between them to represent the station during a flooding event. PCSWMM offers any type of cross sections and volumes for both storage devices and pipes.

Pipe roughness was also added, the default value was set to 1.0 mm. Danish consultants employed at PH – Consults suggested the roughness inside the storm water pipes should be 0.6 mm. This was the recommended roughness under satisfactory conditions. Considered the age of the network, the roughness coefficient was increased.

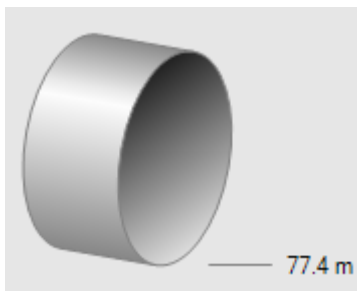


Figure 19: The outfall and its bottom elevation

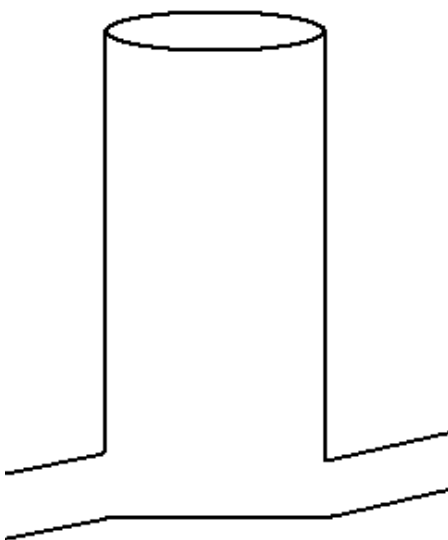


Figure 20: Manhole principle used in PCSWMM

The suggestions from PH – Consult is listed in Table 7.

Table 7: Roughness suggestions from PH - Consults

	v < 1 m/s	v >1 m/s	
		Waste water	Storm Water
Concrete	3.0	1.5	0.6
Plastic	1.5	0.6	0.6

2.4.2 The catchment

The catchment was imported into PCSWMM, along with the pre-calculated properties from ArcMap. All sub catchments were given ID's matching their connected manholes, separated by an index.

The impervious properties had to be divided into two groups: impervious and zero impervious surfaces. The difference between these two is that the zero impervious surfaces have no depression storage. Rooftop areas were added as zero impervious surfaces, while the rest of the developed surfaces were added in the impervious column.

Another parameter called "Width" had to be added for every sub catchment. The width describes the concentration time within the sub catchment. It is defined by dividing the area of the catchment with the average maximum flow length on pervious surfaces. To insert the width, the flow length had to be estimated. The estimation was supported by the length measure tool in ArcMap. The estimation itself was based on the amount of pervious- and impervious surfaces within each sub catchment along with their respectable average slope. As the flow lengths were inserted in the sub catchments, widths were automatically calculated by a tool in PCSWMM called Set Flow Length/ Width. See figures 21 and 22 for demonstration of flow length estimation- and input process in PCSWMM.

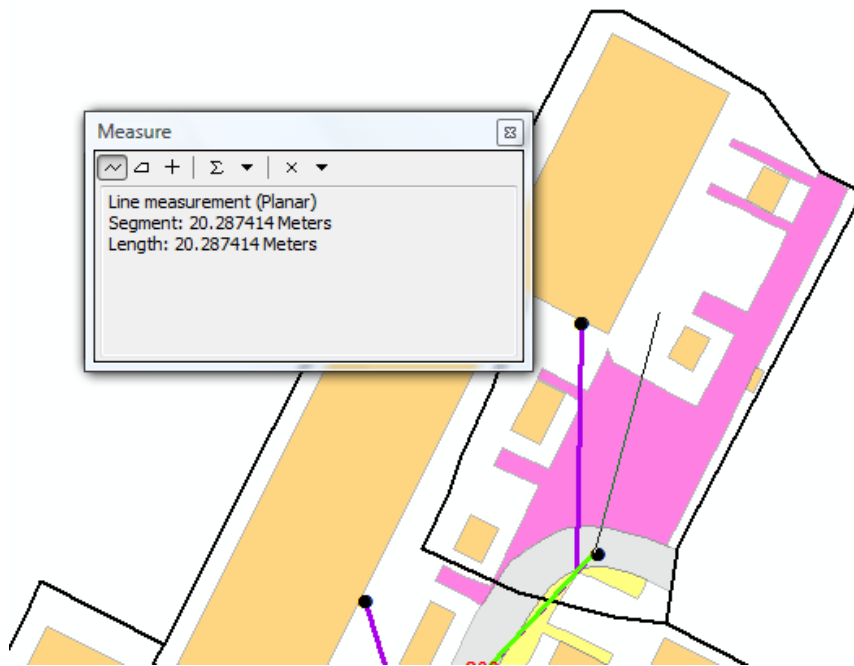


Figure 21: Flow length estimation in ArcMap

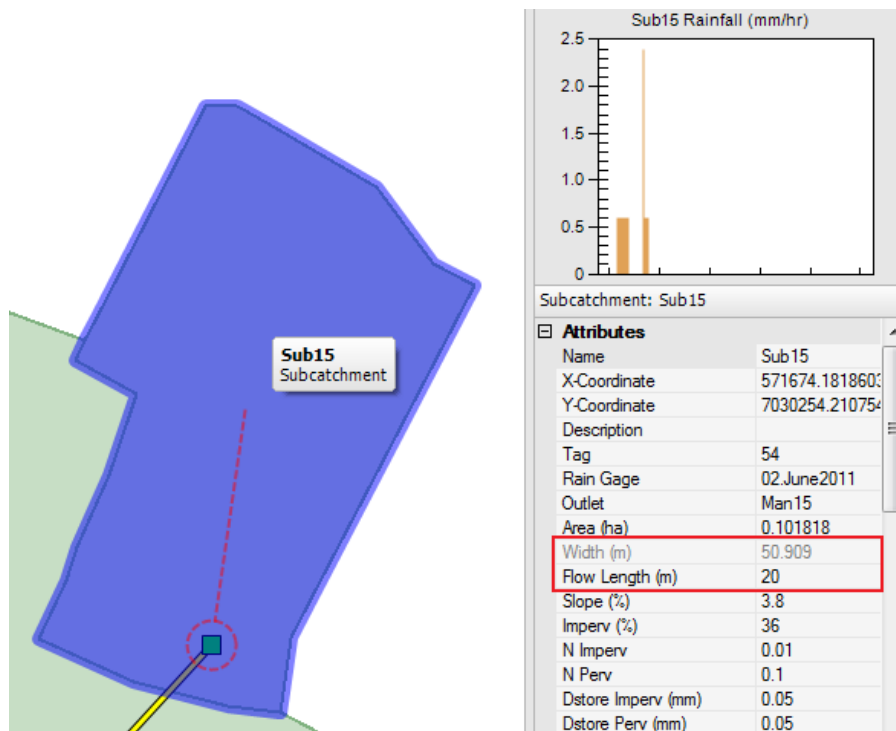


Figure 22: Flow length inserted in PCSWMM

2.4.3 Rainfall events

The rainfall events chosen from 02. June and 16. August were obtained from datasets received from NVE. The event from 02. June was based on data extracted from the Plumatic gauge, and the other was based on data from the Lambrecht gauge.

The precipitation data itself was given as observation values, also called break values. These types of registrations are considered to be reliable according to NVE. Break values is described as observations of changes during an event, meaning that the values register every tip by the gauges at any time, (Harald Viken and Svein Taksdal, 2011). For that reason, the intervals between the registrations were unequal. The dataset had to be converted into equal intervals before it was imported into the runoff model. Then, the datasets were handled in three different ways, with respect to the various import options in PCSWMM. The three principles are as follows:

1. Importing the rainfall event into PCSWMM directly after conversion into 1 minute intervals.
2. Importing the rainfall event into PCSWMM after linear interpolation between the 1 minute intervals.
3. Importing the rainfall into PCSWMM after calculating the increase of precipitation by every minute.

Converting unequal intervals into equal intervals often leads to “uncompleted registrations” between the break values. These gaps were filled with calculated values following the principle of linear interpolation between the break values. This was done to make the rainfall event more realistic, by assuming that it increased or decreased steadily over time before and after the recorded break value. After the linear interpolation operation was completed, the amount of increased precipitation between every minute was calculated. This operation was necessary, since the interpolated values only represented the cumulated amount of precipitation, not the amount of precipitation increase during the time step itself.

In PCSWMM it is possible to import rainfall from both gauges and radars. Datasets from gauges can be imported as Volume (mm), Cumulative (mm) or Intensity (mm/h). The difference between the alternatives volume and cumulative is that the cumulative option takes into the account the interpolated values calculated after conversion into equal intervals. The volume option only requires the actual registration given, without any increased or decreased approaches. The volume input alternative was appropriate for principle 1 and 3, while the cumulative input alternative was appropriate for principle 2.

The Intensity option is only an alternative input parameter to use. In this case where 1 minute intervals were used, conversion from mm to mm/h became a simple operation. The values simply had to be multiplied with 60.

The rain event extracted from 02. June was imported into PCSWMM as both volume- and cumulative input. Followed by principle 1 and 3, two volume inputs were imported. In total three different types of input from the event were to be used. They were all controlled by summarizing the total runoff amount.

The rain event extracted from 16. August was imported as both volume- and intensity input, only followed by principle 1. The duration was about 5 – 6 times longer than the event obtained from June. The two inputs were also controlled by summarization.

The rain fall inputs were compared during the calibration of the runoff model. The purpose of this was to decide which type of input that was most fit to be used for calibration purposes. This was done by comparing the system flow rate with the real flow rate measured by NVE. The flow rate (l/s) and the total volume (m³) were the prioritized parameters. See figures 23 – 33 to study the rainfall events and the input alternatives used for this task.

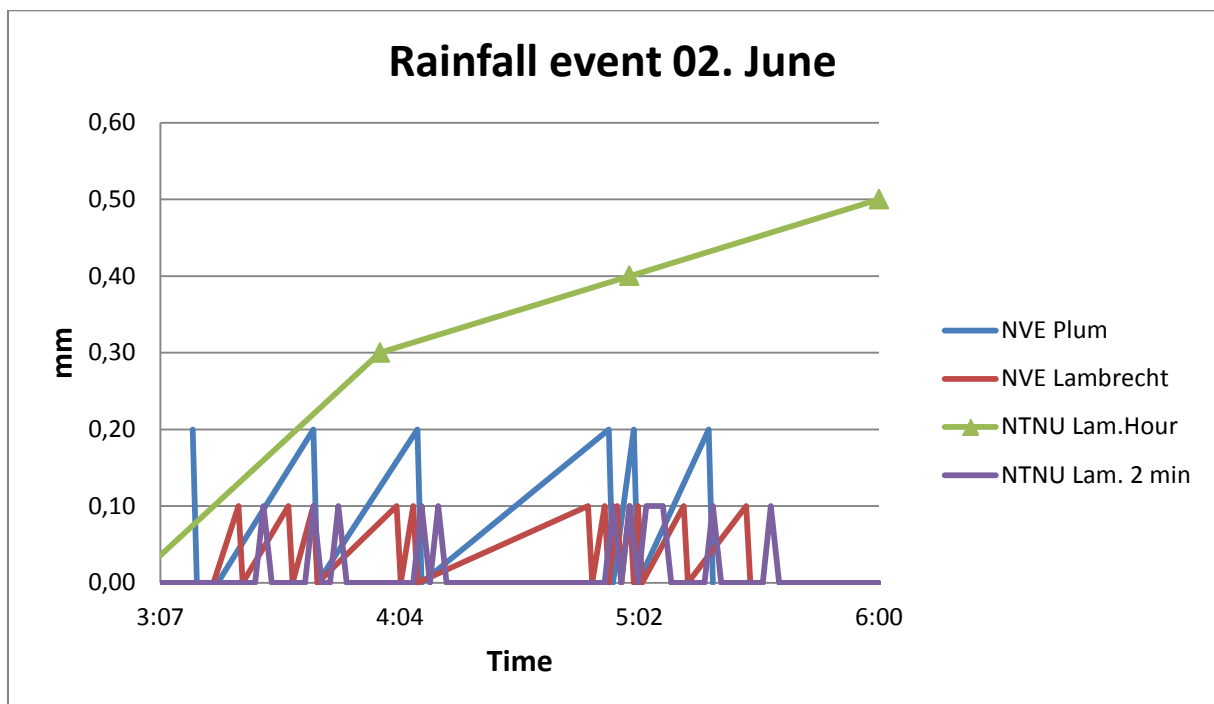


Figure 23: Rainfall event 02. June, scatter chart with straight lines

The total rainfall amounts displayed in the figure above are the same, the difference is only the frequency of registrations.

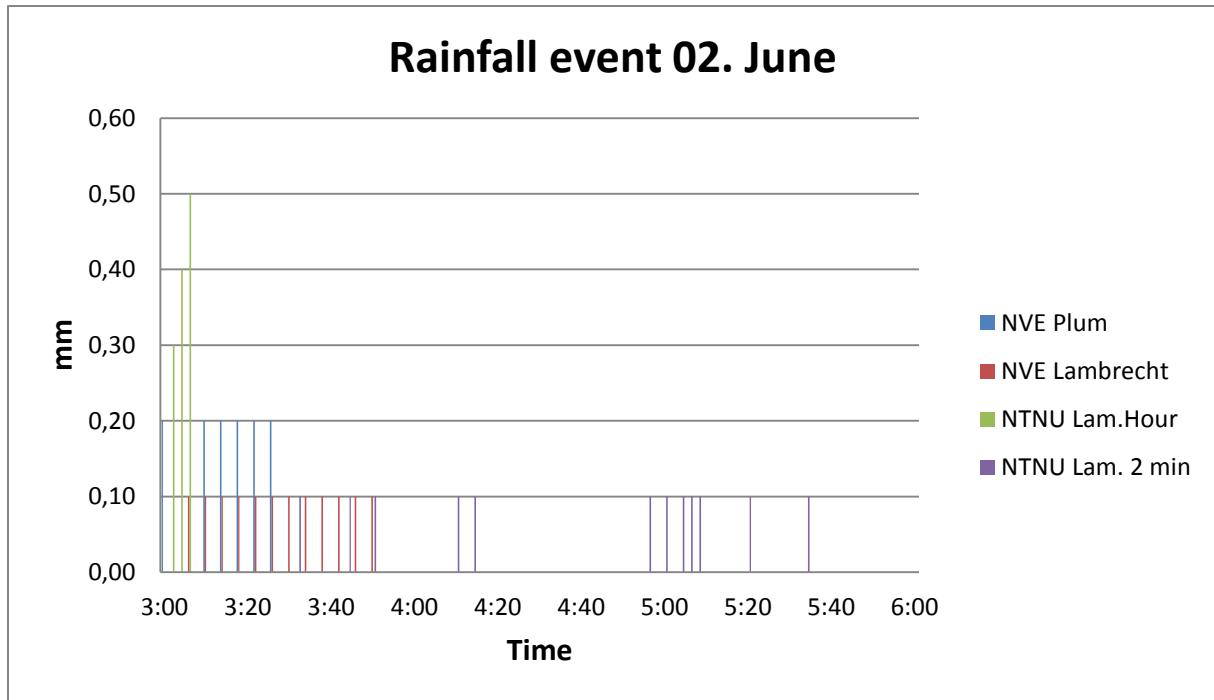


Figure 24: Rainfall event 02. June, clustered column chart

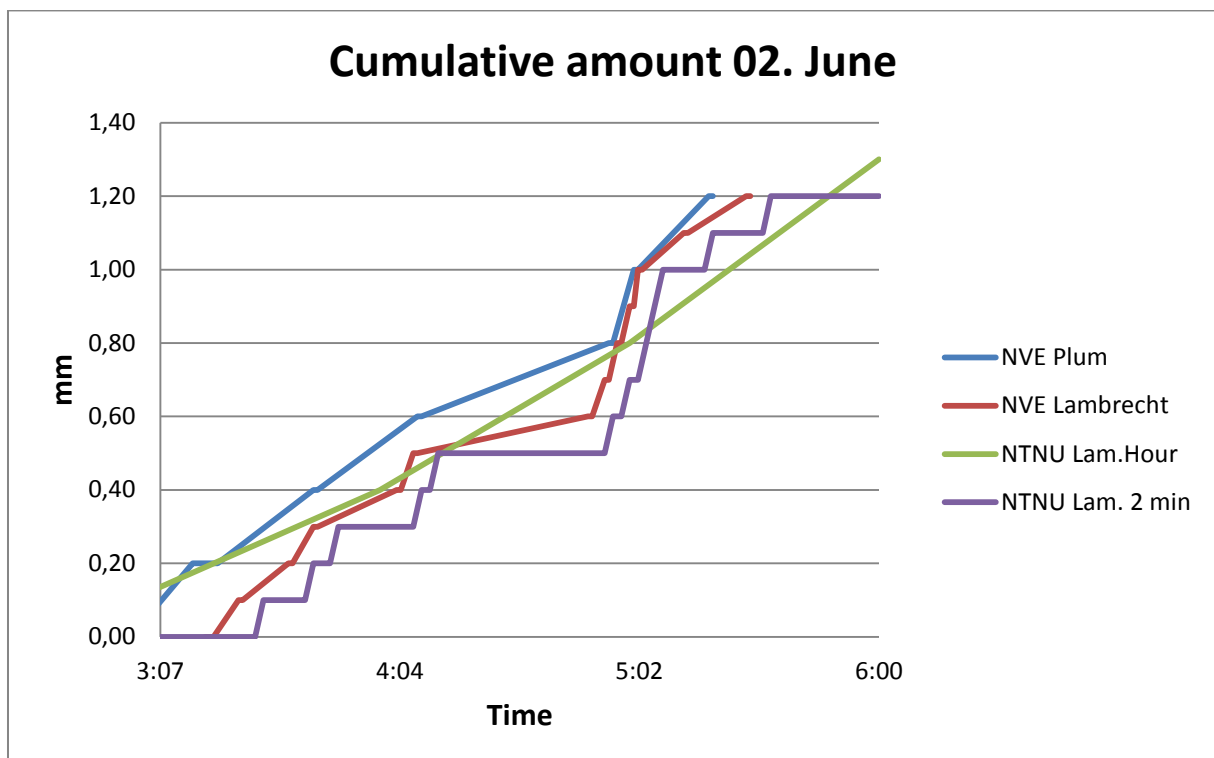


Figure 25: Rainfall event 02. June, cumulative amount

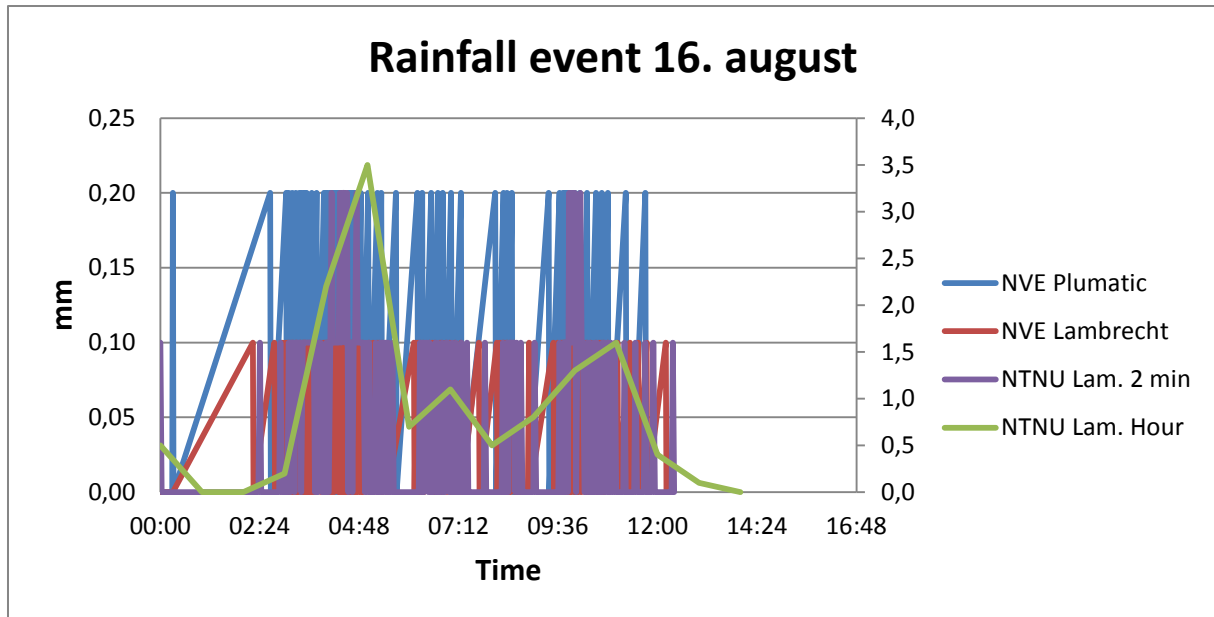


Figure 26: Rainfall event 16. August, scatter chart with straight lines. Secondary axis for NTNU Lam. Hour intervals

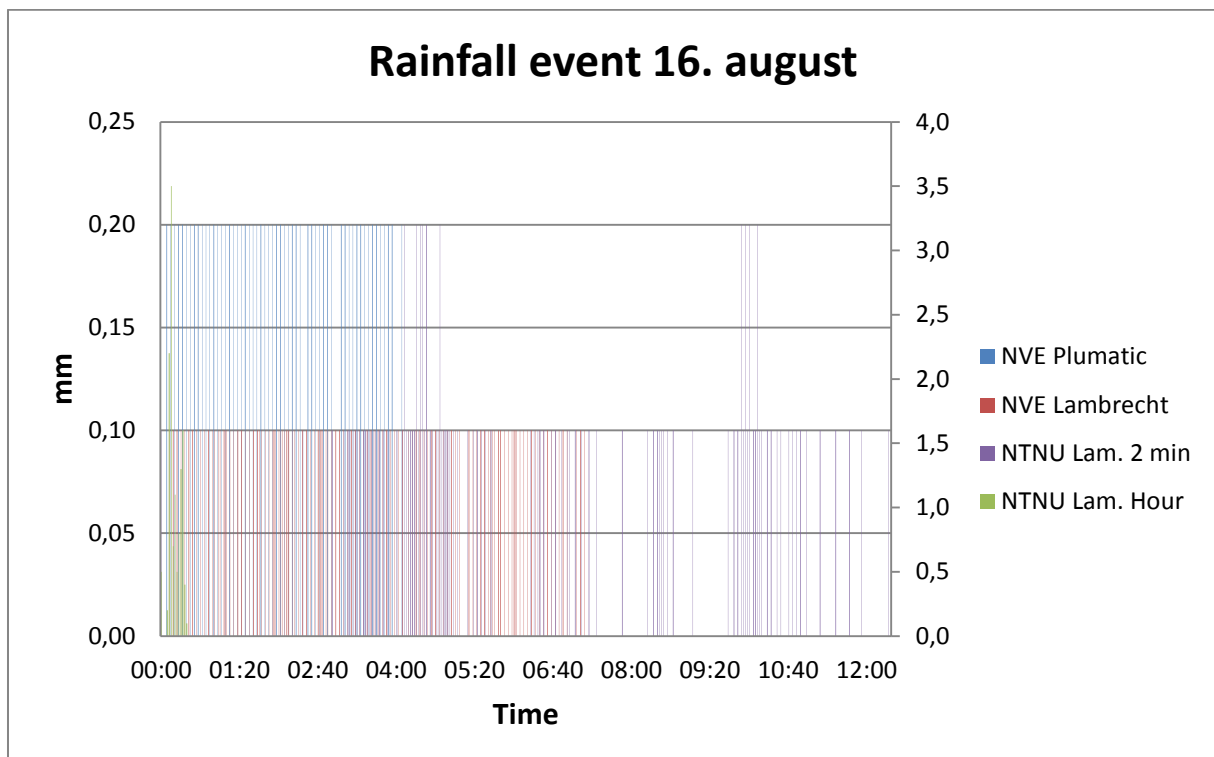


Figure 27: Rainfall event 16. August, clustered column chart. Secondary axis for NTNU Lam. Hour intervals

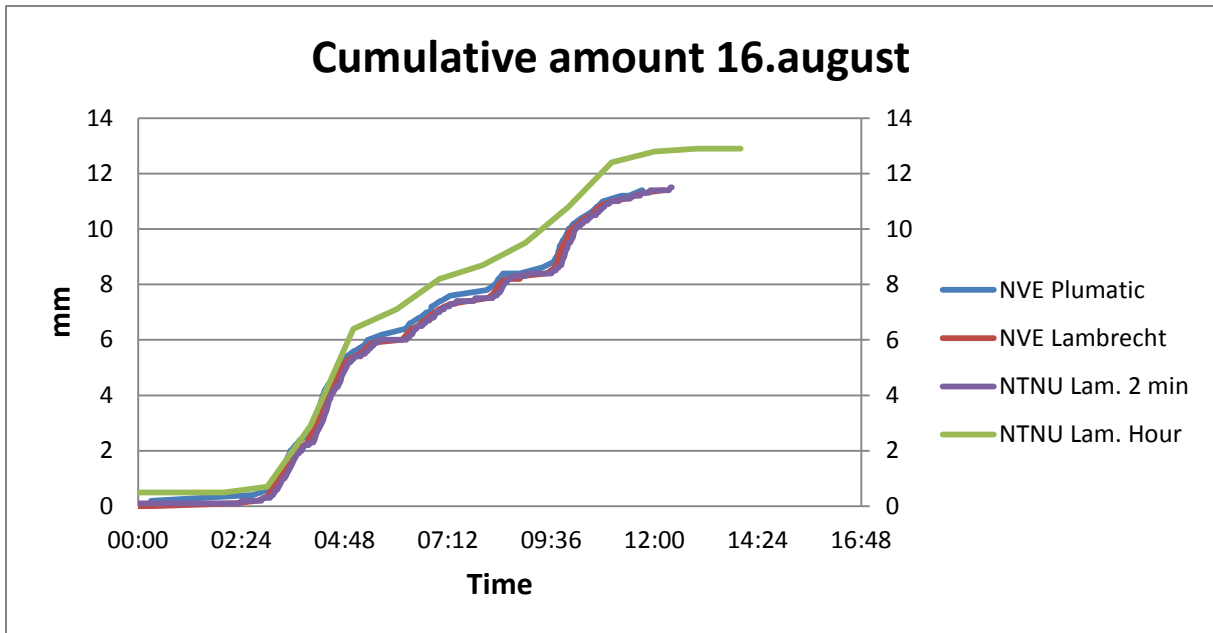


Figure 28: Rainfall event 16. August, cumulative amount. Secondary axis for NTNU Lam. Hour intervals

PCSWMM rainfall inputs:

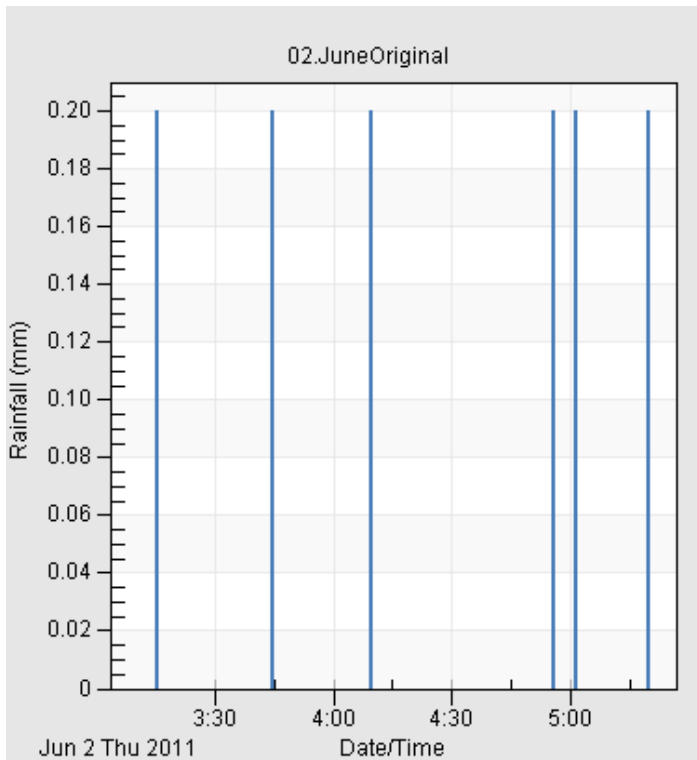


Figure 29: 02. June. Rainfall input following principle 1, imported directly after conversion into 1 minute intervals.

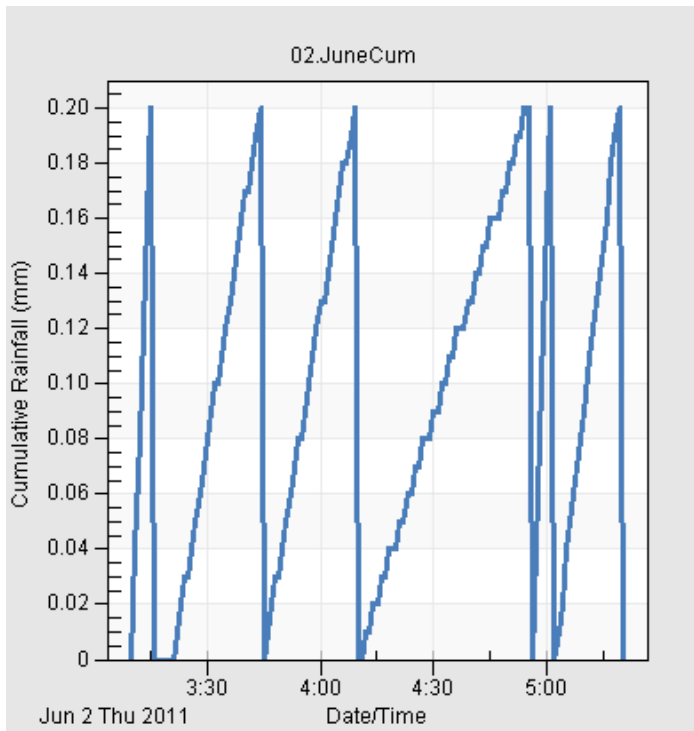


Figure 30: 02. June. Rainfall input following principle 2, imported after linear interpolation

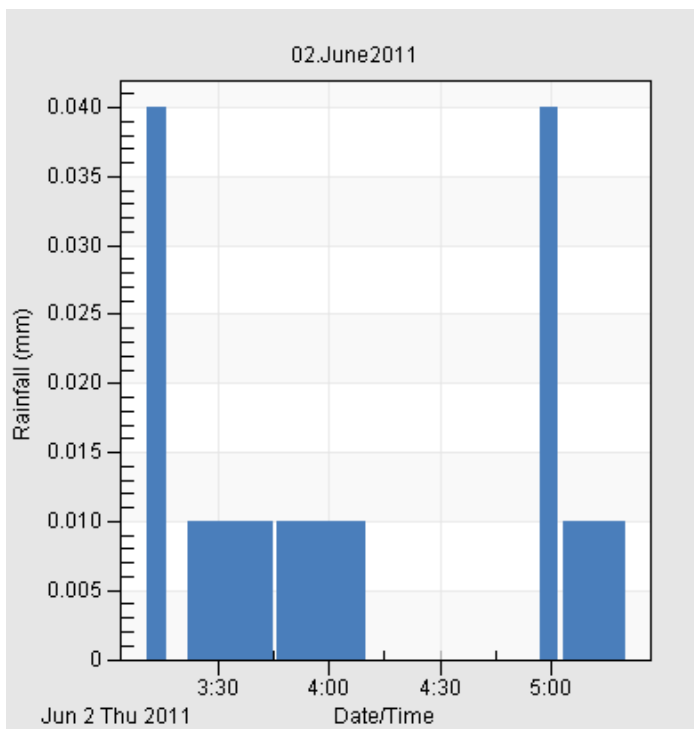


Figure 31: 02. June. Rainfall input following principle 3, increase of the amount of precipitation by every minute.

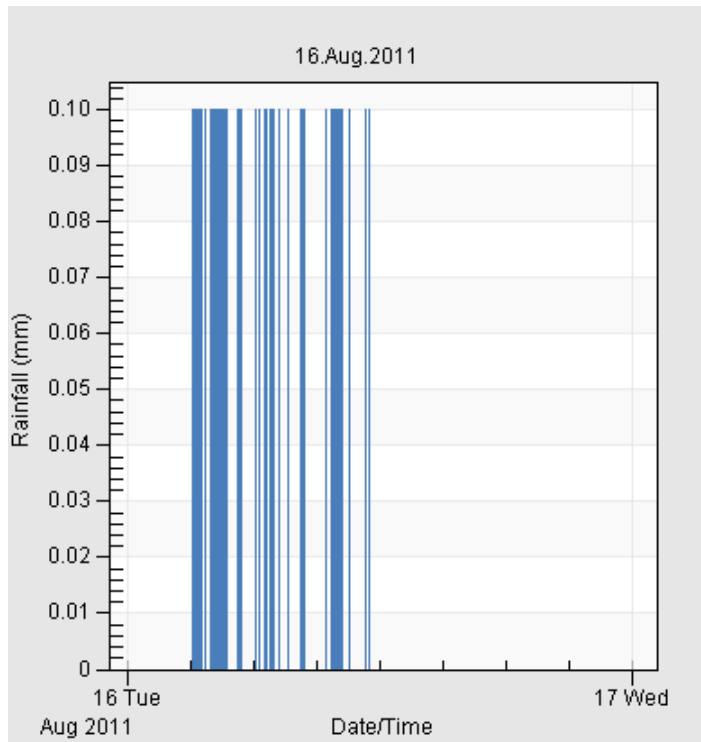


Figure 32: 16. August. Rainfall input following principle 1, imported directly after conversion into 1 minute intervals.

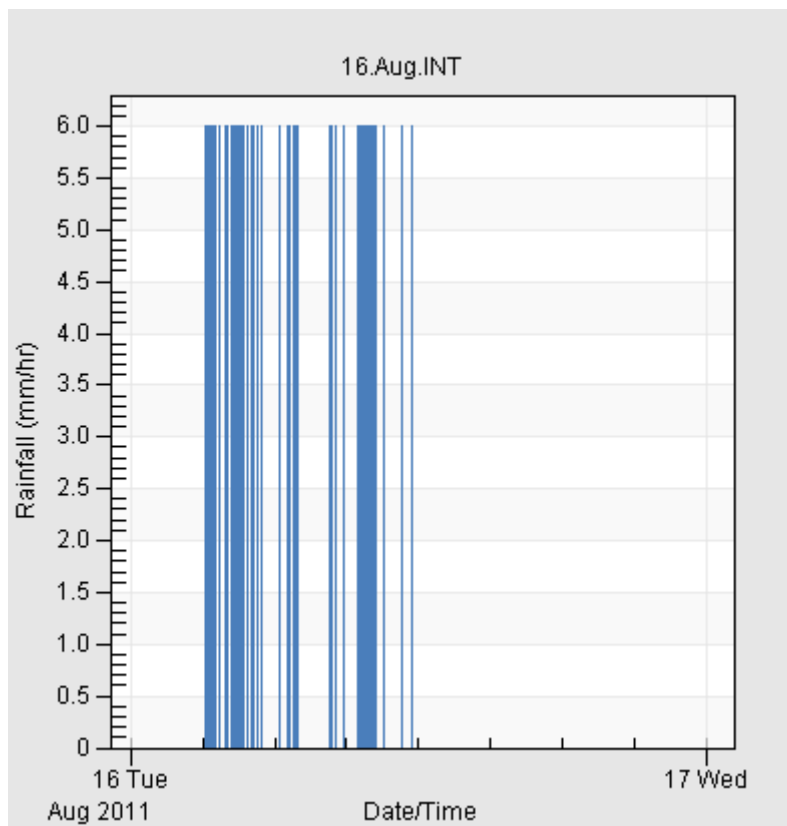


Figure 33: 16. August. Rainfall input following principle 1, imported after conversion into 1 minute intervals followed by conversion into intensity

2.5 Calibration

In this thesis the calibrations focus on the outflow delivered by the entire network system. By comparing the measured outflow with the simulated one, change of parameters would be carried out if necessary to make them match. In this case, flow rate (l/s) and cumulative volume (m³) were the key parameters. NVE supported with files for the measured outflow, the data received was given as 1 minute intervals.

Before the calibrations could take place, a decision about which parameters that could be changed during the process, had to be made. The emphasis was placed on the parameters with relatively great uncertainties. These parameters are listed below:

- Pipe roughness (mm)
- Imperviousness (%)
- Zero imperviousness (%)
- Flow length (m)
- Terrain slope (%)

The inserted default value representing the roughness (1, 0 mm), was based on a very uncertain estimation. The estimation relied on the recommendations given by PH – Consult, taking the age of the network into account. Certain other conditions were not accounted for, such as singularly losses caused by manholes, junctions and bends. These losses can often be of the same scale as the losses inside the pipe network. This depended of the size and formations of the manholes. It is complicated to calculate the exact hydraulic conditions inside them. Except from inlet and outlet losses, changes of direction inside the manholes combined with side connections could make the estimations difficult. Because of these assessments, roughness was considered to be a parameter that could be changed during the calibration, (Norsk Vann Report 172, 2008).

The inserted default values representing the impervious along with zero – impervious surfaces were also very uncertain. Since these values were based on runoff coefficients multiplied by various amounts of surface areas, the imperviousness and zero – imperviousness were considered to be parameters that could be changed during the calibration. Even if the amount of developed areas were properly calculated, the assignments of the runoff coefficients are considered to be partly subjective, (Hydraulic Design Manual, 2009).

The inserted default values representing the flow length (m) was probably the most uncertain parameter of them all. The flow length inserted into every sub catchment was more or less a guesstimation based on the amount of pervious- and impervious surfaces along with the average slope. As earlier explained the flow length helps to adjust the sub catchments width (m), which represents the concentration time in the field. Knowing that the terrain inside the runoff model only consisted of average slopes, its physical appearance was then quite different from the real conditions. The flow length was also based on the amount of impervious surfaces, which itself clearly contained large uncertainties. This could affect the response time in the field. Hopefully PCSWMM will someday be able to import 3D terrain surfaces, so that dynamical slopes could be accounted for.

Documentation of Risvollan Urban Hydrological Research Field, 2011

The average sub catchment slopes exported from the length profiles in ArcMap was considered to be very accurate, since several length profiles were made of them. By principle, it was decided that changing the terrain slope during the calibrations would only happen if absolute necessary.

In addition to the calibrations, results on peak flows would also be presented. These had no impact on the outcome of this thesis, but they could be interesting regarding surface flooding.

3. Risvollan Urban Hydrological Research Field

3.1 Area and topography

The hand drawn field boundary was compared with one of the generated areas performed by the watershed delineation analyses. The analyses were based on minimum sub catchment areas equal to 0.05, 0.1, 0.2, 0.3, 0.5 and 1.0 hectare. As discussed in chapter 2, the ideal count of sub catchments in the field should be 15 to 50. The analyses that included minimum sub areas from 0.05 to 0.3 hectare gave inadequate results. The count of sub catchments far exceeded the upper limit. Analyses including minimum sub areas of 0.5 and 1.0 hectare generated 15 and 7 sub catchments. The analysis based on minimum sub catchment area of 0.5 hectare was chosen as a basis for comparison. Figure 34 shows the comparison between the generated area and the hand drawn area.

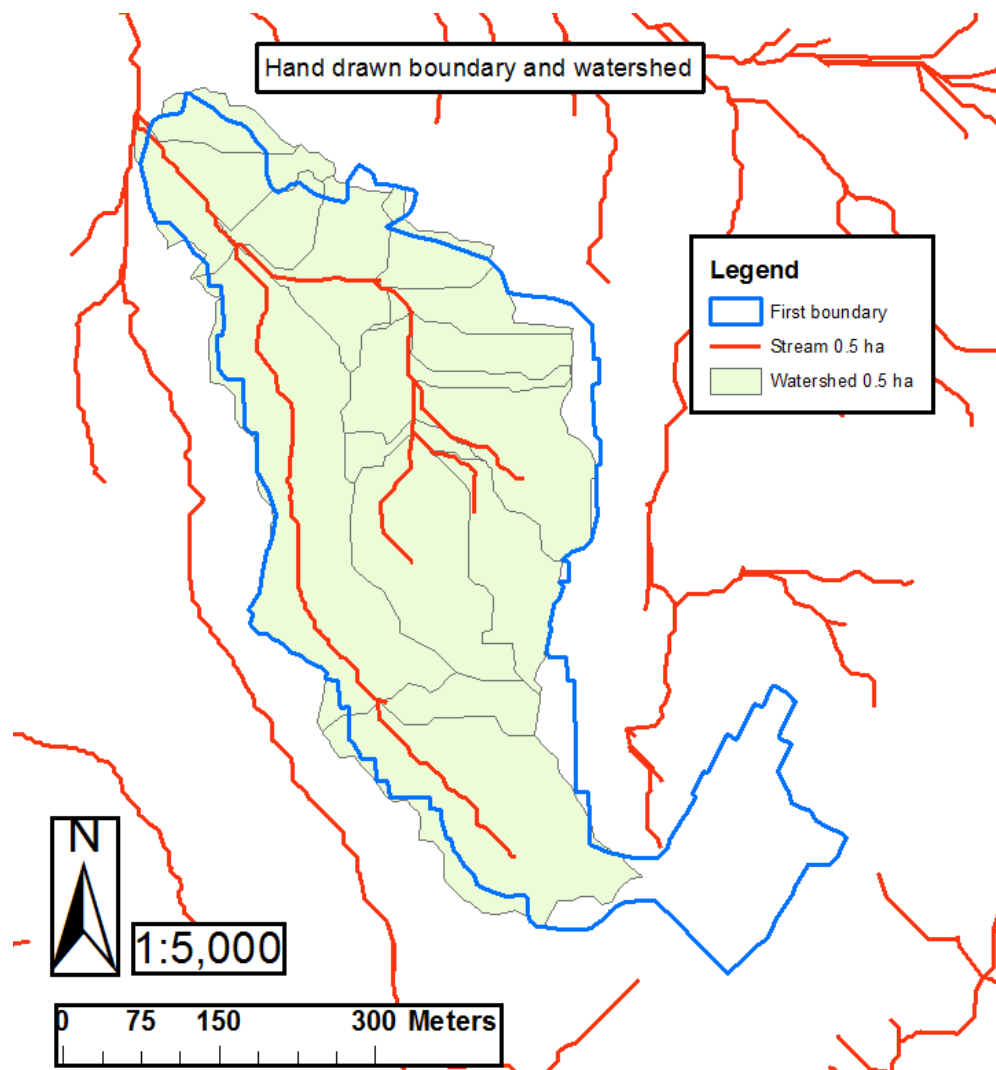


Figure 34: Hand drawn boundary compared with watershed delineation analysis

The generated area seems to be very similar with most of the hand drawn boundary, except for the southeastern corner by the road Marie Sjørdals veg. The streams show that the water paths exit the field boundary there. The generated area was 19.23 hectares, and the hand drawn boundary gave a total of 21.59 hectares. The southeast area was measured to be 3.05 hectares, including 2.19 hectares of developed areas. There was some uncertainty about the runoff contribution from the terrain surface (0.86 ha). Observations during heavy rainfall events didn't reveal exactly which direction the surface water took, with the exception of urban developed areas. It was therefore assumed that 50 % of the terrain gave runoff contribution. A total of 2.62 hectares were not accounted for in the watershed analysis, which meant that the total area should then be 21.85 hectares. However, the hand drawn boundary was a bit incorrect. It included some buildings that weren't connected to the field's storm water system, these parts were removed. Elsewhere the hand drawn boundary was considered to be valid, since it included buildings that were connected to the storm water system. Some of these buildings were located outside the watershed generated boundary. However, there is still considerable uncertainty about the runoff contribution from the surrounding terrain.

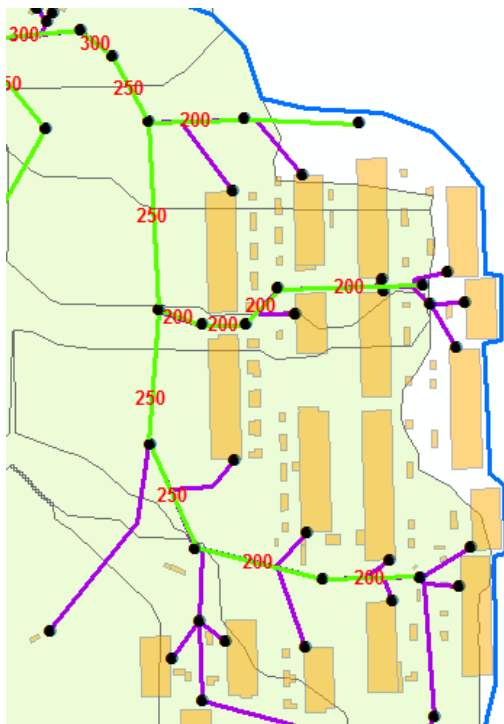


Figure 35: Connected buildings located outside the watershed generated boundary

The final outer boundary was then determined, see Figure 36 on the next page. Its total area was estimated to be 21.27 hectares. The runoff contribution from the terrain surface remains to be fully clarified. This thesis's definition on the main catchments total size, is between 20.84 to 21.70 hectares (21.27 +/- 0.86 ha).

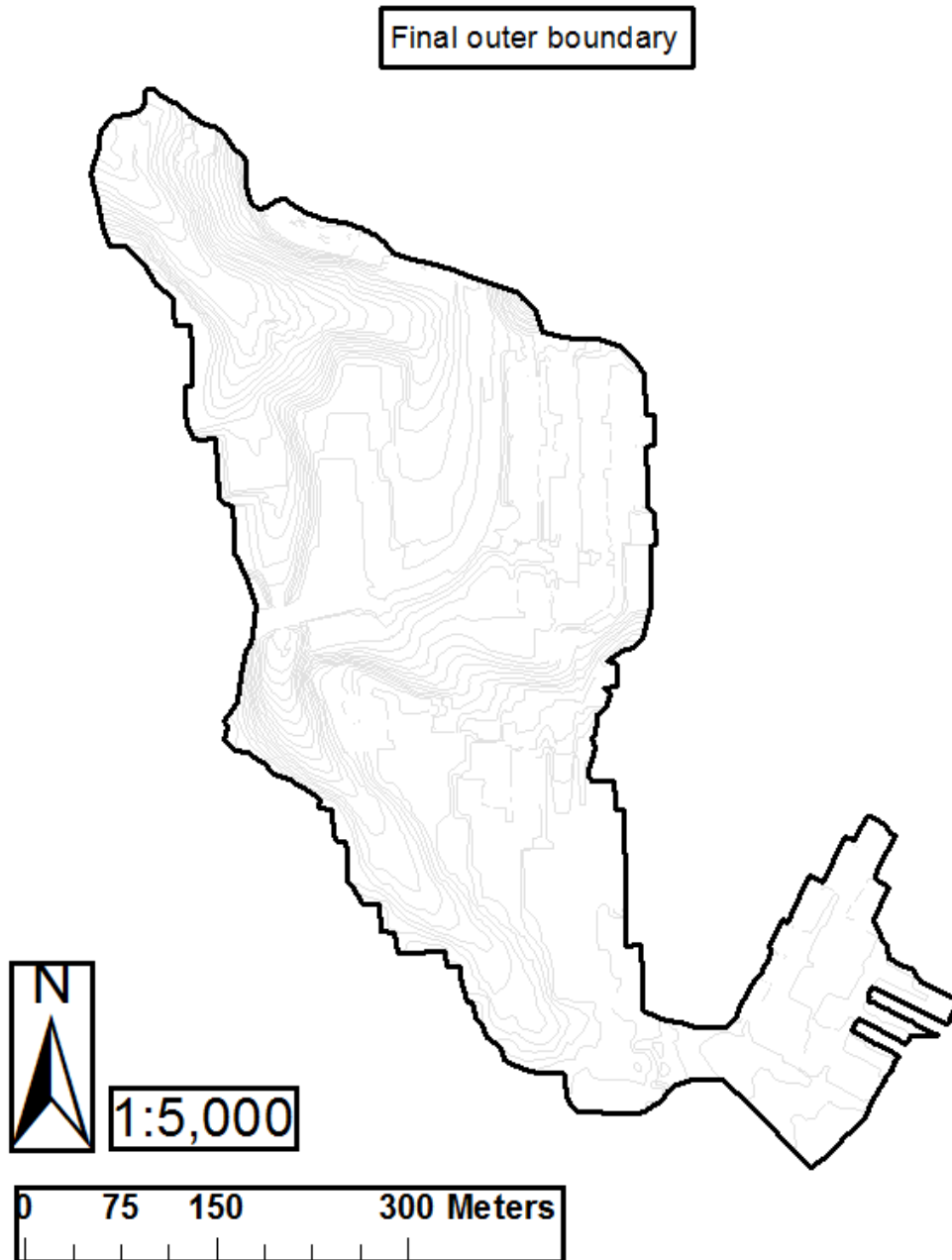


Figure 36: Final outer field boundary

The topography in the area varies greatly. The field consists of both hilly terrain and flat surfaces. The field elevation falls more or less steadily from southeast to northwest towards the station. The highest contour line has elevation +134, the lowest is +83. See Figures on next page for information about the elevation distribution.

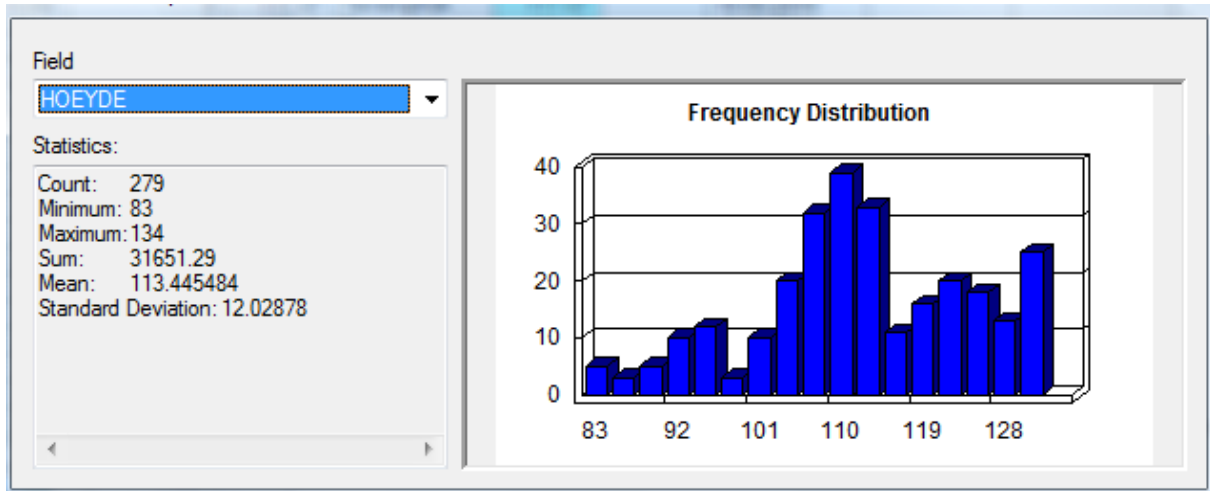


Figure 37: Elevation distribution in the field based on the contour map

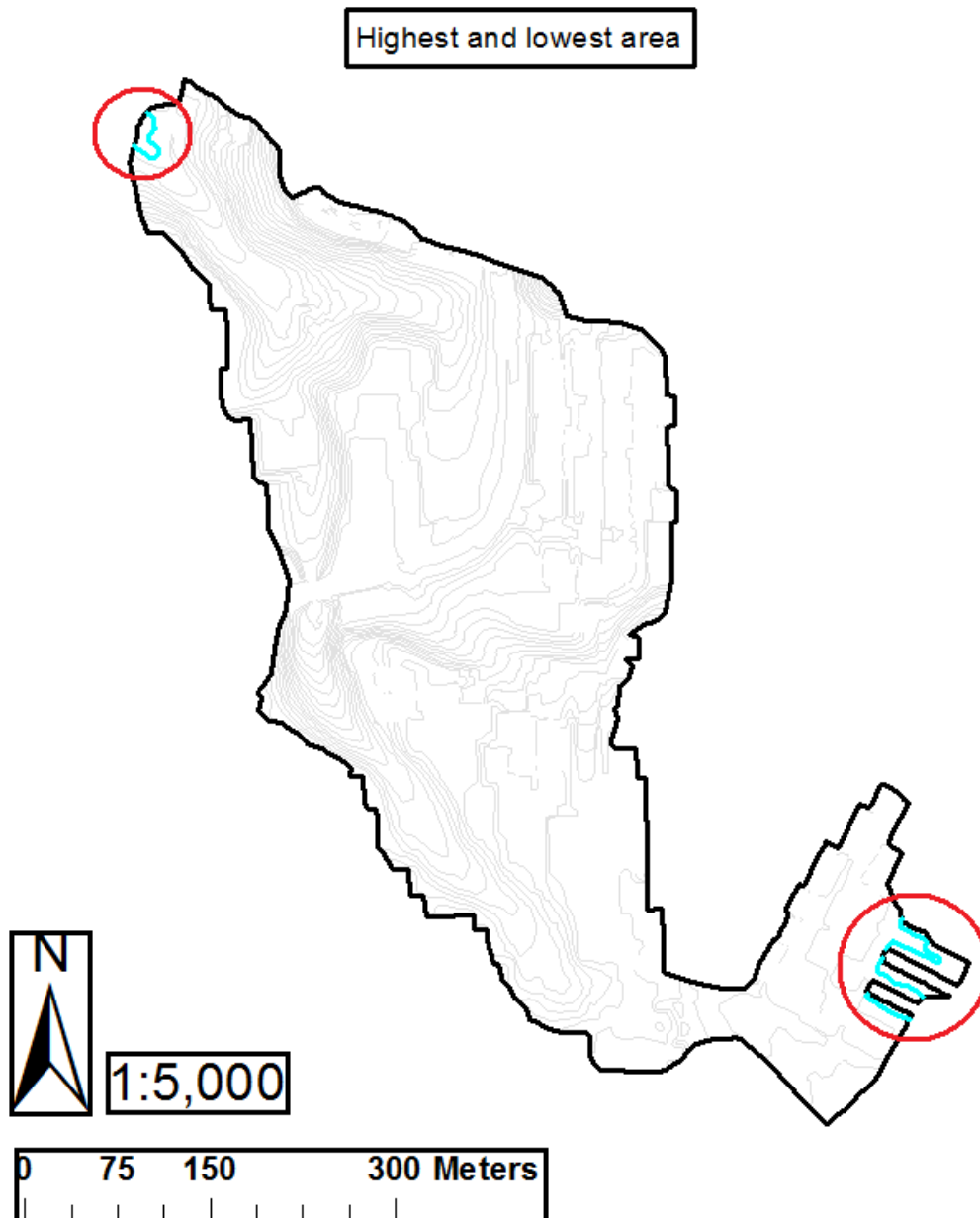


Figure 38: Highest and lowest area in the field, +134 and +83 meters above sea level (m.a.s.l.)

The topography can be presented in several ways, in this thesis with: pictures, TIN – model, DEM, slope map, and spatial representation by ArcScene combined with tilted air pictures. These approaches will be presented here to page 51:



Figure 39: Picture taken during inspections



Figure 40: Another picture taken from inspection

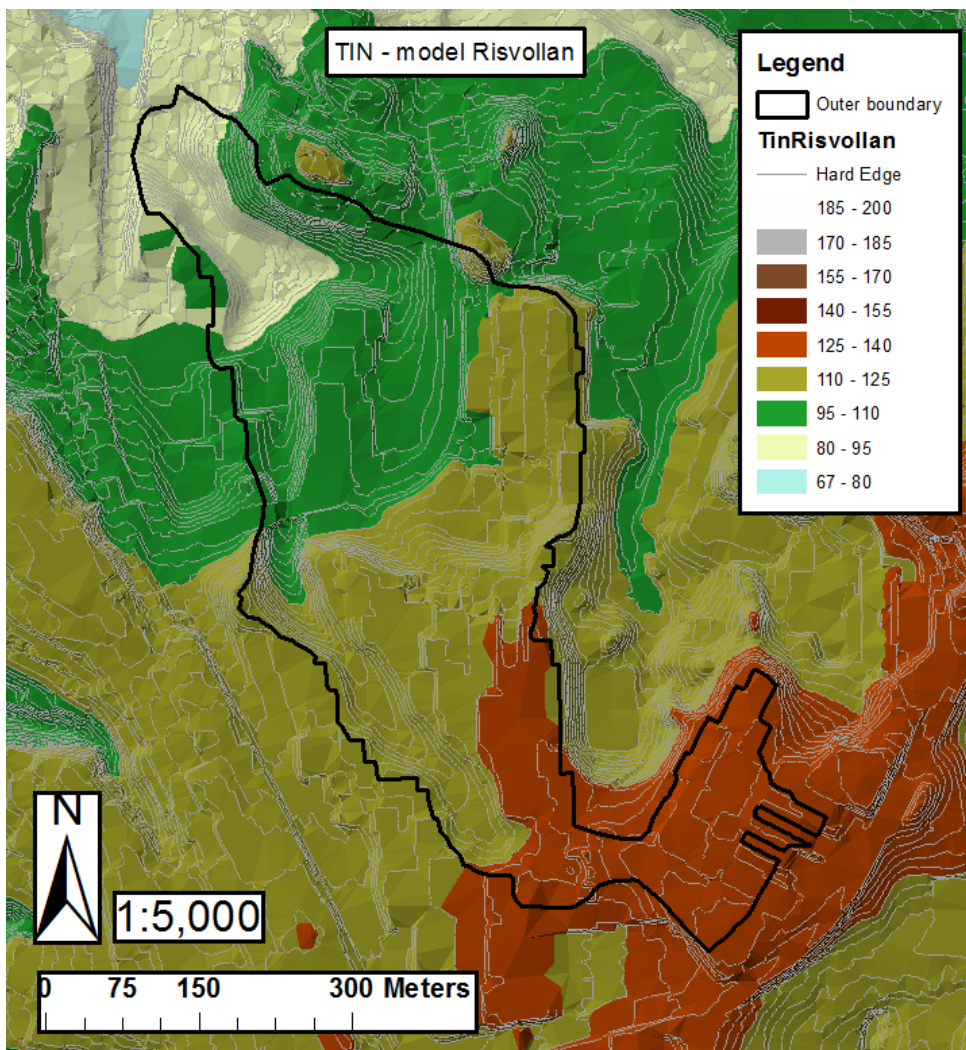


Figure 41: TIN – model of RUHRF with surrounding areas (color scale = elevation range)

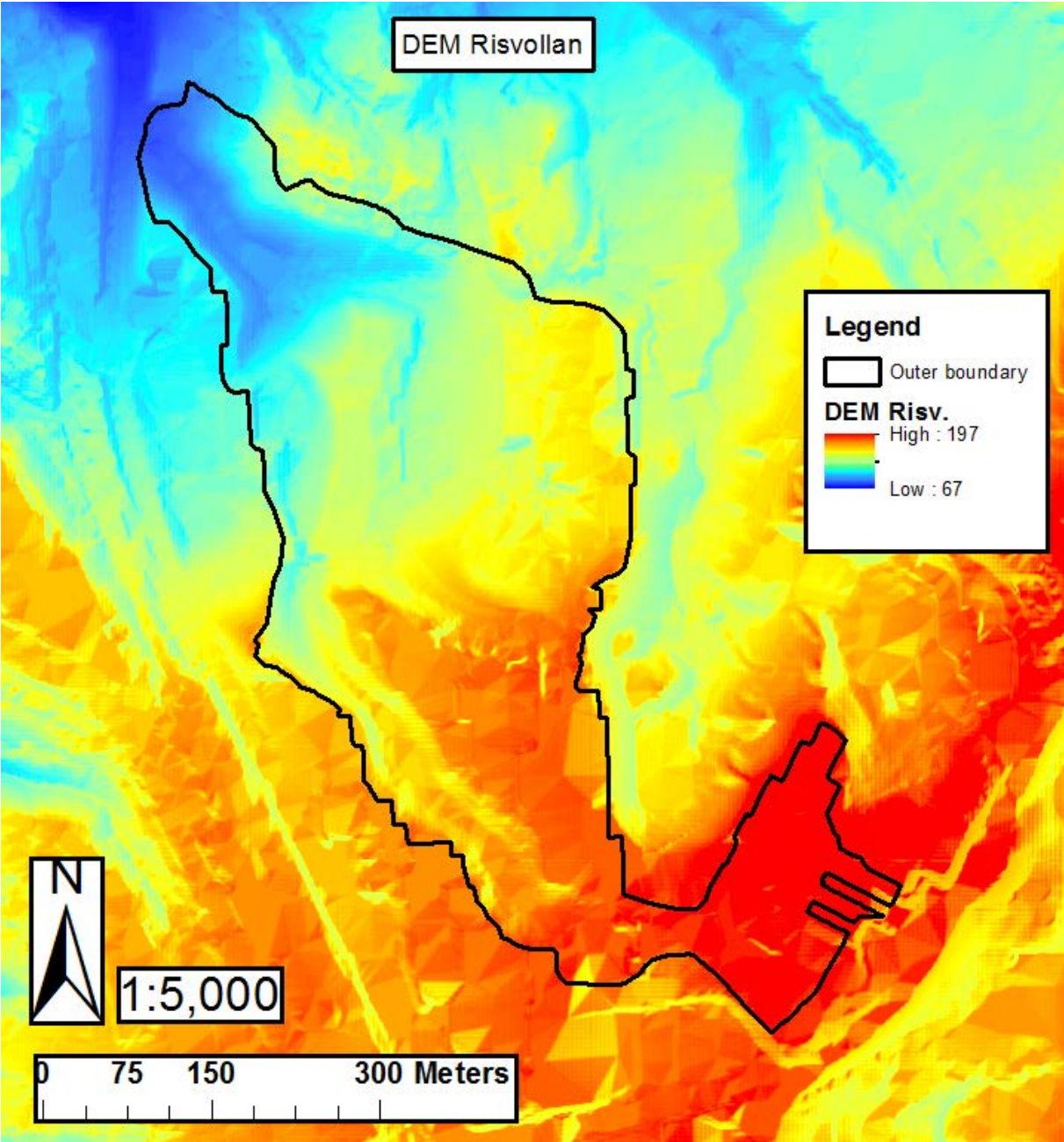


Figure 42: DEM of RUHRF, resolution 1 x 1 meter

The color scale ranges from 67 to 197 m.a.s.l

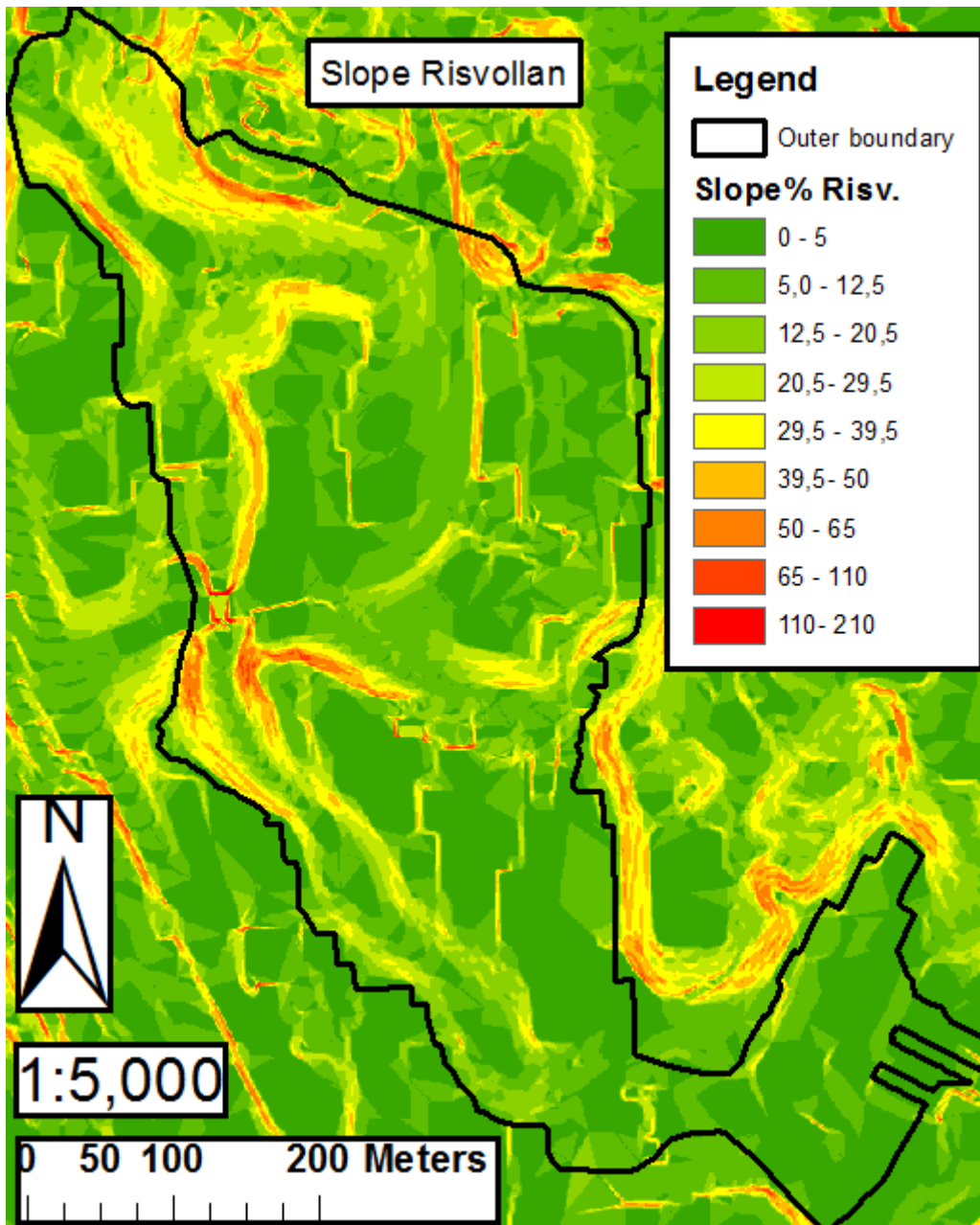


Figure 43: Slope map

The average slope for the entire field was calculated, the result was 10.12 %, equal to 5.78 degrees. The steepest part of the field is located northwest. The red color represents steep slopes, and the green scale represents moderate slopes.



Figure 44: Comparison between ArcScene spatial model and tilted air photo

ArcScene spatial model combined with satellite pictures helped verifying the terrain surface.

3.2 Storm water system

All residents within the field are connected to a separate wastewater system. In this thesis, the storm water system was put into focus.

3.2.1 Manholes

The first manholes were installed in 1969, the last ones in 1981 (Ranveig Høseggen, 2010). Recently, a 1200 mm manhole upstream the station was replaced during the construction of new apartments in autumn 2011. The wastewater manhole next to it was also replaced.

Most of the manholes were built of 1000 mm prefabricated circular concrete components, with manhole cones on the top. Some of them were also 1200 mm in diameter. See Figure 45 below for principle sketch.

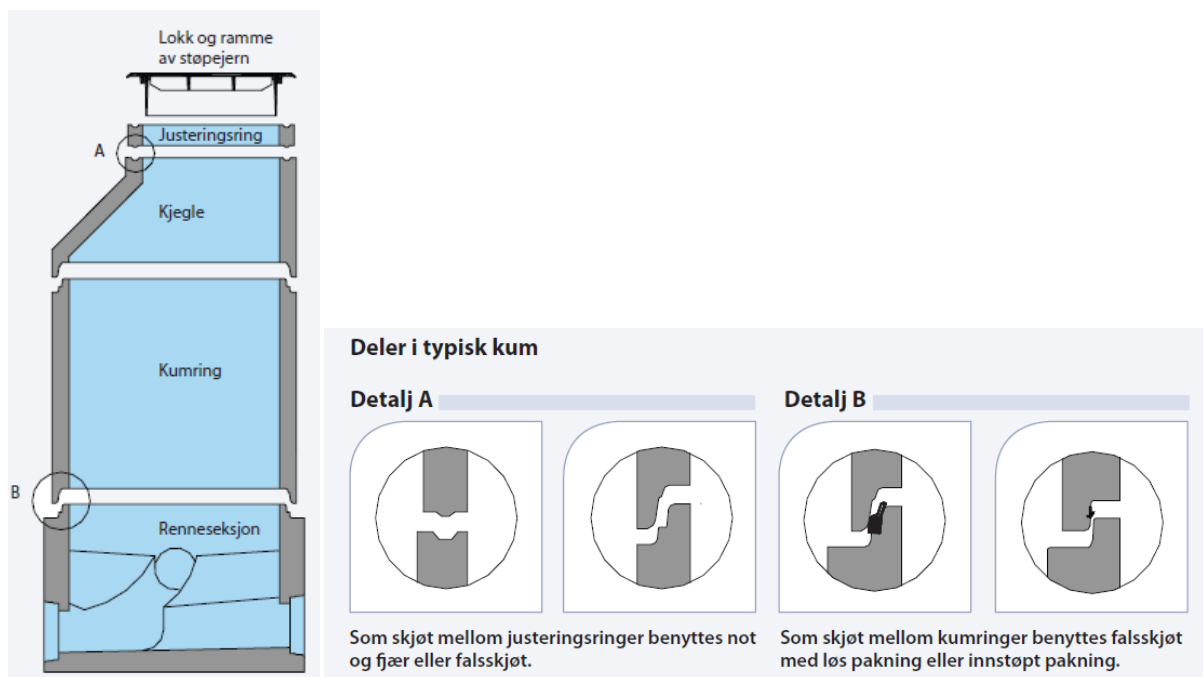


Figure 45: Manhole principal similar to the manholes at Risvollan (rubber joints, detail B) (Basal, 2011)

Figures 46 and 47 next page display the location of the replaced manholes.



Figure 46: Location of replaced manholes



Figure 47: Map location of replaced manholes

Before handling the manhole data, an overview table and figure were created. Some manholes were unfortunately unaccounted for regarding the time of installation. See Figure 48 and Table 8 below.

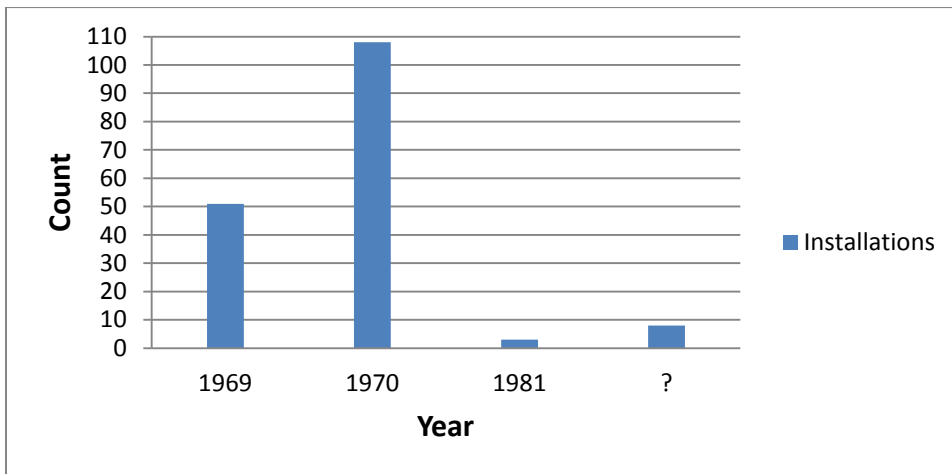


Figure 48: Count of manhole installations before data editing

Table 8: Total count of manholes before data editing

Year	Count
1969	51
1970	108
1981	3
?	8
Grand Total	170

The network system was simplified by the removal of pipes up to 200 mm in diameter, along with the filling of missing data. The total count of manholes then changed considerably, see Figure 49 and Table 9 on next page.

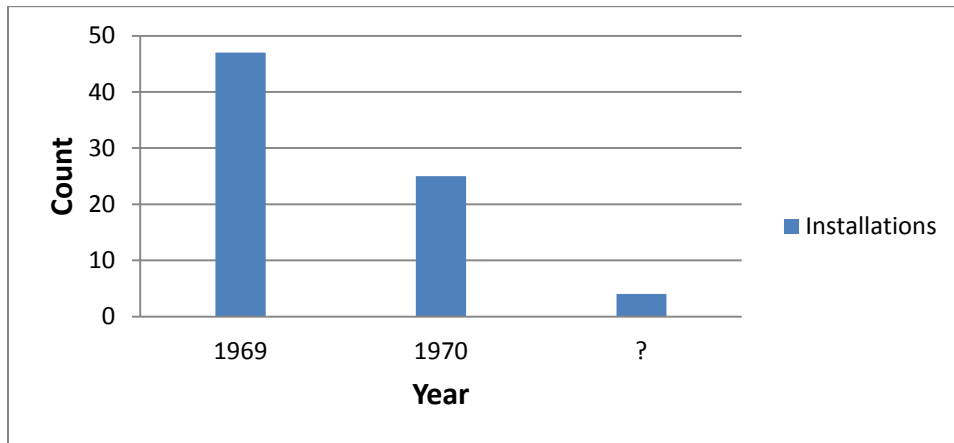


Figure 49: Count of manhole installations after data editing

Table 9: Total count of manholes after data editing

Year	Manholes
1969	47
1970	25
?	4
Grand Total	76

3.2.2 Pipe network

The shape file contained no data telling when the pipes were installed, but it's realistic to assume they were installed at the same time as their connected manholes. As for the manholes with the missing data, it's realistic to assume they were installed at the same time as the residences connected to it.

Most of the pipes are made of reinforced concrete, but some are also made of PVC. The joints between the concrete elements consist of flexible bell and spigot joints including sliding rubber gaskets (Olav Nilssen, 2011).

The table and figure below describes the distribution of the dimensions in the network, before the data was edited.

Table 10: Pipe dimensions and their total lengths before data editing

Dimension mm	Sum length m
110	27
125	89
150	188
200	1038
250	775
300	335
400	601
500	163
800	11
NAN	1453
Grand Total	4680

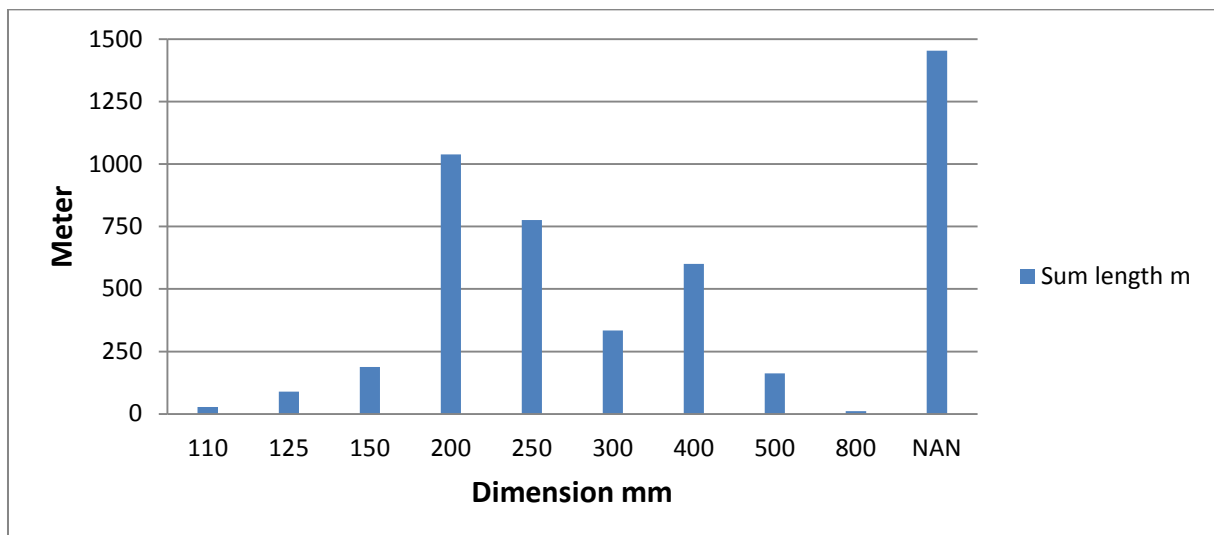


Figure 50: Dimension distribution in the network before data editing

Table 11: Pipe dimensions and their total lengths and volume after data editing

Dimension mm	Sum length m	Volume m3
200	985	31
250	743	36
300	431	31
400	589	74
500	145	29
600	17	5
800	11	6
Grand Total	2922	211

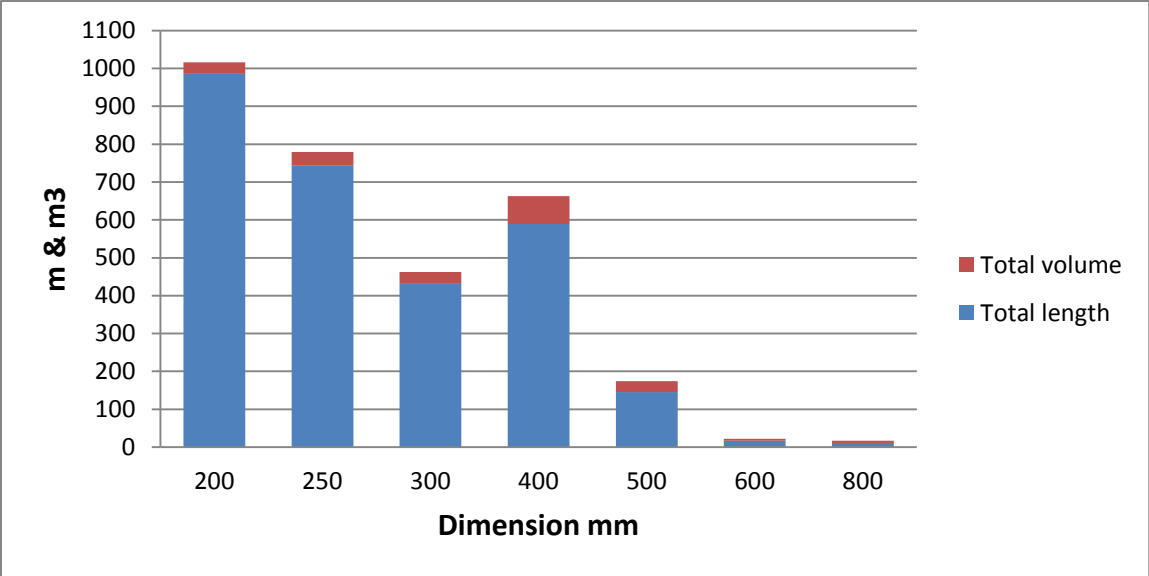


Figure 51: Dimension- and volume distribution in the network after data editing

The pipes are maintained by flushing out the sediments from 1 to 6 times a year, (Olav Nilssen, 2011)

Figure 52 on the next page will display the storm water system as it looked like before data editing.

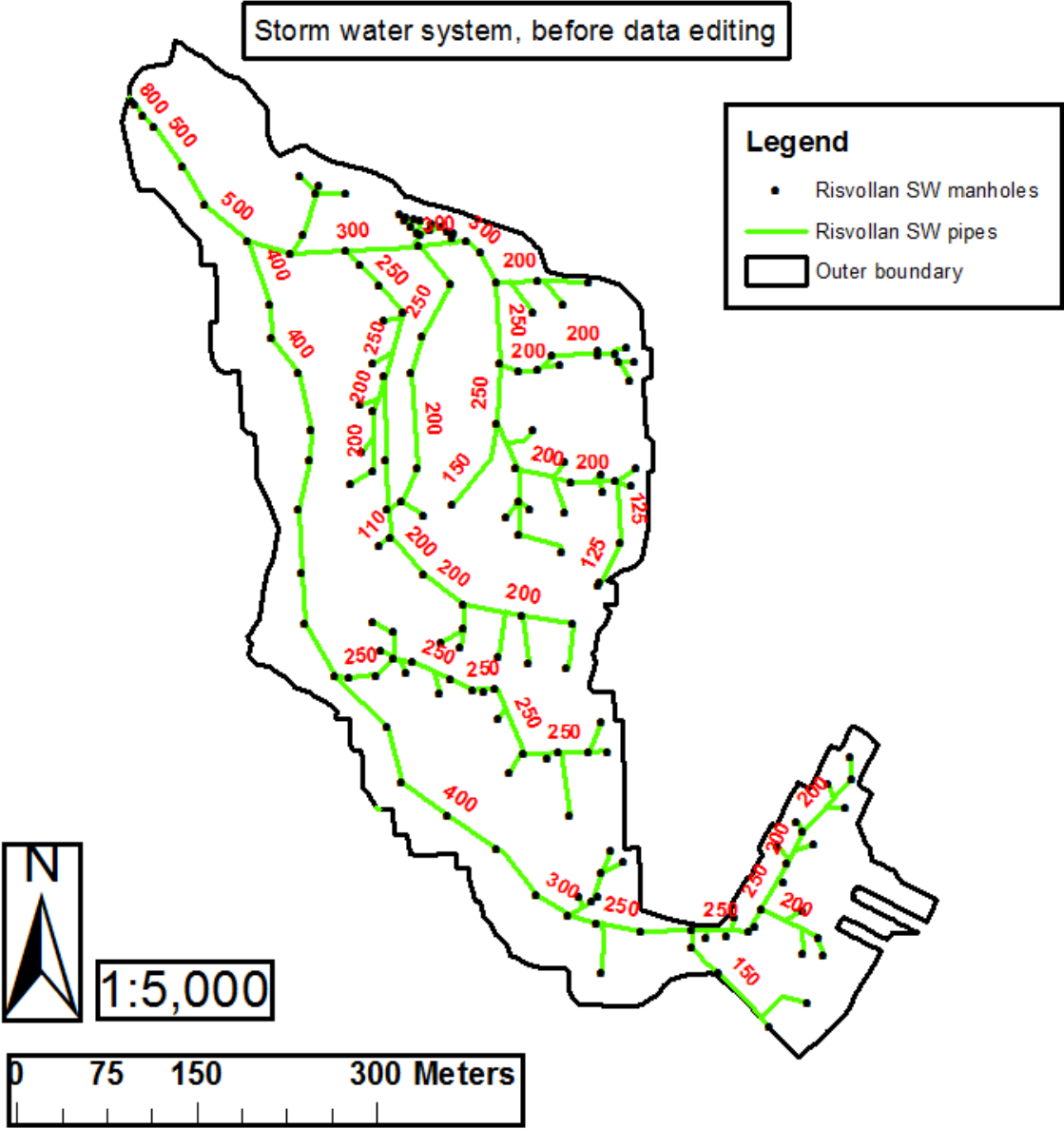


Figure 52: Storm water system before data editing, many dimensions are missing

Figure 53 on the next page will display the storm water system as it looked like after data editing.

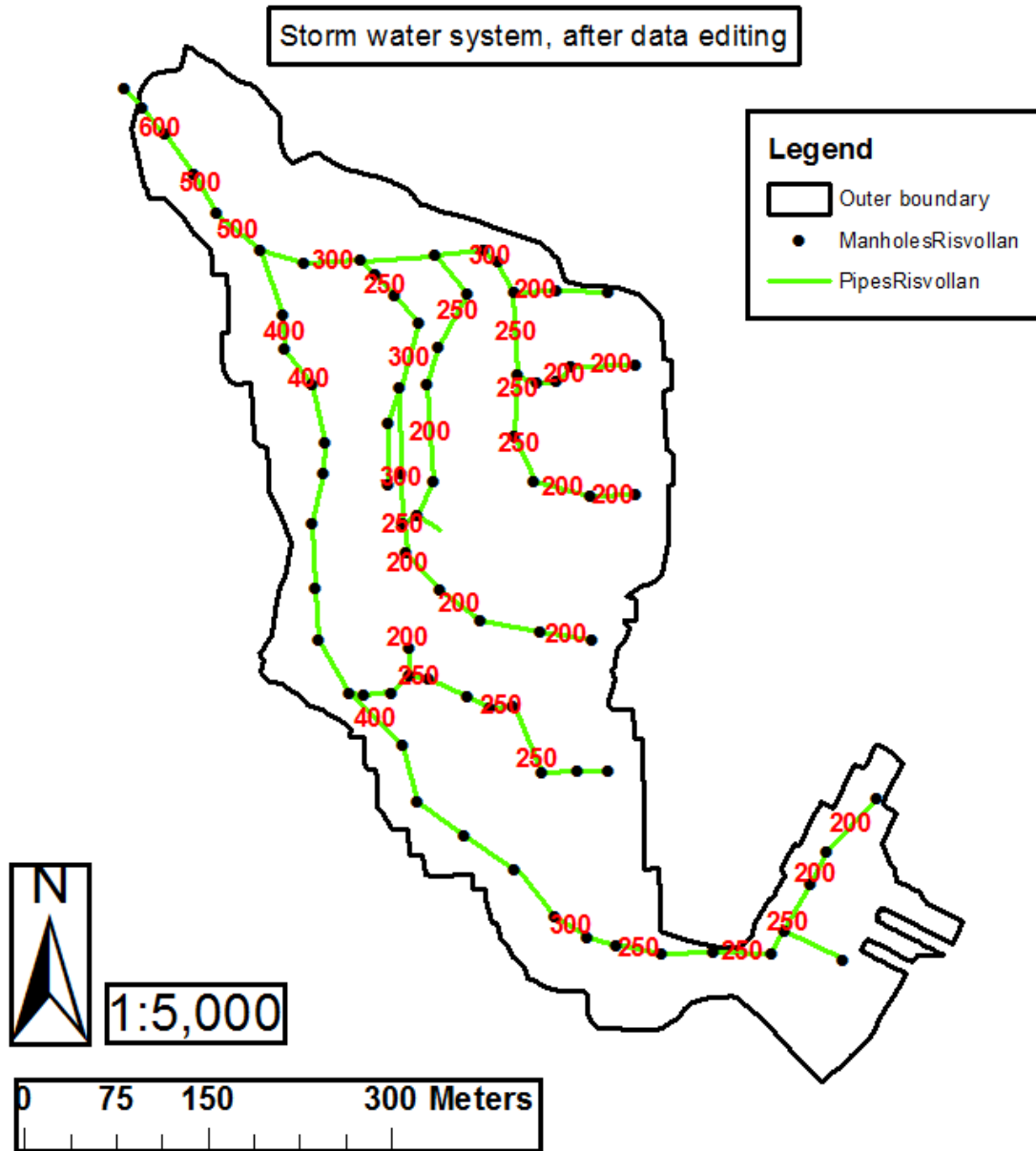


Figure 53: Storm water system after data editing

3.3 Surface characteristics and sub catchments

The analyses of both surface characteristics and sub catchments gave interesting results, especially regarding the count of sub catchments.

3.3.1 Surface characteristics

After digitization of parking lots, driveways and playgrounds, the final surface overview was completed. See Figure 54 and Table 12 to overview the results.

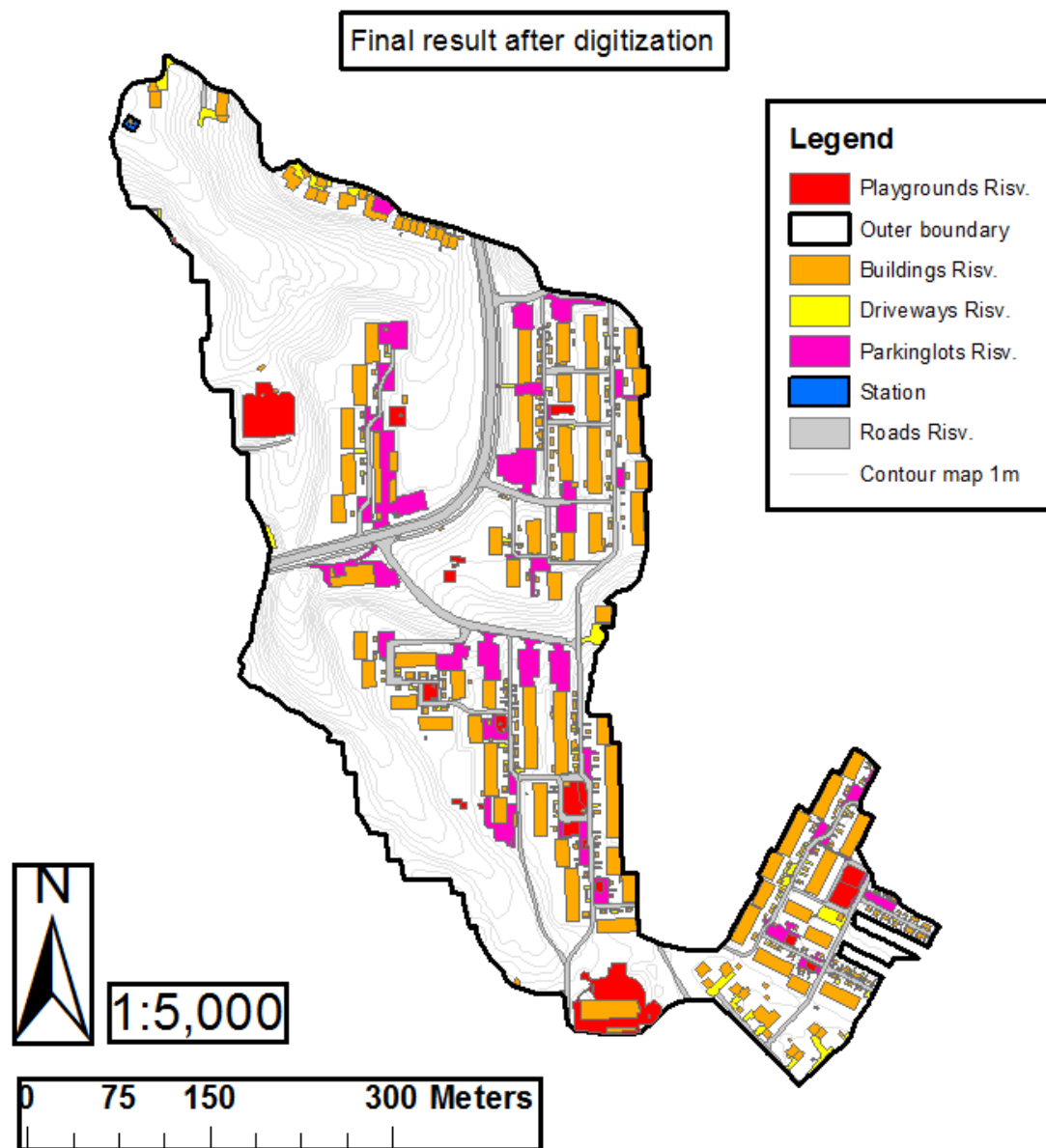


Figure 54: Complete overview of surface characteristics

Table 12: Area distribution and characteristics

Surface	Area dist. (ha)	% dist.	Coefficient C	Imp. area (ha)	% imp. area (ha)
Roofs	2.78	13.06	0.95	2.64	12.40
Roads	1.63	7.67	0.85	1.39	6.52
Parkinglots	1.12	5.26	0.85	0.95	4.47
Driveways	0.34	1.60	0.75	0.26	1.20
Playgrounds	0.58	2.73	0.30	0.17	0.82
Terrain	14.82	69.68	0.25	3.70	17.42
Total	21.27	100		5.41	25.4

The area distribution of the surface characteristics in Table 12 are considered to be valid. The amount of impervious areas was considered to be very uncertain, due to the use of runoff coefficients.

The surfaces were controlled by using the WMS service in ArcMap, see Figure 55 below to view the results.



Figure 55: WMS service used for verification of surface characteristics (polygons made 50% transparent)

Additional analyses

Analyses regarding population distribution in the field and the amount of rooftop units were also conducted, see Figure 56 below. Most of the inhabitants are concentrated in the southeast part, except from a small area in the northeast corner.

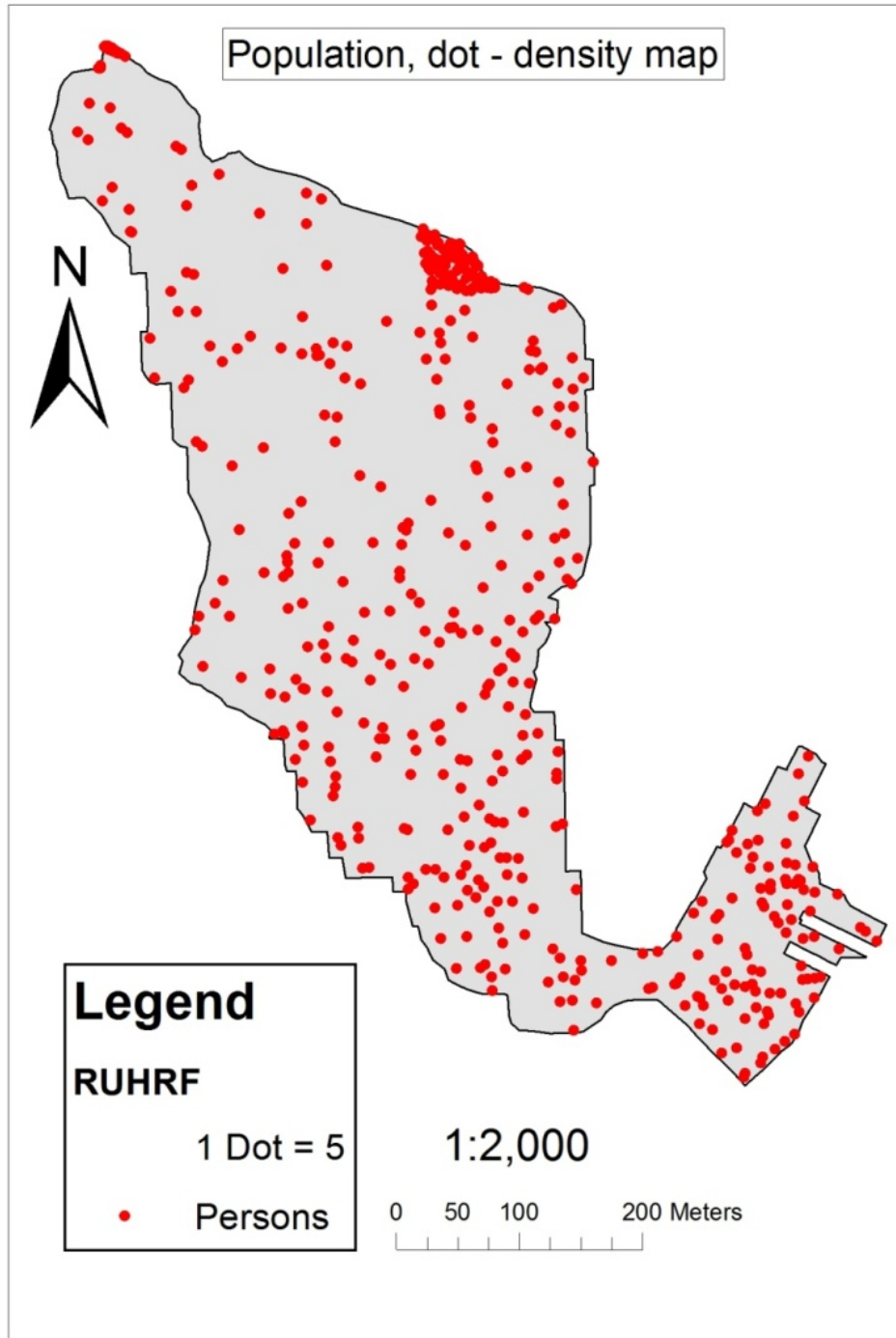


Figure 56: Population distribution in the field (note: scale text error, scale bar is correct)

The total count of roof surfaces in ArcMap was measured to be 351. Total count of surfaces above 40 m² was 95. See figure 57 on the next page to view the statistical results.

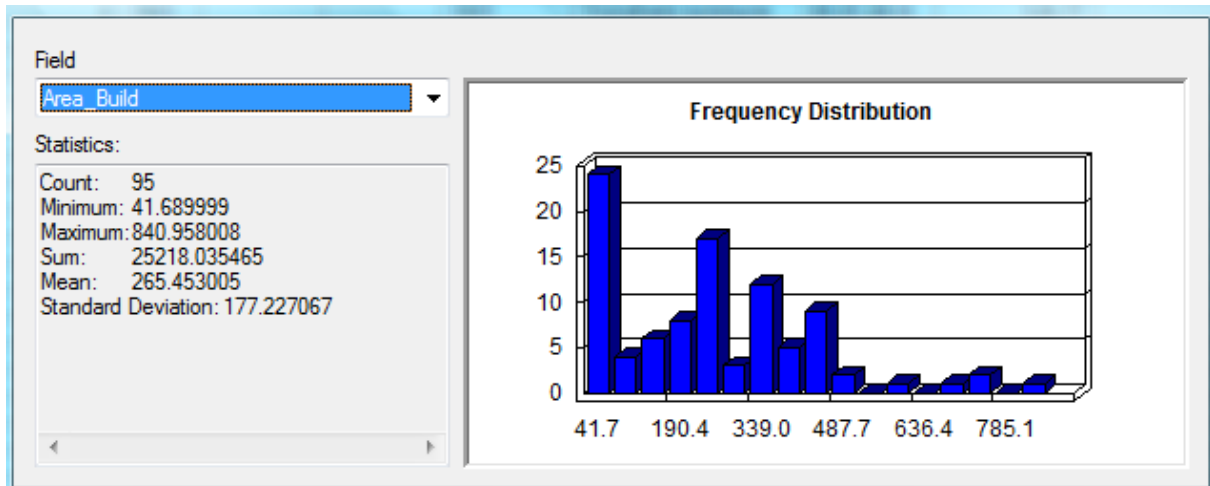


Figure 57: Distribution of rooftops larger than 40 m²

3.3.2 Sub catchments

The sub catchments generated from the watershed analysis were realistic in relation to the terrain formation. However, it did not take into account the storm water system and its connections to the residents. Some of the edges of the sub catchments also “crossed” some of the buildings arbitrarily. In addition, it was necessary to establish new sub catchments for the southeast corner in the field. The generated sub catchments were modified, along with the creation of new sub catchments. When the process was completed, the field consisted of totally 55 sub catchments. This amount exceeded the earlier discussed criteria which were based on a total of 15 – 50 sub catchments. Since all developed surfaces were analyzed, it was assumed that the credibility of these analyses would compensate for the amount of sub catchments. However, it was also mentioned earlier that the function of pervious surfaces has made the determination of runoff coefficients uncertain.

See Figure 58 for illustration of the modification of sub catchments

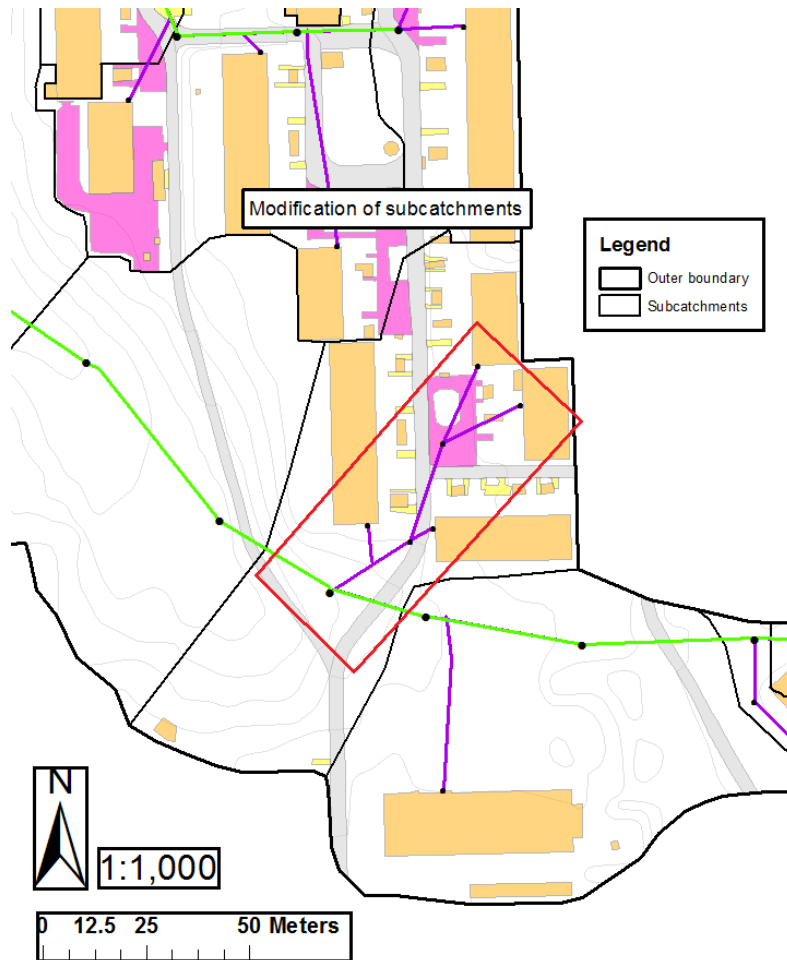


Figure 58: Modifications of sub catchments, connections to the residents were taken into account

As mentioned in chapter 2, associate professor Sveinn T. Thorolfsson and MSc student Stephen Høgeli gave an estimation of a total of 21 sub catchments. Exactly on what basis these estimations are made on is unknown.

Estimations were also given by the Danish Hydraulic Institute (DHI), which generated sub catchments based on Thiessen polygons (Hans Vebjørn Kristoffersen, 2010). Thiessen polygons are made by perpendicular bisectors of the edges of the TIN triangles.

Figure 59 on the next page illustrates the principle of Thiessen polygons. In addition the DHI model of RUHRF is also presented, by Figure 60.

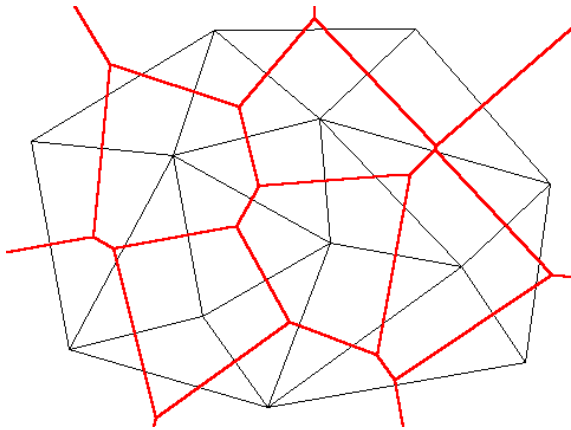


Figure 59: Red Thiessen polygons, TIN – model beneath

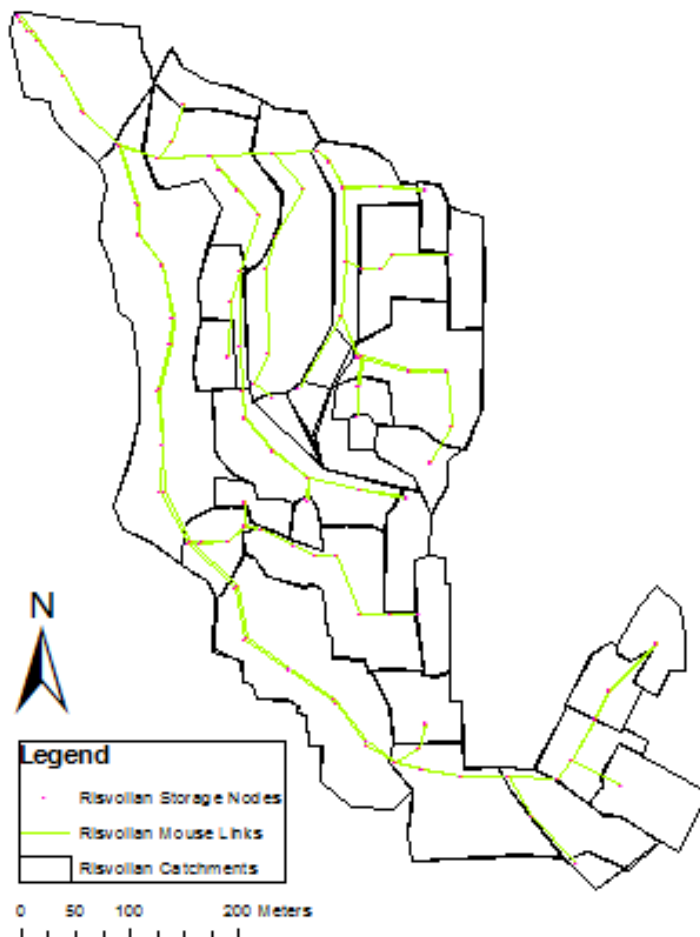


Figure 60: Runoff- and wastewater model of RUHRF, developed by DHI

The model developed by DHI is considered to be very attractive for NTNU students. Especially for those who are planning to write theses about modeling of storm water and or wastewater. Today this model is probably considered to be most accurate one. It is primarily designed for modeling by using the software Mike Urban. The figures 61 and 62 reveal the statistical properties of the sub catchments and the pipe network inside the DHI model.

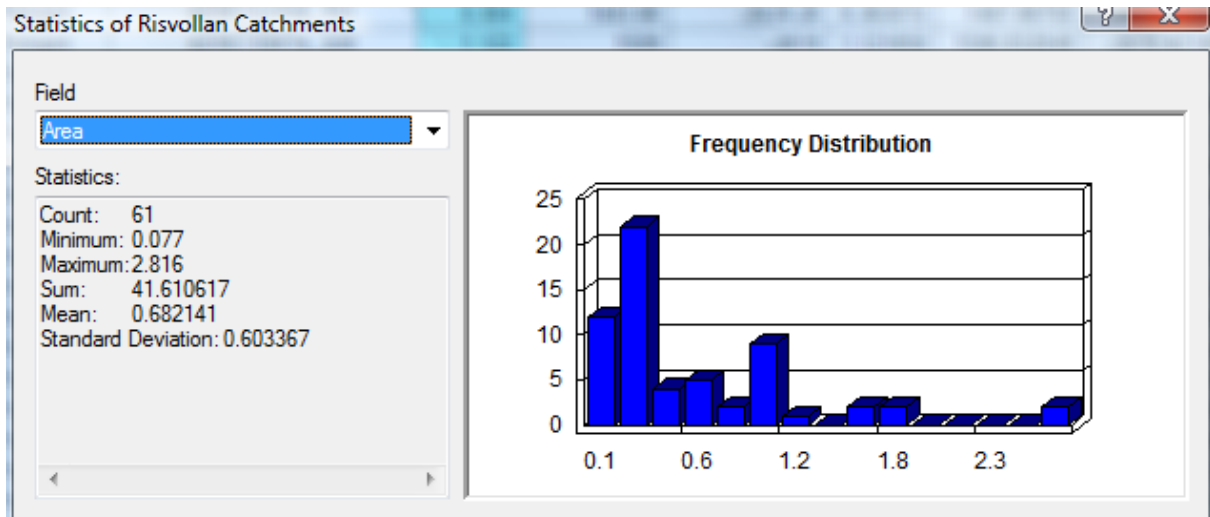


Figure 61: The area distribution of sub catchments, DHI runoff model

The DHI model is divided into 61 sub catchments. Perhaps this result strengthens the thesis's estimation of the total amount of sub catchments.

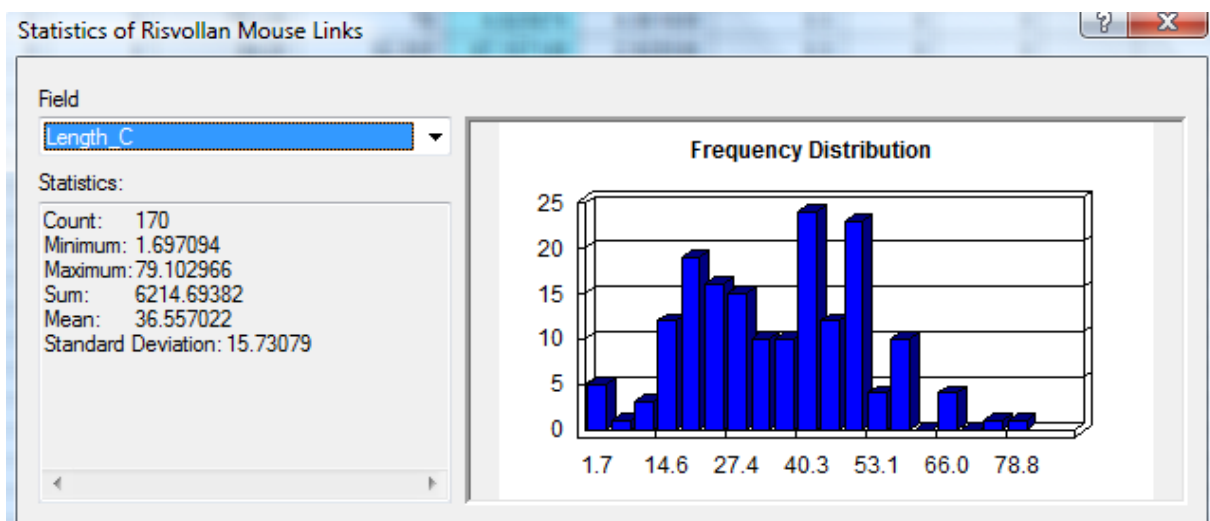


Figure 62: Pipe network statistics, DHI runoff model

After the digitalization- and slope calculations were done, a table and figure were created. See table 13 and figure 63 on next page to view the results.

Table 13: The size and slope of the sub catchments

ID	Area (ha)	Slope %
1	0.33	17.8
2	0.61	23.4
3	0.50	25.3
4	0.31	11.5
5	0.32	17.1
6	0.78	17.1
7	0.24	4.8
8	1.55	7.8
9	1.02	10.2
10	0.32	3.7
11	0.89	13.1
12	0.68	2.2
13	0.31	2.1
14	0.58	2.5
15	0.43	3.0
16	0.66	3.9
17	0.68	7.2
18	0.53	2.5
19	0.63	10.0
20	0.27	1.8
21	0.20	8.7
22	0.34	3.4
23	0.49	9.1
24	0.43	13.6
25	0.35	9.9
26	0.44	7.4
27	0.28	1.5
28	0.26	10.3
29	0.17	4.1
30	0.23	4.9
31	0.33	17.6
32	0.29	10.6
33	0.18	5.3
34	0.18	9.2
35	0.11	7.1
36	0.22	18.8
37	0.17	15.5
38	0.17	26.4
39	0.16	4.4
40	0.26	2.2
41	0.14	4.3
42	0.08	0.5
43	0.22	1.8
44	0.21	5.0
45	0.10	4.0
46	0.13	0.8
47	0.21	9.3
48	0.23	3.6
49	0.50	11.7
50	0.40	22.7
51	0.37	25.9
52	0.61	8.7
53	0.58	8.6
54	0.10	3.8
55	0.49	25.9
Σ	21.27	10.1

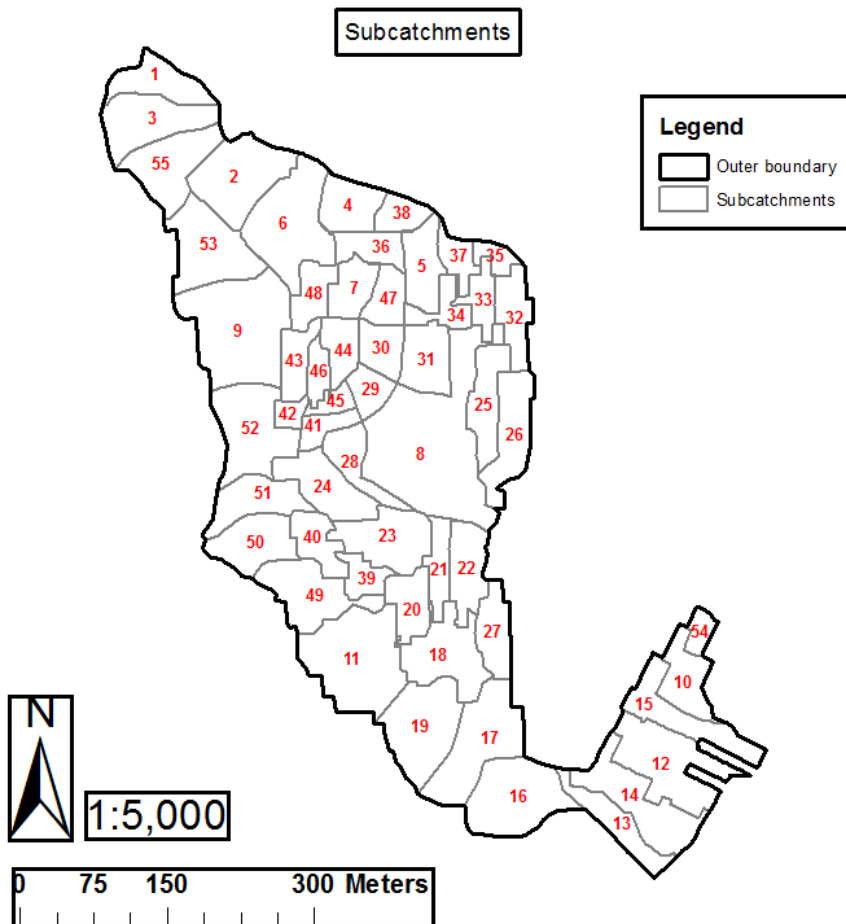


Figure 63: Location of sub catchments

Statistical operations of the sub catchments were also performed, see Figure 64 below.

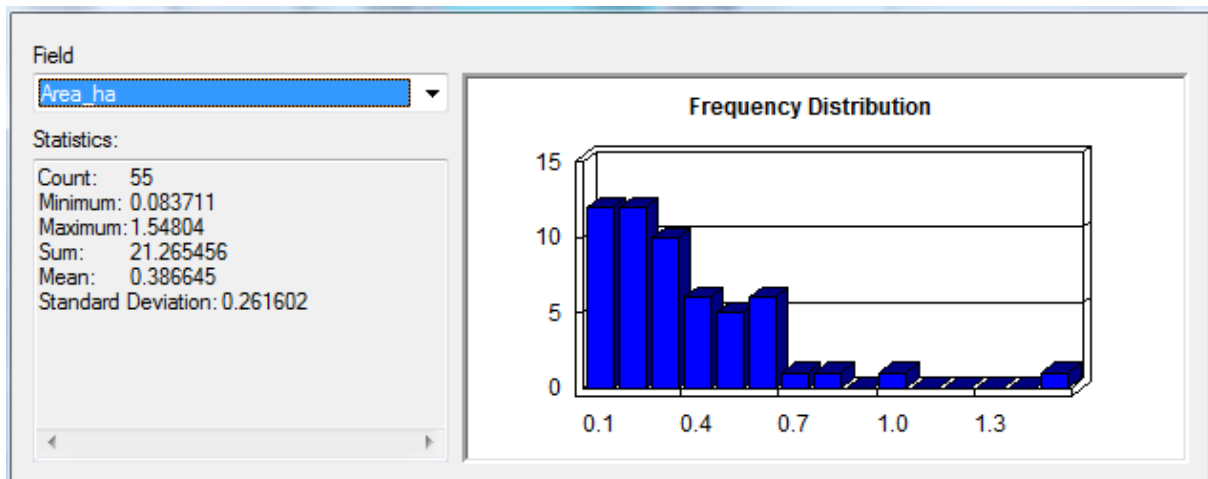


Figure 64: Area distribution of the sub catchments

The average slope is displayed at the bottom of Table 13. The calculation of it was based on the sub catchments individual size in relation to the field's total size. The calculation of average slope within each sub catchment was performed by generation of length profiles.

Three sub catchments were recently developed during late summer and autumn 2011. As mentioned in chapter 2, 27 new apartments were constructed. Another three sub catchments are about to be developed as well, see figure 65 below.

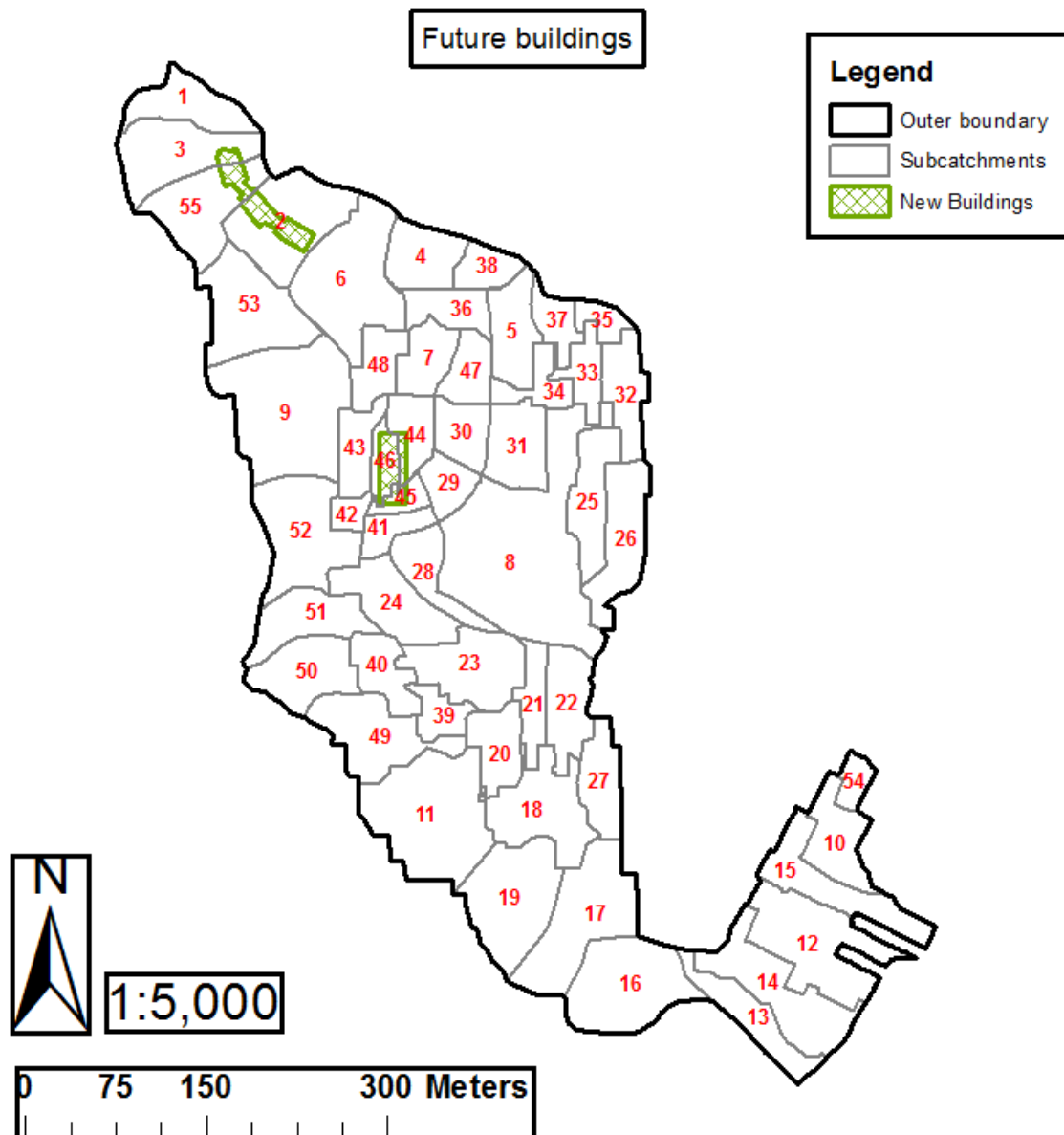


Figure 65: Future buildings in sub catchment 2, 3, 44, 45, 46 and 55.

The replacements of both terrain- and past developed areas were calculated, see Table 14 below. The development sub catchments 2, 3 and 55 are already finished today. See Figure 66 to view the actual construction site.



Figure 66: Construction of 27 new apartments, date taken: 23.08.2011

Table 14: Replacements of terrain- and past developed areas

Sub ID	Sub area m2	New buildings m2	Initial urban areas m2	Final urban areas m2	Initial %	Final %	Increase %
2	6148	1010	874	1884	14	31	16
3	4964	203	109	311	2	6	4
44	2103	234	228	461	11	22	11
45	985	235	572	725	58	74	16
46	1330	855	1071	1157	80	87	6
55	4926	452	53	505	1	10	9

After creation and modification of sub catchments, the spatial model in ArcScene was finally completed. See Figure 67 next page to view the model.



Figure 67: Final spatial model in ArcScene

The spatial model shows that the field is presented in a realistic way.

3.4 RUHS Instrumentation

The RUHS along with its instruments are located within a 95 m² fenced area, and the building itself is about 10 m² large. See Figure 68 below to view the location.



Figure 68: Picture of RUHS

In order to completely understand the composition of new and old instruments available today, a table was created.

Table 15: List of all available instruments and installations (new and old)

Instruments									
Precipitation	Temperature	Humidity	Wind speed	Wind direction	Radiation	Ground temp.	Stormwater	Wastewater	Snow melt
Geonor	Vaisala HMP45	Vaisala HMP45	Young	Young	Klipp & Zonen	Campbell 107	Ultrasonic	Stillingwell	Pressure sensor
Lambrech	Thermometer						Stillingwell	Paper roll	Ballcock
Plumatic	Temp. Sensor						Meter line	PB - flume	Snow lysimeter
							Meter stick		
							Paper roll		
							V - notch weir		

The most important instruments and installations related to this thesis will be further described. The instruments and installations are as followed:

1. Geonor gauge (instrument)
2. Lambrecht gauge (instrument)
3. Plumatic gauge (instrument)
4. V – notch weir (permanently mechanical installation)

3.4.1 Geonor

The Geonor gauge was installed early may in 2011. It measures precipitation by collecting- and weighing it in a bucket. The sensor records the weight every second. The increase of weight gives the basis for calculating the expected contribution. The instruments total capacity is 1000 mm, more or less enough to measure the entire annual precipitation. However, the bucket should be checked and emptied frequently due to debris (leafs and dusts) which can accumulate over time. During the winter months a mixture of antifreeze liquid and methylated spirits are necessary to add into the bucket. If the temperature is colder than – 15 degrees Celsius, a mixture of 1.5 liters antifreeze liquid and 2.0 liters of methylated spirits is necessary. To avoid evaporation during the summer, 0.4 liter thin oil has to be added. The oil should be replaced once a year.

The instrument is connected to NTNU's CR1000 logger, which generates resulting files on both hour and two minute intervals. In the two minute file, the average bucket weight in mm for every last minute is registered. In the hour file, the increase of precipitation in mm for every last hour is registered, (Tone Muthanna and Helge Aarøen, 2011).

The gauge replaced an old pluviograph which has been out of service for a long time.



Figure 69: Geonor T200 – B gauge



Figure 70: Geonor T200 – B gauge opened



Figure 71: The old pluviograph

For more information about the Geonor gauge, see Appendix CD.6.

3.4.2 Lambrecht

The Lambrecht gauge is a German produced pluviograph, which is based on the tipping bucket principle. The volume per tip is equivalent to 0.1 mm. Every tip is registered by an electrical impulse, recorded by the loggers. The instrument is equipped with thermostatically heater, which enables it to measure precipitation at temperatures down to -20 degrees Celsius. The maximum capacity is up to 75 tips per minute, or 7.5 mm per minute. Since the tipping bucket's volume equals to 0.1 mm, it is possible to develop a formula for conversion into intensity (l/s*ha):

$$i \text{ (l/s)} = ((0,1 \text{ mm} * 10000 \text{ m}^2 * 1000 \text{ l/m}^3) / (1000 \text{ mm/ m} * 10000 \text{ m}^2 * 120\text{s})) * n$$

Where n = the count of tip per every second minute

By converting from 10000 m² to ha, the formula can be simplified by rewriting it:

$$i \text{ (l/s*ha)} = [1000\text{l}/1\text{ha} * 120 \text{ s}] * n = 8.333 * n$$

(Thorolfsson, S.T., & Høgeli, S.A. 1994)

The instrument is connected to both CR1000 and NVE's Sutron logger. As for the Geonor gauge, CR1000 logger generates files on both hour and two minute intervals for Lambrecht. Both of these files record the increase in mm with respect to their belonging intervals (increase each hour, and every second minute). (Tone Muthanna and Helge Aarøen, 2011).



Figure 72: Associate Professor Sveinn T. Thorolfsson explains about the Lambrecht gauge



Figure 73: The top of the Lambrecht gauge

Sometimes the tipping bucket can get stuck, or it jumps off either one or both supports on each side. Regularly inspections at least once a month is needed to control this. It is also necessary to check if debris has accumulated on top of the instrument, (Harald Viken, 2011).

3.4.3 Plumatic

The Plumatic gauge follows the same principle as the Lambrecht gauge. Only difference is that it is not equipped with thermostatically heater, and its tipping bucket equals a volume of 0.2 mm. The gauge is only operative in temperatures from 0 – 50 degrees Celsius, which means it's temporary out of service before May and after October. The cooperation between DNMI and Kongsberg weapons factory resulted in the development of this instrument. Its maximal capacity is 35 tips per minute, or 7.0 mm per minute. The instrument is considered to be very stable, since it rarely ceases to work in its respectable period of measurement. As for the Lambrecht gauge, it is possible to convert the amount of precipitation into intensity. The formula is virtually the same:

$$i \text{ (l/s)} = ((0,2 \text{ mm} * 10000 \text{ m}^2 * 1000 \text{ l/m}^3) / (1000 \text{ mm/ m} * 10000 \text{ m}^2 * 120\text{s})) * n$$

Where n = the count of tipp per every second minute

By converting from 10000 m² to ha, the formula can be simplified by rewriting it:

$$i \text{ (l/s*ha)} = [2000\text{l}/1\text{ha} * 120 \text{ s}] * n = 16.667 * n$$

(Thorolfsson, S.T., & Høgeli, S.A. 1994)



Figure 74: The Plumatic gauge



Figure 75: The top of the Plumatic gauge

Regularly inspections at least once a month is needed to check the instrument for debris.

3.4.4 V – notch weir

The V – notch weir was installed by Trondheim Municipality, and was ready for use in 1986. The purpose of its function is to continuously create a relationship between the water surface level and the flow rate. It is then possible to measure the flow at any time with different instruments.

Relationship: $Q \text{ (l/s)} = f(H)$

Upstream the sharp crest there is a rectangular basin, which function is to establish stable flow rates before the water enters the crest. In theory this means that subcritical conditions must be established upstream the crest (Froude number < 1.0), and the transition between the subcritical and supercritical conditions has to be located directly above the crest (Froude number $= 1.0$). To optimize these conditions, the 600 mm concrete pipe upstream the station was replaced by an 800 mm concrete pipe. About 6 meters of length were replaced. The basin itself is only 2 meters long, theoretically 0.3 – 0.9 meter to short, (Appendix C).



Figure 76: The V – notch weir



Figure 77: The V – notch weir from another angle

The notch angle is 100.7° and the total height is 57,6 cm. By using the Kindsvater – Shen formula, the total capacity was calculated to be approximately 420 l/s. The result was heavily depended of the choice of the contraction coefficient C_e (0.58), which meant that the result contained some uncertainty. In addition, the 17 cm gap between the upper crest and the concrete floor was excluded from the calculation. See Figure 78 to view the sketch of the V – notch weir.

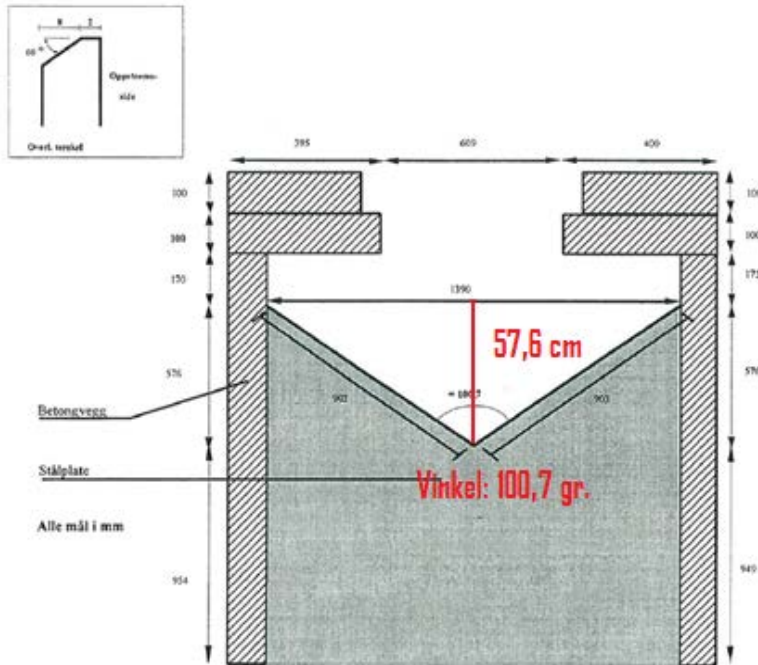


Figure 78: V – notch weir sketch, theoretical maximum height calculated from the angle (Thorolfsson, S.T., & Høgeli, S.A. 1994)

Kindsvater – Shen formula:

$$Q = \frac{8}{15} * C_e * \tan \frac{\Phi}{2} * \sqrt{2g} * H^{\frac{5}{2}}$$

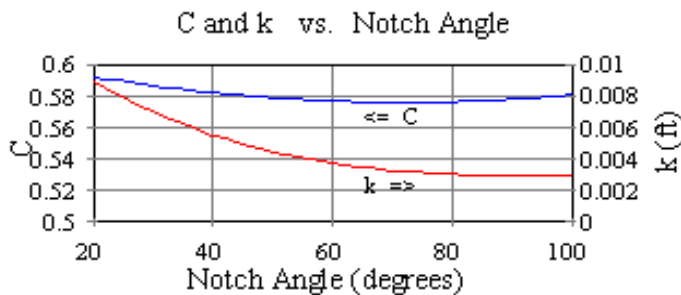


Figure 79: Contraction coefficients in relation to the angle. The “k” coefficient is related to a rewritten formula, which takes into account American units.

- C_e = Contraction coefficient (discharge coefficient)
- Φ = Notch angle (degrees)
- H = Head (m)

Compared with an empirical diagram developed by NVE and NTNU, the calculated result seemed to be realistic, see figure 80 below. However, the gap above the crest increases the capacity up to 900 l/s (Thorolfsson, S.T., & Høgeli, S.A. 1994)

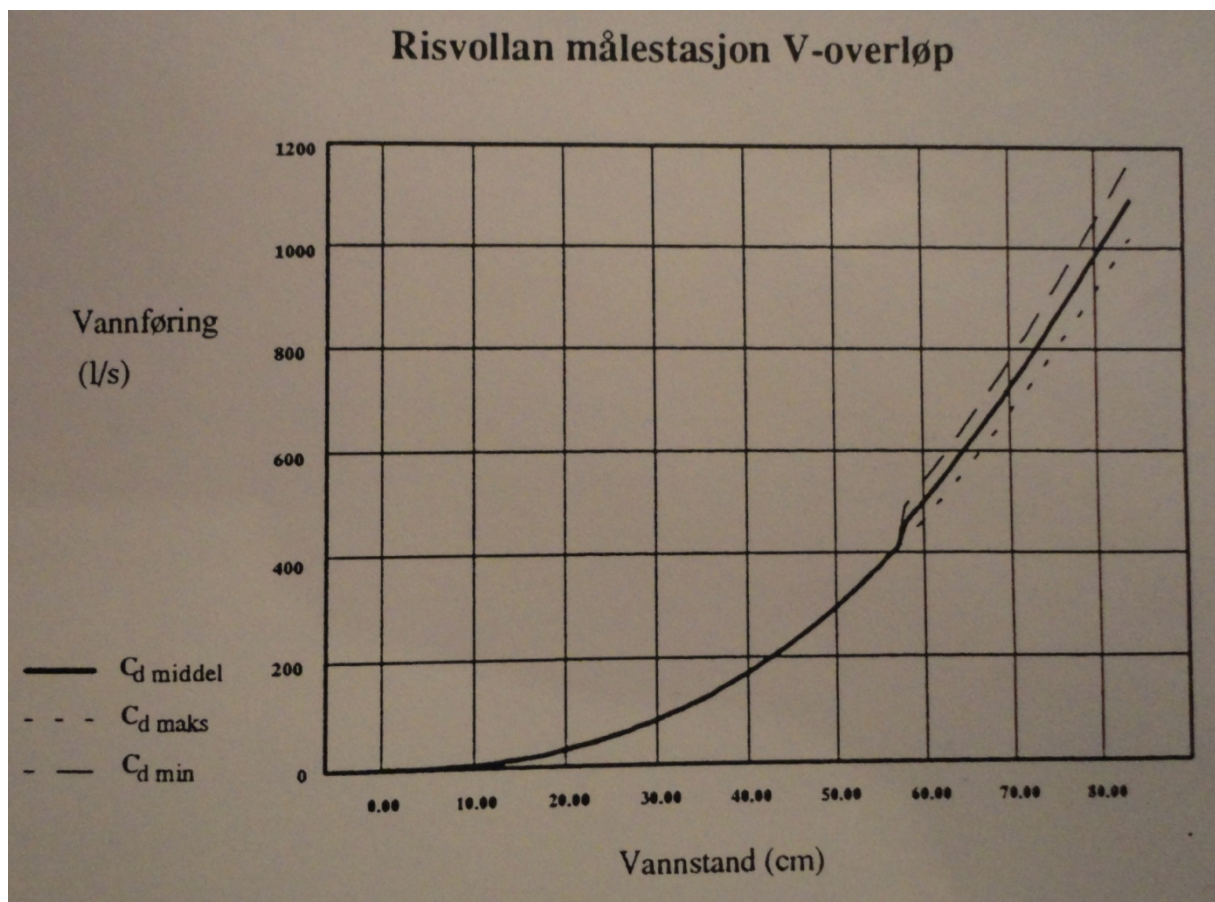


Figure 80: Empirical diagram developed by NVE and NTNU

NVE has also developed a table that focus on the consequences of failure during the registration of water level.

Table 16: Percentage of deviation based on water level

V-notch weir (cm)	Probable flow (l/s)	Deviation (+ cm)	Measured flow (l/s)	Error (%)	Volume error (m ³ /day)
5	1.4	0.5	1.7	21	32
5	1.4	1.0	2.2	36	68
10	7.7	0.5	8.7	11	85
20	42.8	0.5	45.5	6	234
30	117	0.5	122	4	425
40	240	0.5	247	3	650
40	240	1.0	255	6	1312
60	656	0.5	671	2	1186

The results in Table 16 are based on V – notch weir with crest angle equal to 120°

In addition, a combination of failure between the stilling well, the signal amplifier, the crest, the counter and the basin has been assessed by associate professor Sveinn T. Thorolfsson. It was assessed that the stilling well contained 2% error, the crest 5%, the signal amplifier 2%, the counter 2% and the basin 5% error. The combination of these failures would finally result in 8% error, but this is related to the old system. However, it could very well be an indication of the combination of failure also today.

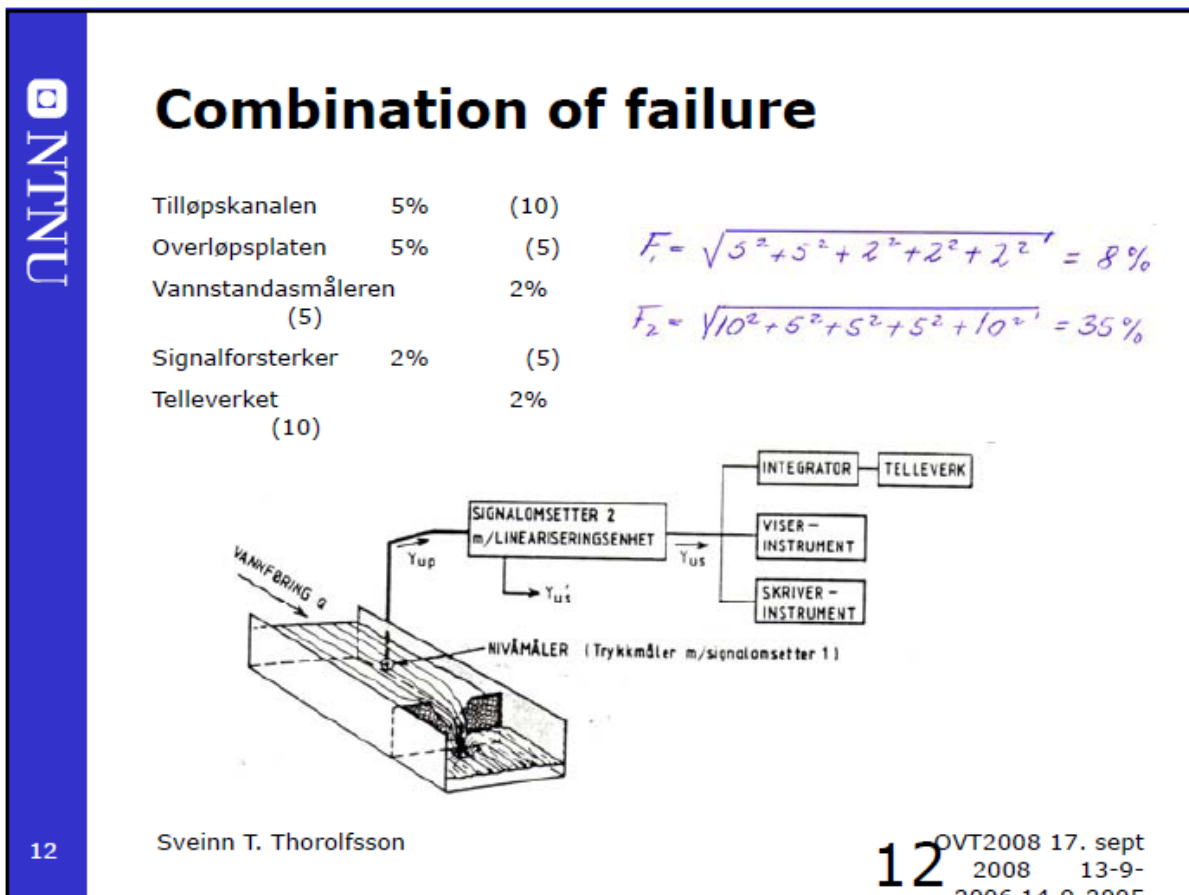


Figure 81: Assessment of the combination of failures

Earlier, a pressure sensor at the bottom of the basin measured the depth. Basically its parameter was based on measuring the pressure $P = \gamma H = \rho g H = 1000 \text{ kg/m}^3 \cdot 9.81 \text{ m/s}^2 \cdot H(\text{level m})$, (Teklu, 2010).

Aanderaa was the fabrication of the sensor. The instrument was eventually replaced by the ultrasonic sensor. The mechanical stilling well has been in operation almost from the beginning after the installation of the V – notch weir. Shuttle is the fabrication of the ultrasonic sensor. It displays the flow rate every 5 seconds. Both stilling well and the sensor transmit signals to the Sutron- and the Shuttle logger. NVE collect and stores the data. See Appendix CD.6 for more information about these instruments.

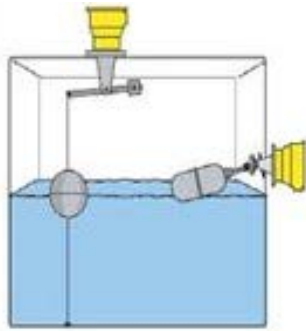


Figure 82: Stilling well

NVE register the storm water flow rate, and is able to provide with data files containing 1 minute intervals. In addition they also provide day values for the last two months, which can be downloaded for free from their website.

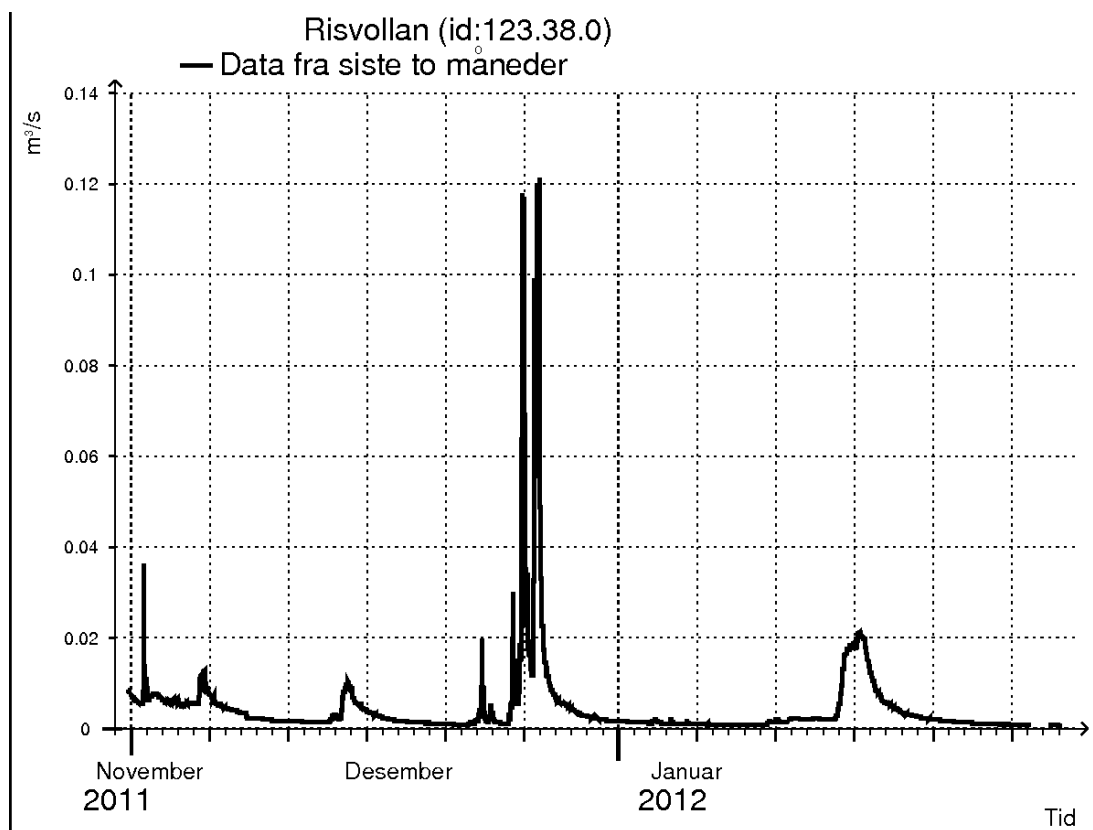


Figure 83: Runoff diagram downloaded from NVE's website



Figure 84: Shuttle logger



Figure 85: Shuttle ultrasonic sensor

In addition to the sensor and the stilling well, manual readings are possible. A wire with a marker attached on it is constantly moving up and down depending of the flow rate. Parallel to it, a line with mm scale measures the attached marker. Also a meter stick with cm scale is attached to the wall inside the basin.



Figure 86: Meter stick



Figure 87: Wire and line with scale

In summer and autumn 2007 the station experienced flooding due to overloaded system downstream it. The water literally poured out the front door, and the flow rate was estimated to be as much as 1300 – 1400 l/s. According to senior engineer Olav Nilssen employed at Trondheim Municipality, such events are highly unlikely to be repeated after the improvement of the network systems downstream the station. As earlier mentioned a combined system exists there, and it is about to be reconstructed into a separate system. The storm water part will consist of pipes that lead the water downstream to an upcoming improved creek named Fredlybekken (Birgitte Johannessen, 2011). The creek leads the water further into the river Nidelva, see Figure 88 next page.

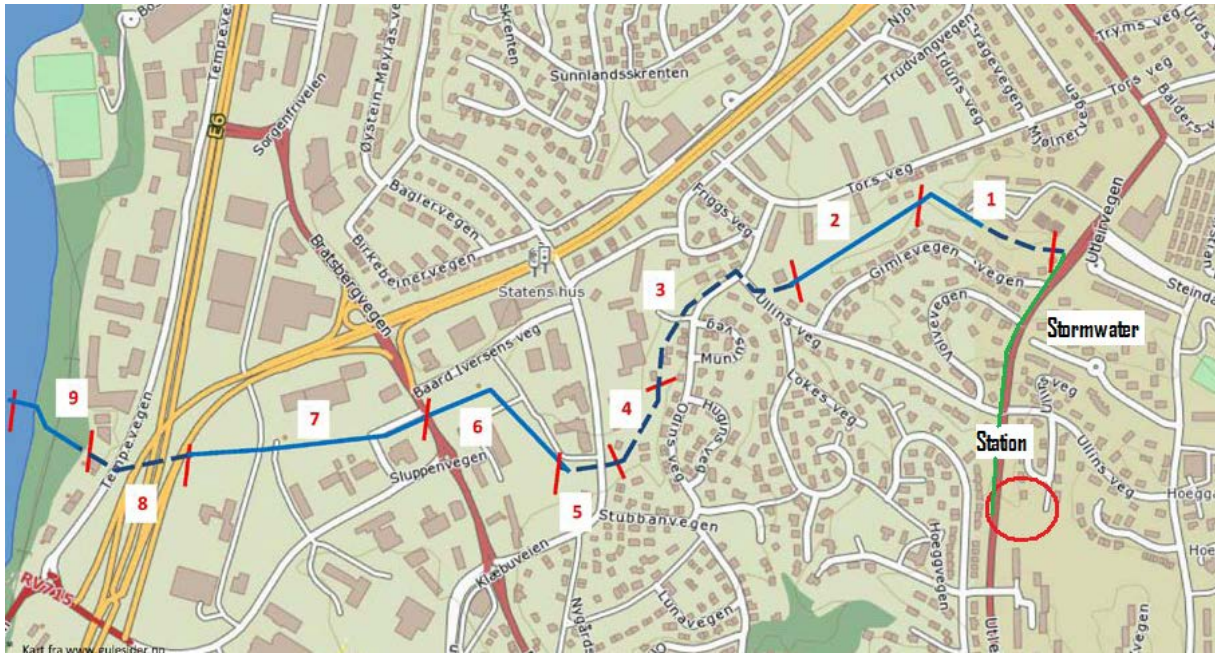


Figure 88: The creek Fredlybekken is marked blue, the connection with RUHRF is marked green

Below, some advantages and disadvantages are listed:

Advantages:

1. V –notch weir are able to operate during all seasons.
2. It gives reliable and good data, especially in ideal conditions (Protected against frost events, normal discharges and no sediments).
3. Usually cheap to construct and install.

Disadvantages:

1. The amount of sediments (floating and sinking) will over time increase inside the basin (disturbing the discharge by the crest and eventually plug the connection pipe into the stilling well). The basin had to be emptied once during the construction period of the new apartments. The sediment layer at the bottom was almost 30 cm thick in some parts of the basin.
2. Biofilm growth at the bottom of the V – crest.
3. Cannot handle extreme rain events, large discharges can easy create flooding.

For more information about the V – notch weir, see Appendix C.

3.4.5 Other instruments

1. Temperature and air humidity (Vaisala HMP45)

The instrument measures the temperature in Celsius degrees and the relative humidity in percentages.

Relative humidity is defined by this formula:

$$\phi = \frac{e_w}{e^*_w} \times 100\%$$

where:

e_w = Ratio of partial pressure of water vapor (H₂O)

e^*_w = Saturated vapor pressure of water at a prescribed temperature

The instrument transmits data to the CR1000 logger, data files with hour and 2 minutes intervals are generated (Tone Muthanna and Helge Aarøen, 2011)



Figure 89: Temperature- and humidity sensor

2. Temperature sensor

The sensor transmits data to the Sutron logger. In addition, another sensor is also placed at the rain garden outside the catchment. Both data sets are collected and stored by NVE.

3. Thermometer

An ordinary thermometer that measures the temperature in Celsius degrees is available for manual readings.

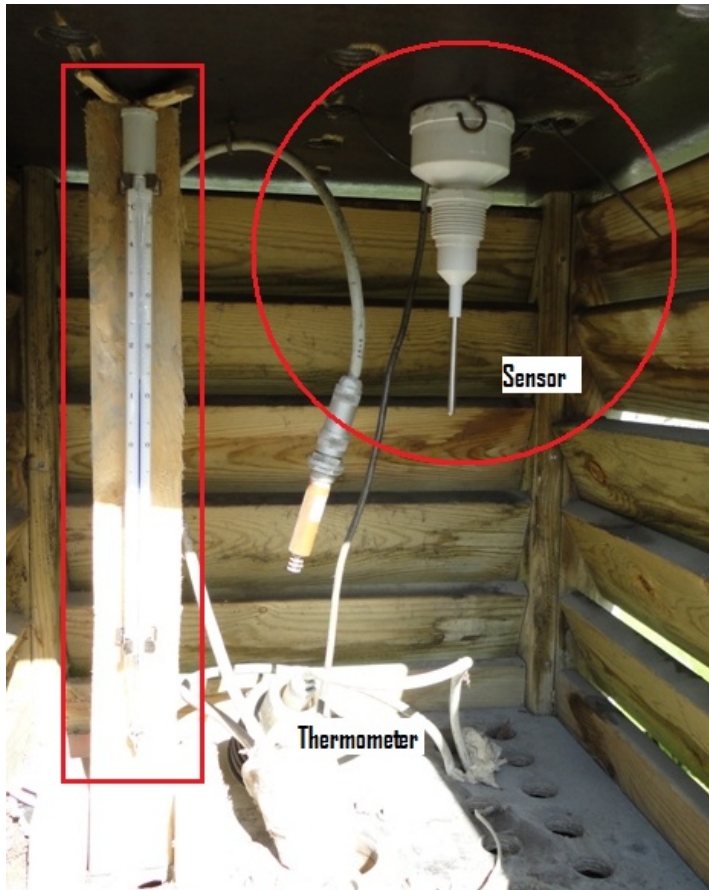


Figure 90: Thermometer and sensor

4. Wind speed and wind direction (R.M. Young 85004, SDI - 12)

The instrument measures the wind speed (m/s) and the direction (degrees) every second, and transmits the data to the CR1000 logger. In addition to the files containing hour and 2 minutes intervals, a further two files with 1 minute and 10 minute intervals are generated. Parameters such as average and maximum speed along with change of direction are included into the dataset.

The range of wind direction is 360 degrees, where 0 represents north. The logger calculates the direction (θ_1) by using this routine:

$$\theta_1 = \arctan (U_x/U_y)$$

$$\text{Where: } U_x = (\sum \sin \theta_i)/720 \text{ and } U_y = (\sum \cos \theta_i)/720$$

(θ_i is the representative direction by each of the last 3600 registrations for the last hour)

(Tone Muthanna and Helge Aarøen, 2011)



Figure 91: Young instrument for measurement of wind speed and wind direction

5. Solar radiation measured by Klipp & Zonen, CMP 11

Short wave radiation (300 – 2800 nm) measured every second, and transmits the data to the CR1000 logger. Data files generated contains hour and 2 minutes intervals.

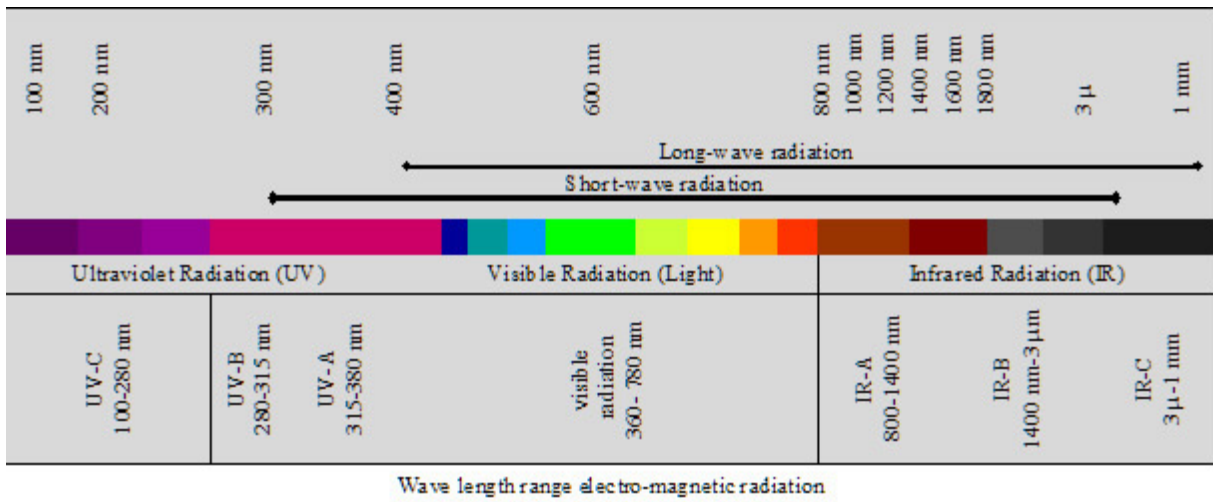


Figure 92: Definition of different types of radiation



Figure 93: The short wave instrument

(Tone Muthanna and Helge Aarøen, 2011)

6. Ground temperature, Campbell 107

Campbell 107 is a sensor that measures the ground temperature in Celsius degrees, and transmits the data to the CR1000 logger. The generated data files contain hour and 2 minutes intervals. The sensor is buried approximately 15 cm beneath the surface, (Tone Muthanna and Helge Aarøen, 2011).



Figure 94: Location of ground temperature sensor

7. PB – flume

The PB – flume is not directly considered to be an instrument, but more like an installation. It works by the same principle as the V – notch weir, to create subcritical conditions in the inflow basin before the wastewater reaches a critical point. As mentioned in previous sub chapter, a relationship between the flow rate and the water level is then established. The uncertainty in the flow measurements is considered to be between $\pm 5 - 10\%$. NVE collects and stores the data sets, (Thorolfsson, S.T., & Høgeli, S.A. 1994).



Figure 95: The PB – flume

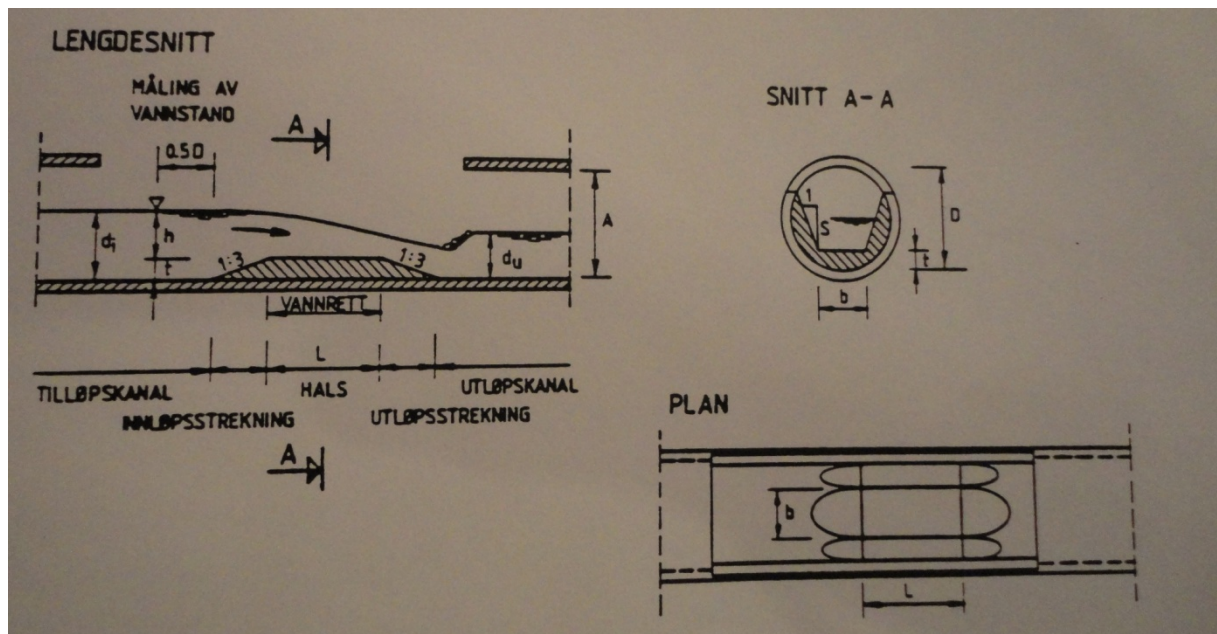


Figure 96: Principle sketch of the PB – flume

8. Snow lysimeter

The snow lysimeter is a rectangular container that collects the snow before it melts. A pipe connects the bottom of the container to another container inside the station. The registration of snowmelt amount is performed by a pressure sensor and a ballcock instrument. The ballcock works by the same principle as the stilling well. The pressure sensor registers the water level and transmits the data to the Sutron logger. When the logger registers too much pressure, a pump is activated so the container can be emptied automatically. In addition, a scale (mm) is attached to the container so that it's possible to perform manual readings, (Thorolfsson, S.T., & Høgeli, S.A. 1994).

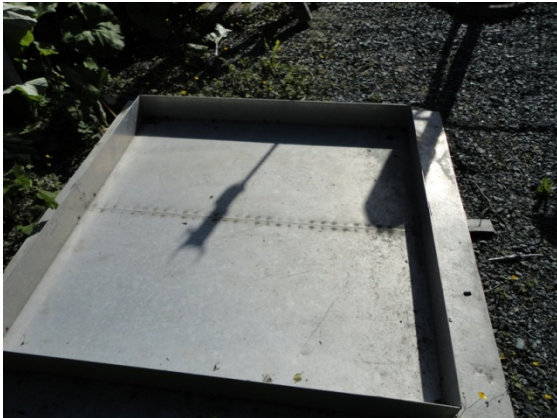


Figure 97: Snow lysimeter



Figure 98: The snowmelt container

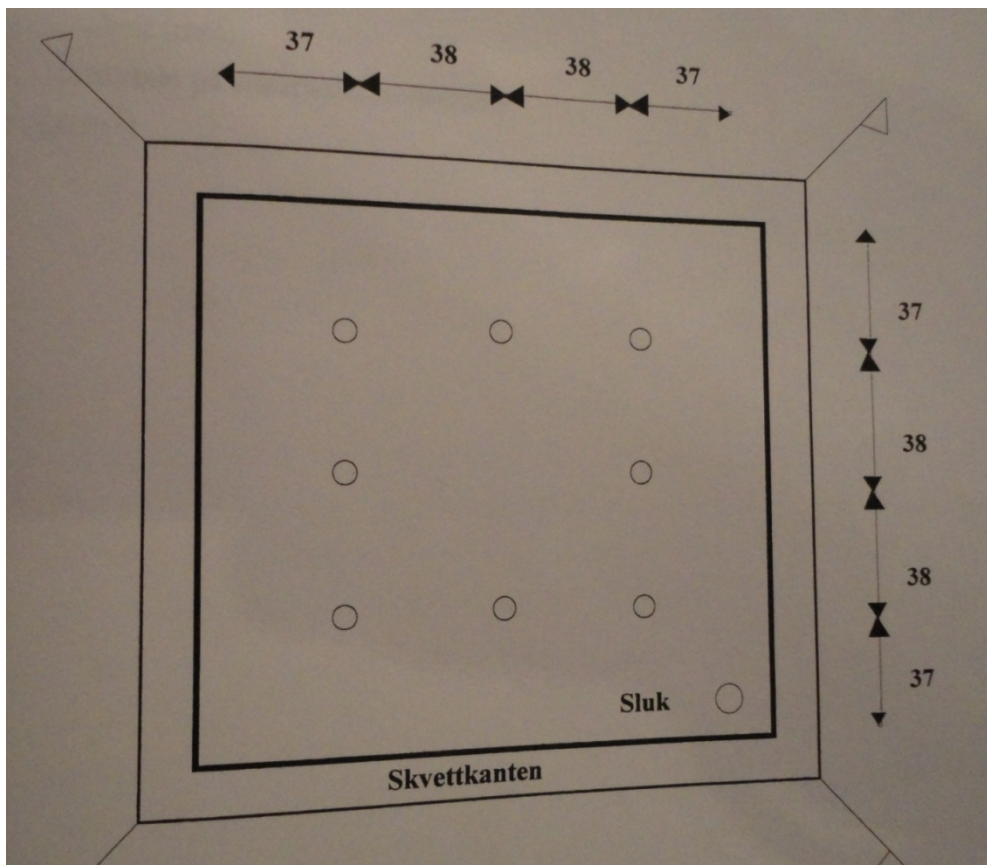


Figure 99: Principle sketch of the snow lysimeter

9. Paper rolls

The two old paper rolls that earlier measured the storm water and the wastewater are still available, and partially operational. They register the water level from the stilling wells, but only for a week, before they have to be screwed up again by a steel spring, (Thorolfsson, S.T., & Høgeli, S.A. 1994).

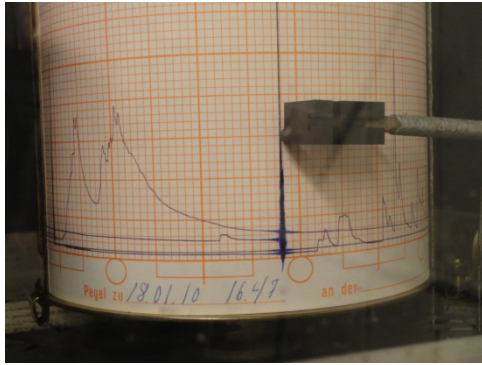


Figure 100: Paper roll storm water

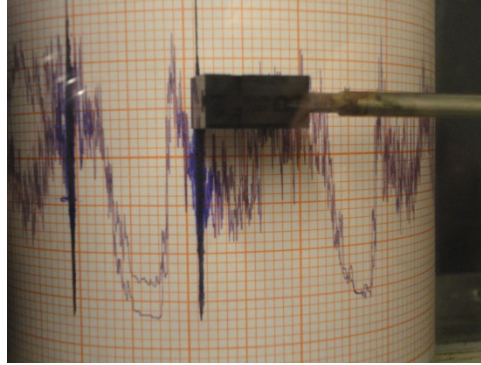


Figure 101: Paper roll wastewater

3.5 RUHS Transmission System

The transmission system has been changed regularly since the station was built. However, the most crucial changes took place since the beginning of 2010 until May 2011. During the same period, the main responsibilities of the station were also changed. These changes were implemented to ensure that NTNU had an independent logging system in addition to NVE's system. The need for an updated logging system along with new instrumentation was vital as well. The reason for this was to further customize the weather station for research purposes, (Sveinung Sægrov, 2011)

Trondheim Municipality is responsible for the surrounding area by the location of the station. In addition they also make sure that the V – notch basin is being emptied of sediments, but only after the notice from inspections conducted by NTNU. Regarding inspections and maintenance of the instruments, NTNU has now the main responsibility. Earlier the NVE had that responsibility, now they are only responsible for the collection of data sets. See figures below to view the old and the new transmission system.

Documentation of Risvollan Urban Hydrological Research Field, 2011

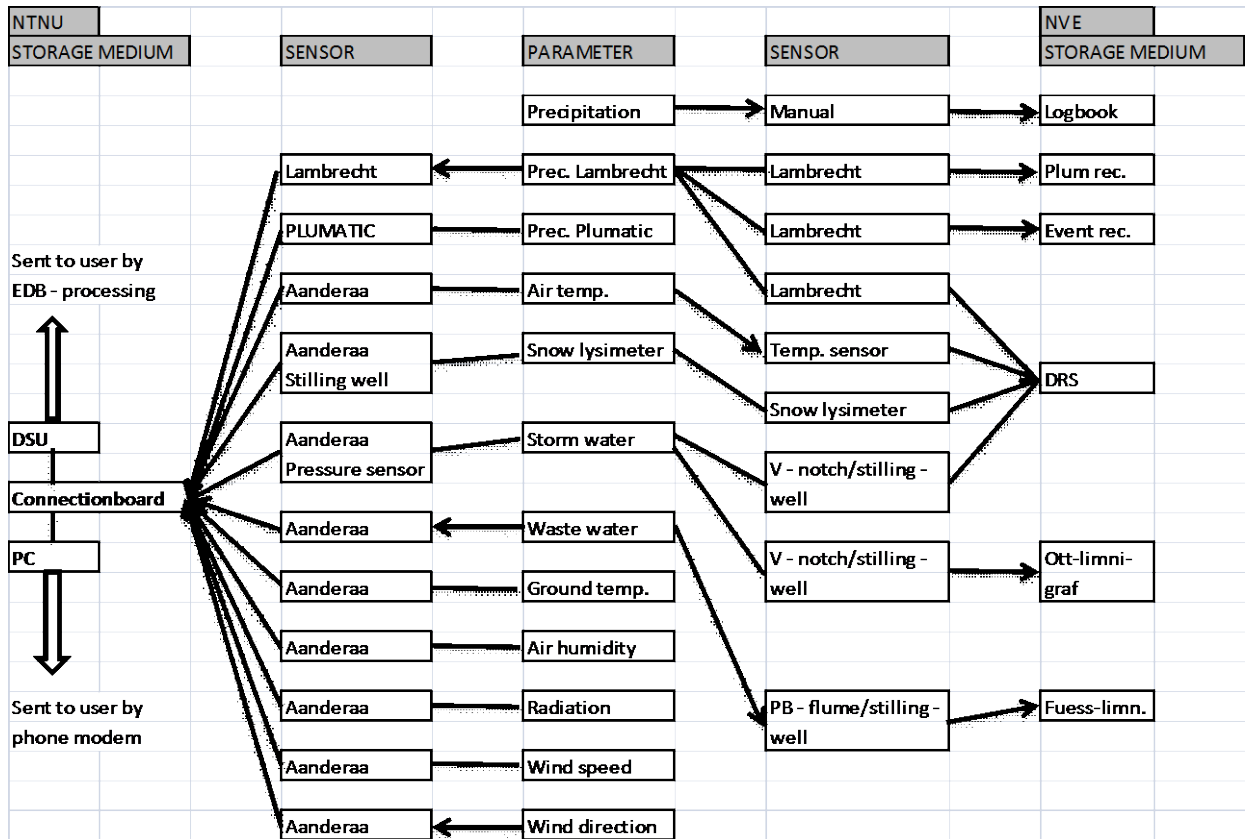


Figure 102: Old transmission system

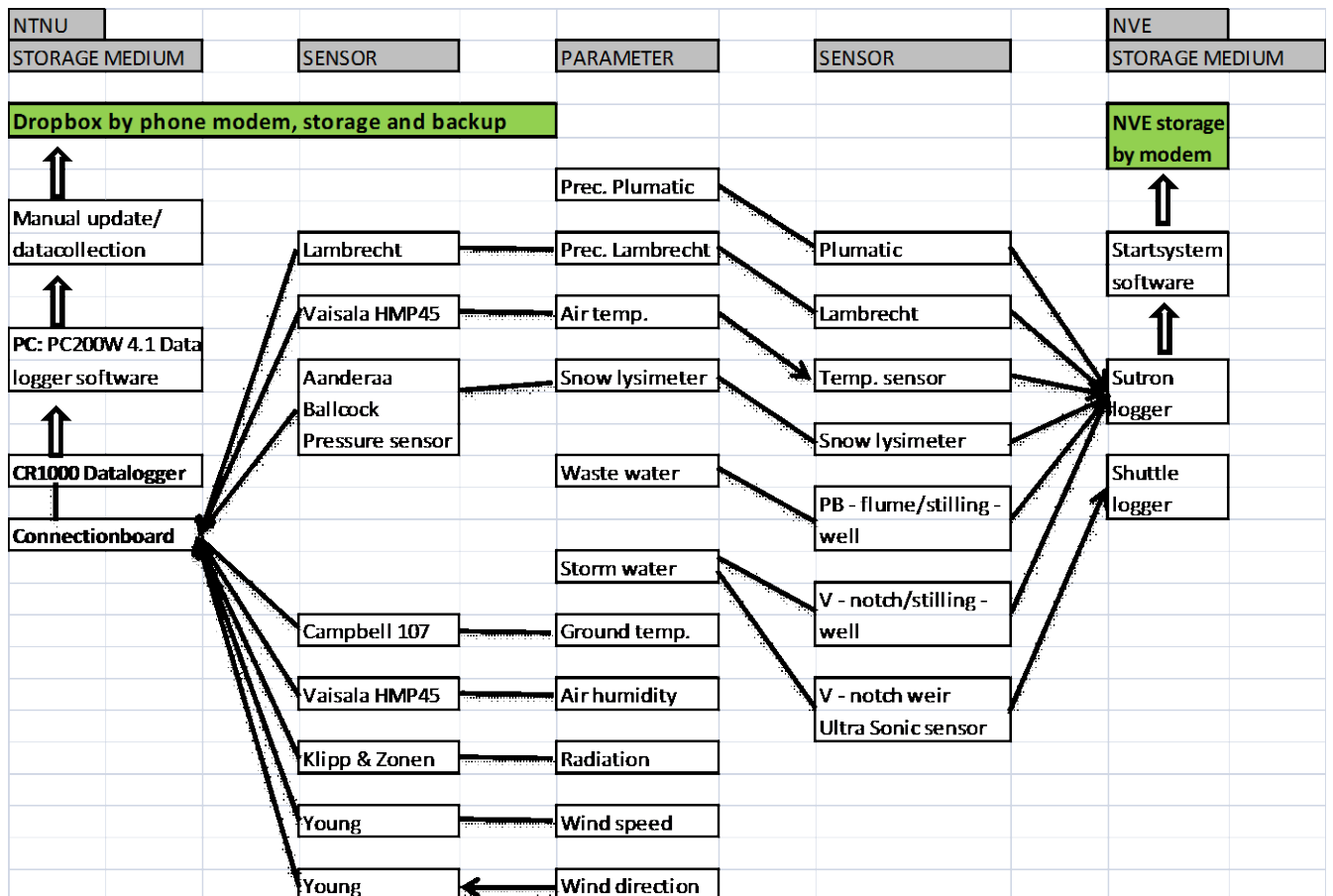


Figure 103: New transmission system

Documentation of Risvollan Urban Hydrological Research Field, 2011

The main thing is that the old Data Storing Unit (DSU) log system was replaced by the new Campbell CR1000 log system. This was followed by replacements of old instruments.

The DSU system was able to collect and store 65.530 ten-bits-words, a total capacity equivalent to 4 months of data storage. However, the data files contained 2 minutes intervals, which reduced the total duration to 1 week. The full unit then had to be replaced with a new one. In addition, an available PC with proper software was able to read the data sets and store it into a disc.

The Campbell CR1000 system has a total capacity of 4Mbyte, storing the data as text files with DAT – format. Two files containing hour and 2 minute intervals are generated, and they include arithmetic, trigonometric and statistical calculations. In addition, two files containing 1 minute and 10 minute intervals are generated for the wind speed- and direction. The system has a backup battery in case the operating power lapses. The total capacity is 152 days (\approx 5 months), before the old data sets are continuously being replaced of the new ones (ring memory). A PC with proper software (PC200W 4.1 Data logger Support software) is able to read the current data sets and store it into the hardware drive or in other locations. Today the data is transferred into an external web storage called Dropbox. This does not happen automatically, a button named “Collect data” inside the software needs to be pushed each time somebody is visiting the station for inspection.



Figure 104: The CR1000 connection board

Parameter	Value	Unit
RecNum	228896	VH_1 sek
TimeStamp	03.06.2011 02:37:50	VR_1 sek
ID	1 065,00	NB2_2_m_mm
Prog_dato	161 210,00	NB2_1_t_mm
Batt_V	13,81	NB2_h_i_2_m
Intern_gr_C	23,15	NB2_h_i_t
LF_prst	32,28	NB2_vipp
LT_gr_C	11,18	
GS_Wpm2	1,48	
R	43,98	
RA_01	43,64	
RR_1	0,40	
R_f	1 223,91	
T_107_gr_C	11,56	
VH_3_sek	0,37	

Figure 105: Current data displayed on the PC screen

For information about the Sutron logger and the Shuttle logger, see Appendix CD.6

It might be an advantage to connect the measurement of storm water and wastewater to the CR1000 logger as well.

4. Precipitation gauges

In this chapter, the results from the comparison between different gauges and logger data sets will be presented. Precipitation data from May to December was used as basis for these comparisons, along with a couple of rainfall events. In addition, previous records and comparison between these will also be presented. These records include annual precipitation since 1986. Finally, the chapter will go through the simulated results that helped developing the water balance equation for Risvollan. In addition, climate changes will be discussed.

4.1 Comparison between instruments

Monthly precipitation is presented for Geonor, Lambrecht and two Plumatic gauges. One of the Plumatic gauges belonged to Voll weather station. Table 17 below shows the results from the analyses.

4.1.1 Monthly precipitation

Table 17: Monthly precipitation from May to December

	→ Input values		Monthly precipitation mm autumn 2011							
	→ Incomplete									
	→ Invalid data				NVE					
	NTNU	NTNU	NTNU	NTNU	Lambrecht	Plumatic	Voll (Yr.no)	Voll (met.no)		
Month	Geonor hour	Lambrecht hour	Geonor 2 min	Lambrecht 2 min	Break values	values	day Int.	Break values	Input values	
May	393	72	1285	72	70	73	51	50	72	
June	463	83	1740	83	83	87	81	81	83	
July	182	88	4023	79	80	68	69	69		
August	300	146	6323	130	129	119	115	115		
September	373	90	17143	83	36	36	125	125		
October	210	81	3931	75	79	106	95	95		
November	#	#	#	#	90	98	59	59		
Average	#	93	#	87	81	84	85	85		
Min	#	72	#	72	36	36	51	50		
Max	#	146	#	130	129	119	125	125		
Total	#	559	#	521	477	489	536	535		

Data for both Geonor and Lambrecht gauge were partially incomplete, and the monthly total was simply invalid for May and June. To correct this, average data from primarily NVE's registrations replaced the invalid data. This was because NVE collects data from the same location. If NVE had incomplete data, average data from Voll station replaced the invalid data. Incomplete precipitation data from the Geonor gauge were not corrected, simply because all data were invalid.

Abnormal values were detected during the summarizations of Geonor registrations. Despite of removing these, there were still enough individual values to generate enormous amounts of data.

There is no explanation for the abnormalities, except from the gauge may have been tested regularly after installation. The testing could include adding water directly into the gauge to see if the CR1000 logger detects the changes. The gauge detects the weight of the bucket, which means if someone rests their hands on it or lifts it off and puts it back on the container, it could disturb the normal pattern of registrations. This could perhaps explain why the total amount from the 2 minute interval data was so much greater than the total amount from the hour interval data; maybe it detects more violent changes.

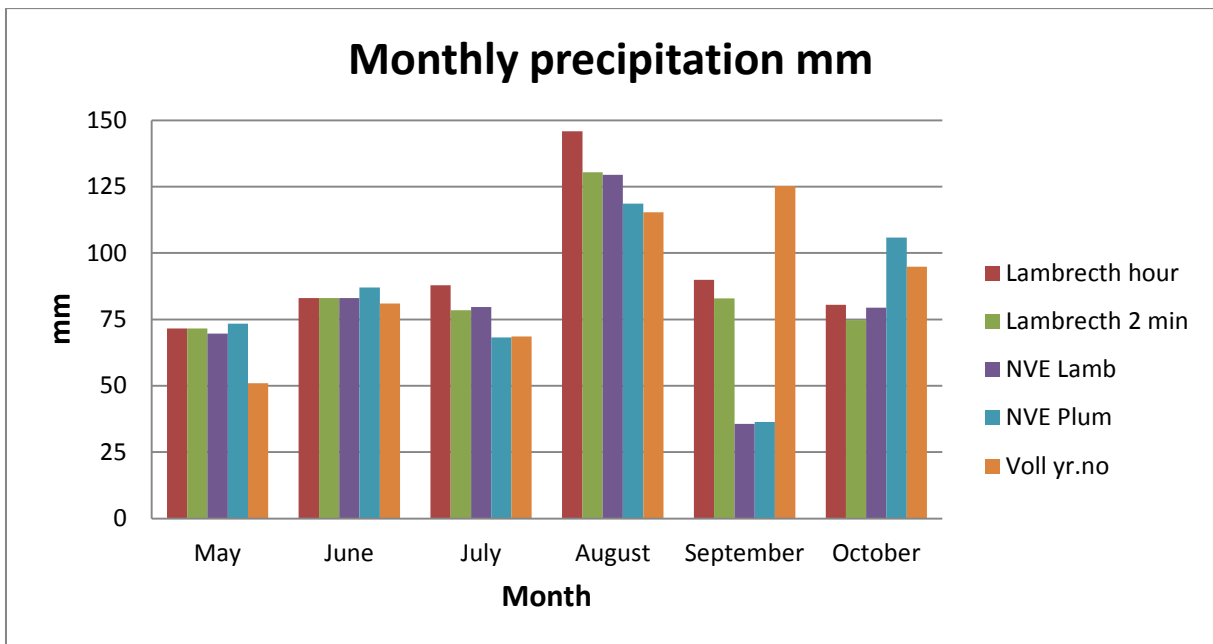


Figure 106: Monthly precipitation from NTNU (CR1000), NVE (Sutron) and Voll (DNMI)

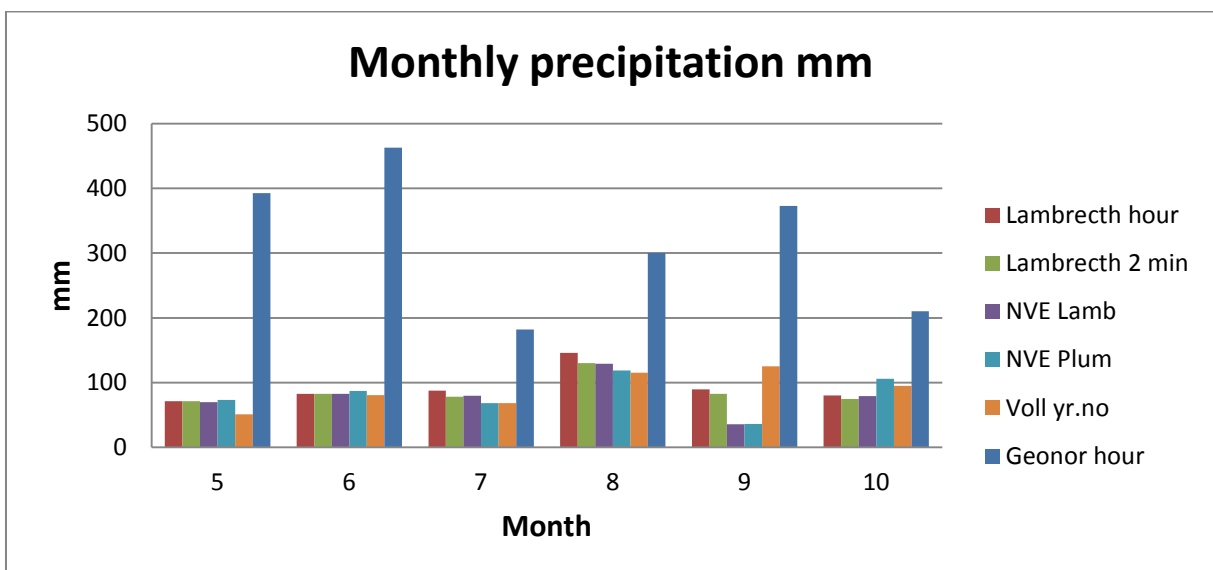


Figure 107: Monthly precipitation including Geonor hour intervals data

The Geonor gauge illustrated a similar pattern of monthly precipitation development. However, the precipitation data itself was too large. The hourly interval data alone had an average deviation of up to 374 % compared to the other data sets.

Monthly statistics:

The precipitation data from the Geonor gauge was excluded due to large deviations from the other gauges.

The calculated average of Lambrecht and Plumatic registrations was considered to be the most valid. Figure 108 below shows how much the other registrations deviate from NVE's.

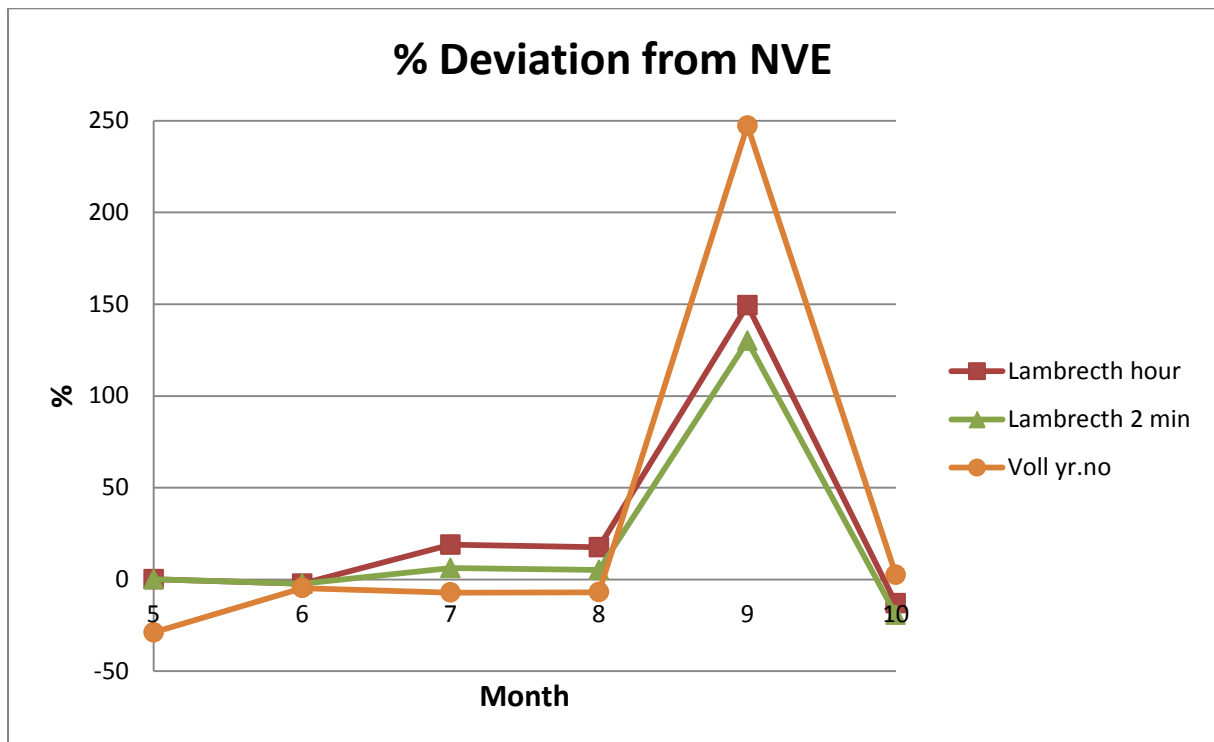


Figure 108: Percentage of deviation from NVE's average of Plumatic and Lambrecht registrations

Overall average deviation of collected Lambrecht precipitation data from the CR1000 logger was estimated to be +24.2%.

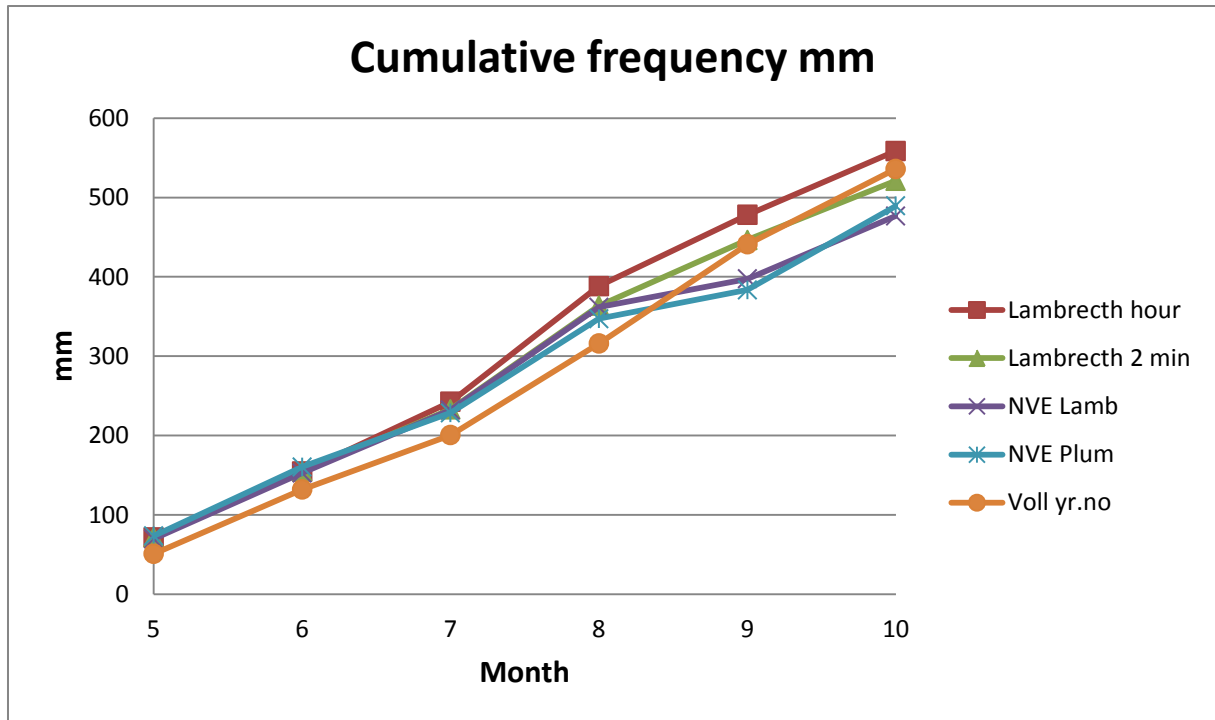


Figure 109: Cumulative developments per month

4.1.2 Weekly precipitation

As for the monthly precipitation data, the same procedure was done with the weekly precipitation data (input values, exclusion of Geonor).

Table 18: Weekly precipitation in 2011

Week	Precipitation mm week 18 - 48							
	NTNU Geonor hour	NTNU Lambrecht hour	NTNU Geonor 2 min	NTNU Lambrecht 2 min	NVE Lambrecht	NVE Plumatic	DNMI Voll day	DNMI Voll break.
18	2	2	0	2	2	3	1	1
19	17	17	0	17	17	16	17	17
20	10	10	0	10	10	11	9	9
21	17	17	847	17	17	20	15	15
22	19	16	918	26	15	20	21	21
23	20	20	521	20	20	20	20	20
24	23	18	262	17	17	15	26	26
25	22	20	251	19	19	16	15	15
26	44	34	470	30	30	26	11	11
27	41	21	822	16	16	14	29	29
28	32	6	894	6	6	5	4	4
29	51	26	921	24	25	21	23	23
30	37	15	1141	15	15	13	11	11
31	34	3	1167	3	3	3	1	1
32	89	58	1402	51	50	44	37	37
33	96	58	1796	51	51	49	56	56
34	65	26	1542	22	22	21	9	9
35	43	6	936	6	3	3	16	16
36	90	10	1357	9	9	9	20	20
37	92	37	3712	34	36	36	66	66
38	8	9	9134	8	7	7	7	7
39	76	35	2961	33	33	33	33	33
40	57	35	726	33	35	48	37	37
41	51	20	1348	20	20	16	24	24
42	53	36	562	33	33	31	22	22
43	28	4	664	4	5	7	4	4
44	0	0	0	0	4	4	8	8
45	0	0	0	0	4	5	5	5
46	0	0	0	0	27	28	23	23
47	0	0	0	0	19	16	16	16
48	0	0	0	0	37	45	28	28
Average	43	21	#	20	19	19	20	20
Min	2	2	#	2	2	3	1	1
Max	96	58	#	51	51	49	66	66
Total	1116	557	#	523	604	604	613	613

Some data weren't collected from the CR1000 logger due to unavailable time during the phase of this thesis.

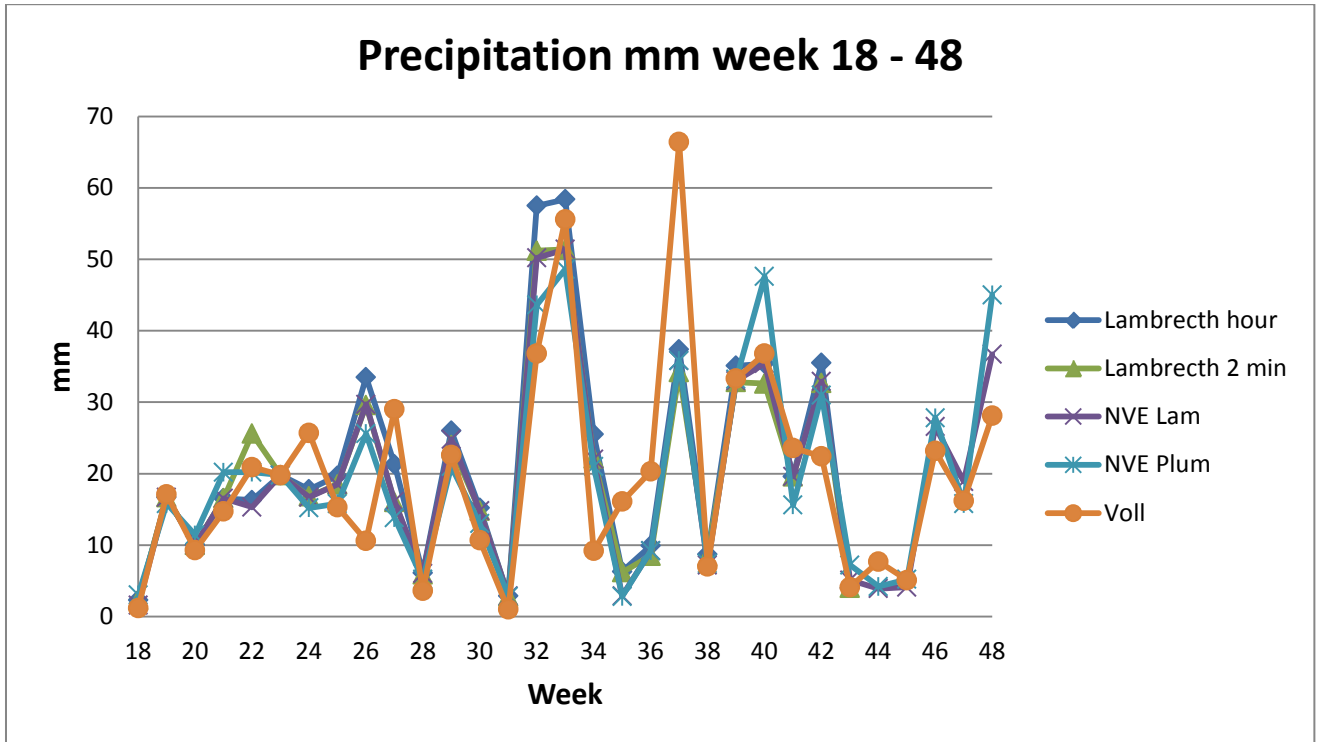


Figure 110: Weekly precipitation in 2011

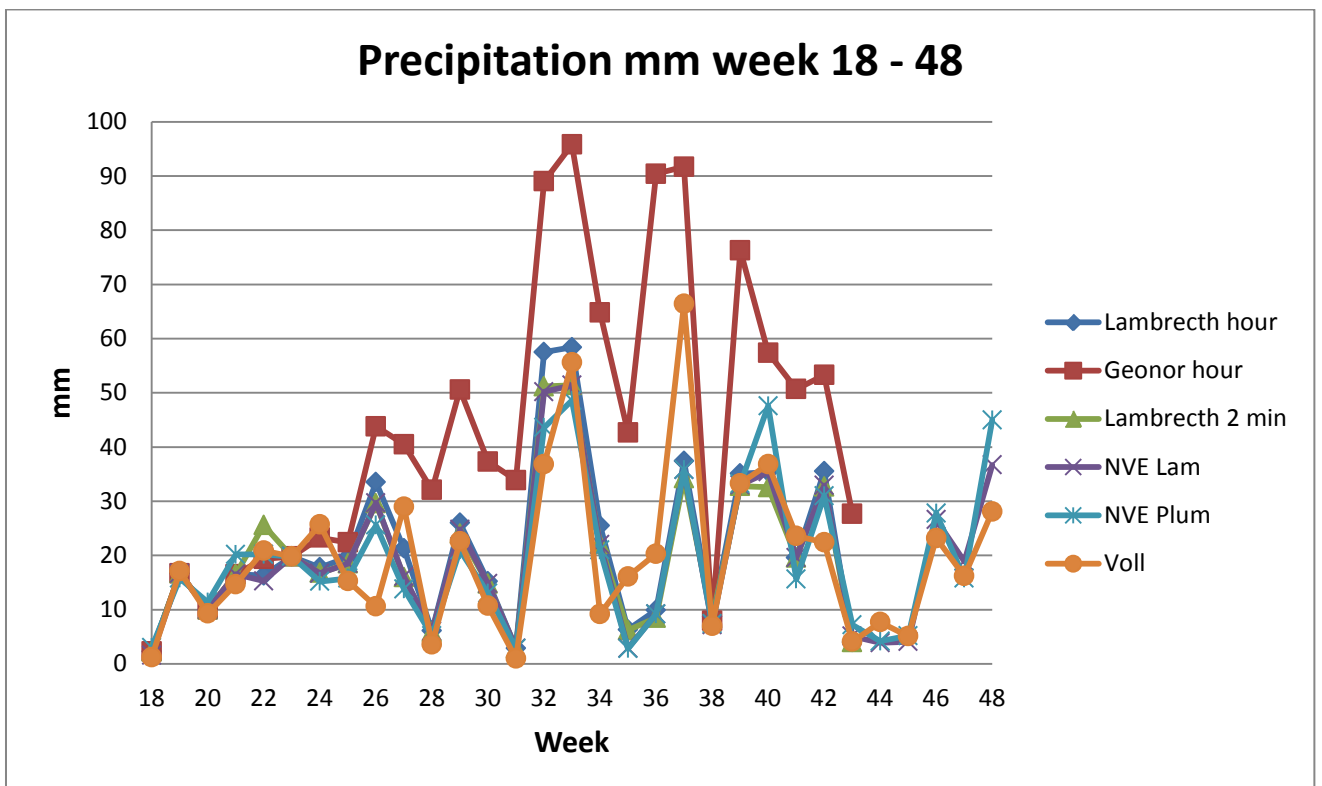


Figure 111: Weekly precipitation in 2011 including Geonor hour intervals data

Weekly statistics:

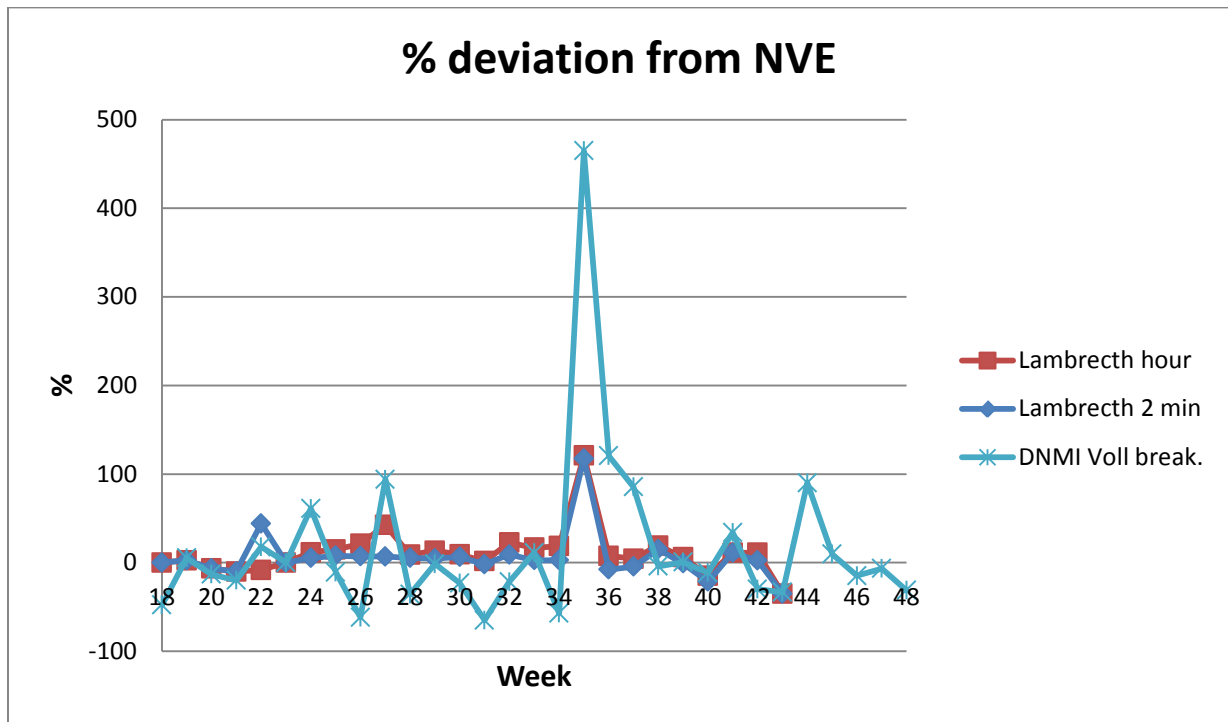


Figure 112: Percentage of deviation from NVE

In week 35, there's a greater deviation between the registrations from Voll station and the RUHS (465%). The reason for that may be local conditions; rainfall events are rarely uniform over large areas. Moreover, the precipitation data from Voll deviated relatively much throughout the period. Overall average deviation of collected Lambrecht precipitation data from the CR1000 logger was here estimated to be +8.75%. This result showed that comparison between instruments based on analyses of weekly precipitation instead of monthly precipitation, could change the average deviation with 15%.

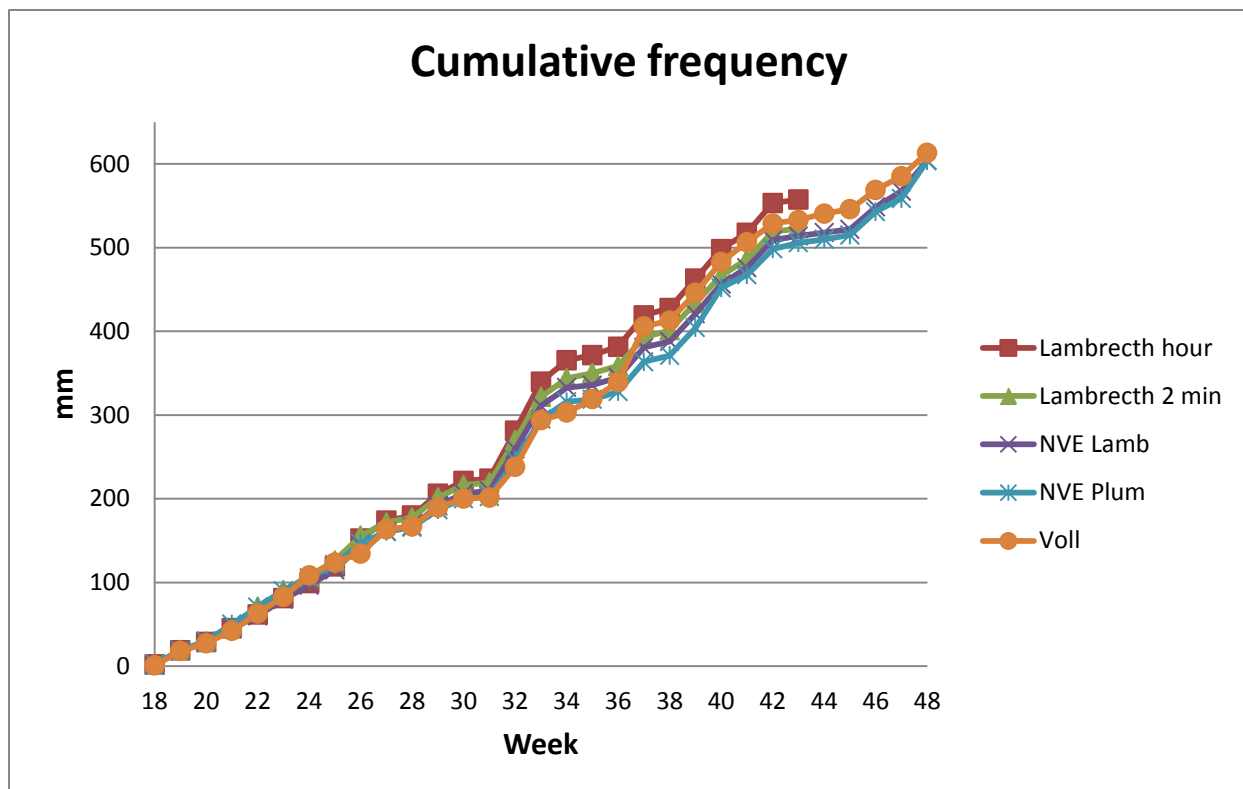


Figure 113: Cumulative developments per week

The comparison between the gauges showed that the Geonor gauge was very inaccurate, especially regarding the data values itself. However, it illustrated some of the developments both in increase and decrease synchronously with the other gauges.

The Lambrecht precipitation data collected from CR1000 logger shows throughout the period that the values are slightly higher than the precipitation data collected from the Sutron logger.

To see daily variations of runoff, temperature and wind speed for each month, see Appendix CD.7.

4.1.3 Rainfall events

The rainfall events that were chosen for calibration in PCSWMM, did also work as basis for comparison between the gauges. However, this time only the total precipitation from the Lambrecht and the Plumatic gauge was compared.

The rainfall event extracted from June lasted for about 2 hours and 20 minutes, and the total amount of precipitation was measured to be 1.2 mm. Tables 19 and 20 with Figure 114 below show the individual precipitation data collection from both CR1000- and Sutron logger.

02. June 2011

Table 19: Precipitation data from CR1000 (Lambrecht) and Sutron (Lambrecht and Plumatic), 02. June

Prec. Data	mm
NVE Plumatic	1.2
NVE Lambrecht	1.2
NTNU Lam. Hour	1.3
NTNU Lam. 2 min	1.2

Table 20: Intensity and duration of rainfall event from 02. June

	Duration hour	Duration min	Average mm/min	Average mm/hour
NVE Plumatic	2:20	140	0.009	0.51
NVE Lambrecht	2:11	131	0.009	0.55
NTNU Lam. Hour	3:00	180	0.007	0.43
NTNU Lam. 2 min	2:06	126	0.010	0.57

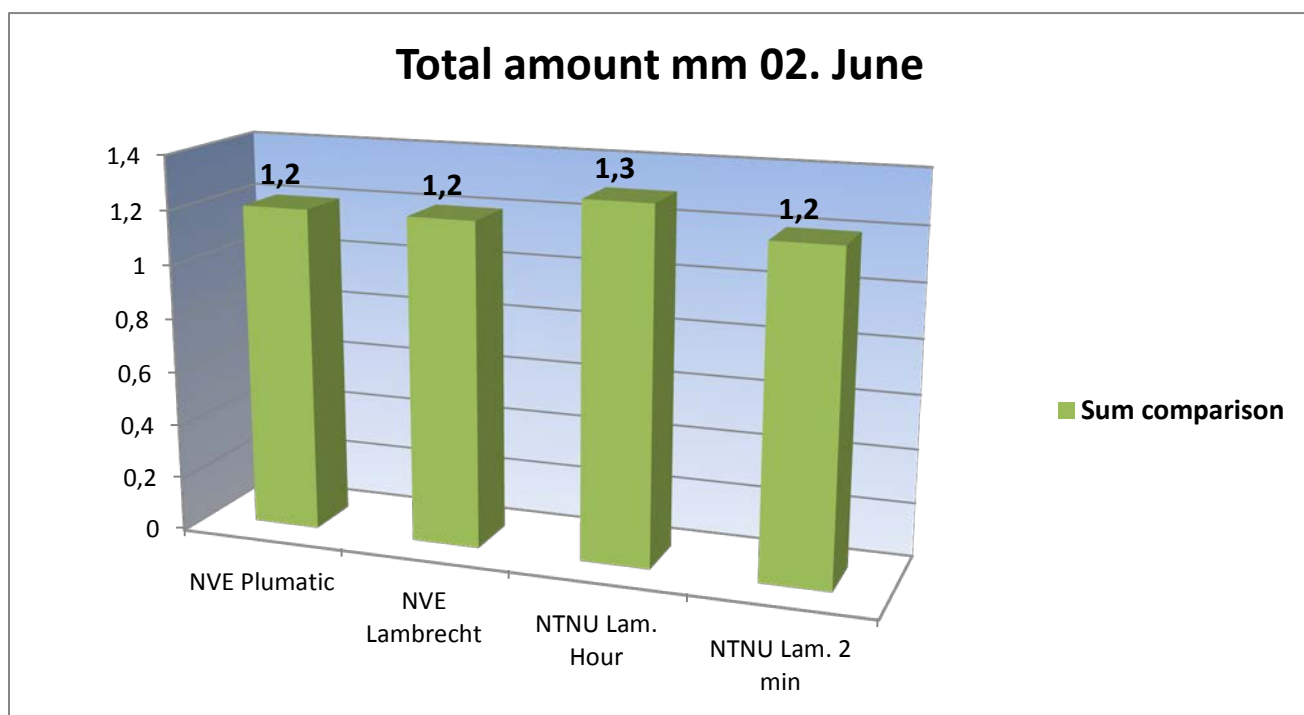


Figure 114: Precipitation data from CR1000 (Lambrecht) and Sutron (Lambrecht and Plumatic), 02. June

In sub chapter 2.4.3, figures show both relative- and cumulative development for this event. The same gauges were also used there.

For this event, it was barely any difference at all. Something that must be taken into account is that the comparison only involved two gauges based on four individual registrations. However, these gauges and their respective data sets were considered to be the most valid ones.

16. August 2011

The rainfall event extracted from June lasted for about 12 hours, and the total amount of precipitation was measured to be about 12 mm. Tables 21 and 22 with Figure 115 below shows the individual precipitation data collection from both CR1000- and Sutron logger.

Table 21: Precipitation data from CR1000 (Lambrecht) and Sutron (Lambrecht and Plumatic), 16. Aug.

Prec. Data	mm
NVE Plumatic	11.4
NVE Lambrecht	11.4
NTNU Lam. Hour	12.9
NTNU Lam. 2 min	11.5

Table 22: Intensity and duration of rainfall event from 16. August

	Duration hour	Duration min	Average mm/min	Average mm/hour
NVE Plumatic	11:26	686	0.017	1.00
NVE Lambrecht	11:55	715	0.016	0.96
NTNU Lam. Hour	12:00	720	0.018	1.08
NTNU Lam. 2 min	10:02	602	0.019	1.15

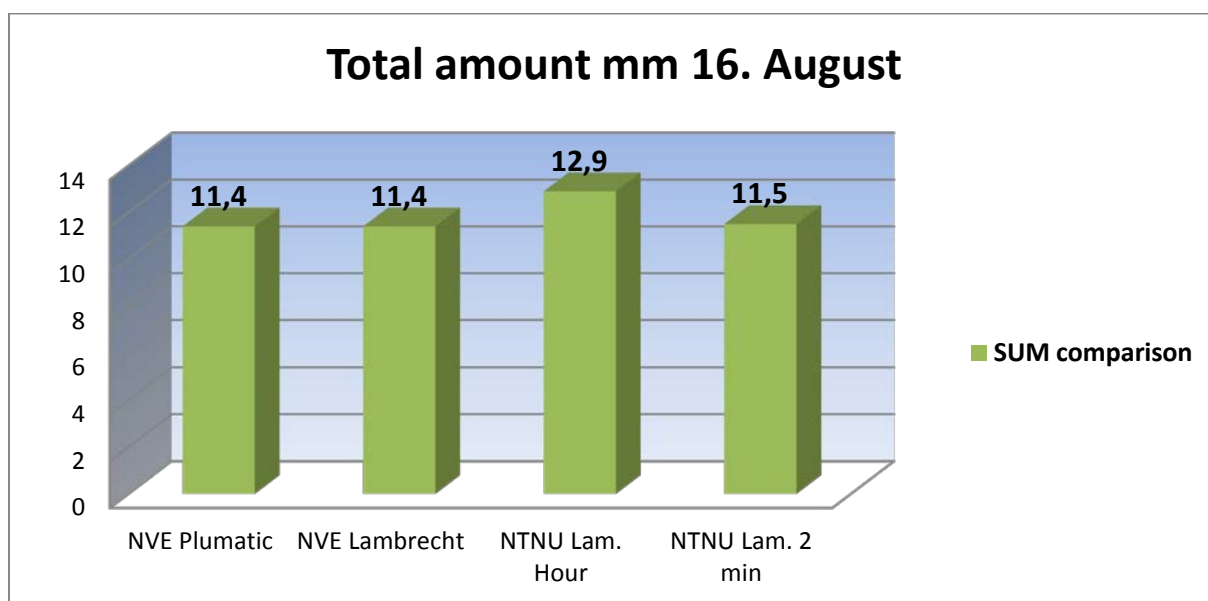


Figure 115: Precipitation data from CR1000 (Lambrecht) and Sutron (Lambrecht and Plumatic), 16. Aug.

In sub chapter 2.4.3, figures show both relative- and cumulative development for this event. The same gauges were also used there.

What was common for the analyses of monthly precipitation, weekly precipitation and the rainfall events was that the precipitation data collected from the CR1000 logger always seemed to be slightly higher than the precipitation data collected from the Sutron logger. The exact reason for that is not known at this moment.

4.2 Previous precipitation records

Table 23 below shows the monthly precipitation at RUHS since 1986. Some data were missing in 1986 and 1988.

Table 23: Monthly precipitation at RUHS since 1986

	Precipitation mm Risvollan																		
	January	February	March	April	May	June	July	August	September	October	November	December	Sum	Average	Development %	Max	Min		
1986	0	0	0	0	0	0	24	38	155	83	31	16	347	29	#	155	0		
1987	84	109	3	64	62	79	86	118	106	33	57	192	993	83	#	192	3		
1988	9	30	49	93	58	21	0	0	0	0	165	151	575	48	#	165	0		
1989	205	93	31	5	75	46	77	103	86	116	49	104	989	82	0	205	5		
1990	69	48	207	63	82	23	116	84	90	64	89	95	1029	86	4	207	23		
1991	38	60	31	46	93	134	64	67	161	62	59	118	932	78	-9	161	31		
1992	260	108	72	21	57	64	79	105	30	77	61	85	1019	85	9	260	21		
1993	86	141	96	22	67	58	90	144	79	133	0	67	982	82	-4	144	0		
1994	62	8	100	45	33	114	44	112	99	86	115	66	883	74	-10	115	8		
1995	65	123	79	100	87	83	38	77	40	114	76	59	941	78	7	123	38		
1996	10	76	43	6	43	72	66	42	24	81	70	108	639	53	-32	108	6		
1997	128	95	176	141	60	78	25	48	182	127	27	15	1101	92	72	182	15		
1998	66	178	92	20	48	79	54	135	21	86	4	1	785	65	-29	178	1		
1999	73	140	40	86	37	89	128	36	21	107	68	65	890	74	13	140	21		
2000	161	98	133	22	34	105	48	108	26	26	12	34	807	67	-9	161	12		
2001	21	80	44	40	75	58	73	0	71	65	224	37	788	66	-2	224	0		
2002	61	91	82	36	24	101	41	33	136	45	14	84	748	62	-5	136	14		
2003	183	10	17	44	68	56	42	145	73	88	22	179	927	77	24	183	10		
2004	12	11	39	1	56	69	54	49	256	46	194	197	983	82	6	256	1		
2005	185	90	27	42	19	68	23	138	121	47	101	156	1017	85	3	185	19		
2006	135	128	50	35	58	43	69	48	87	106	91	131	979	82	-4	135	35		
2007	163	61	58	106	72	18	134	128	162	135	120	22	1176	98	20	163	18		
2008	81	137	73	21	42	88	44	76	64	95	151	43	915	76	-22	151	21		
2009	134	100	75	24	69	82	134	80	259	94	25	53	1129	94	23	259	24		
2010	44	35	130	60	48	107	67	52	79	91	9	75	796	66	-29	130	9		
2011	80	42	166	76	55	95	81	130	86	93	94	86	1084	91	36	166	42		

2.7

What was interesting to determine was the annual development through these years, to see if there are indications of increase of precipitation. Since some data were missing from 1986 and 1988, the average development was estimated from 1989 (1989 starts at 0 %). The average development since then was estimated to be 2.7 %. It was also interesting to estimate the annual average linear growth from 1987 to 2011 and from 1990 to 2011, see Figure 116 below.

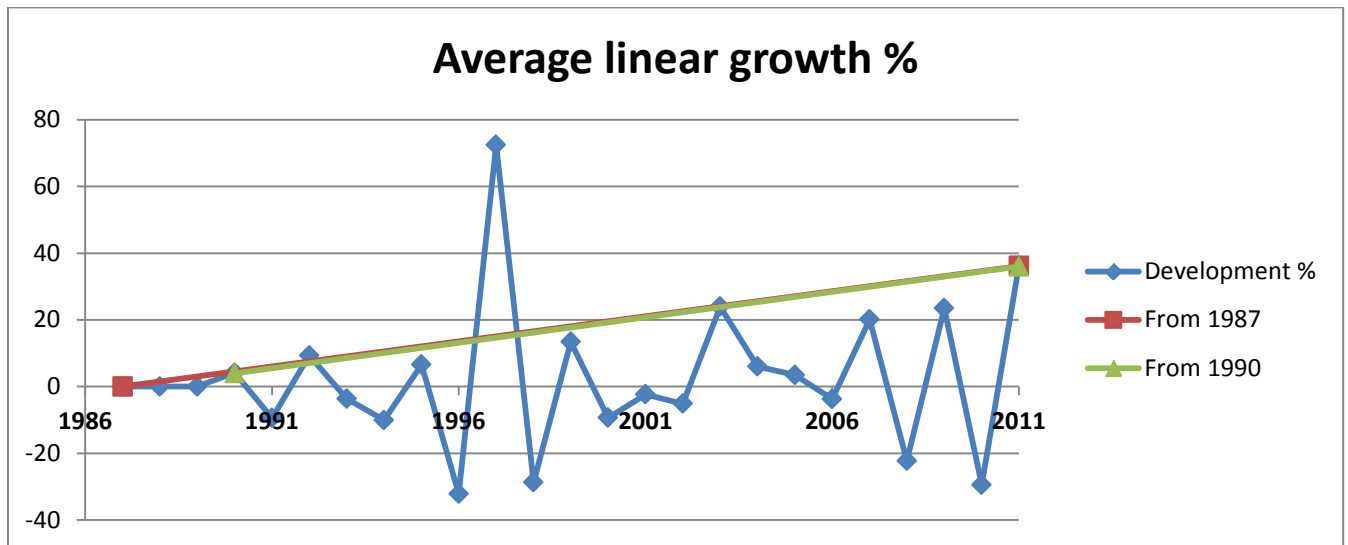


Figure 116: Average linear growth from 1987 and 1990

Linear average growth from 1987 to 2011: **1.5 %**

Linear average growth from 1990 to 2011: **1.7 %**

The blue line in Figure 116 illustrates the percentage of the annual development from year to year.

Figure 117 and 118 shows the monthly variations each year, and the monthly development in relation to the years.

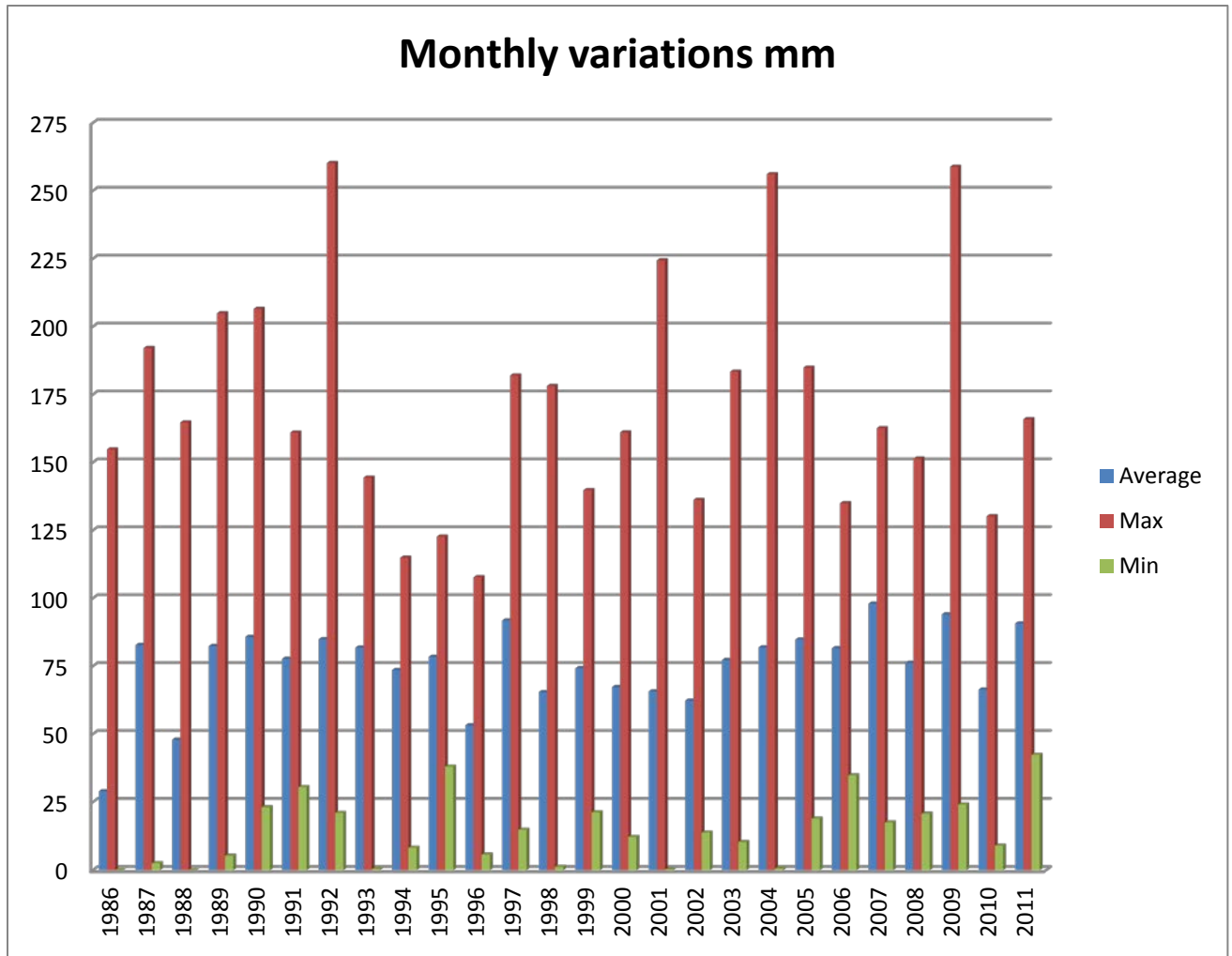


Figure 117: Monthly variations mm

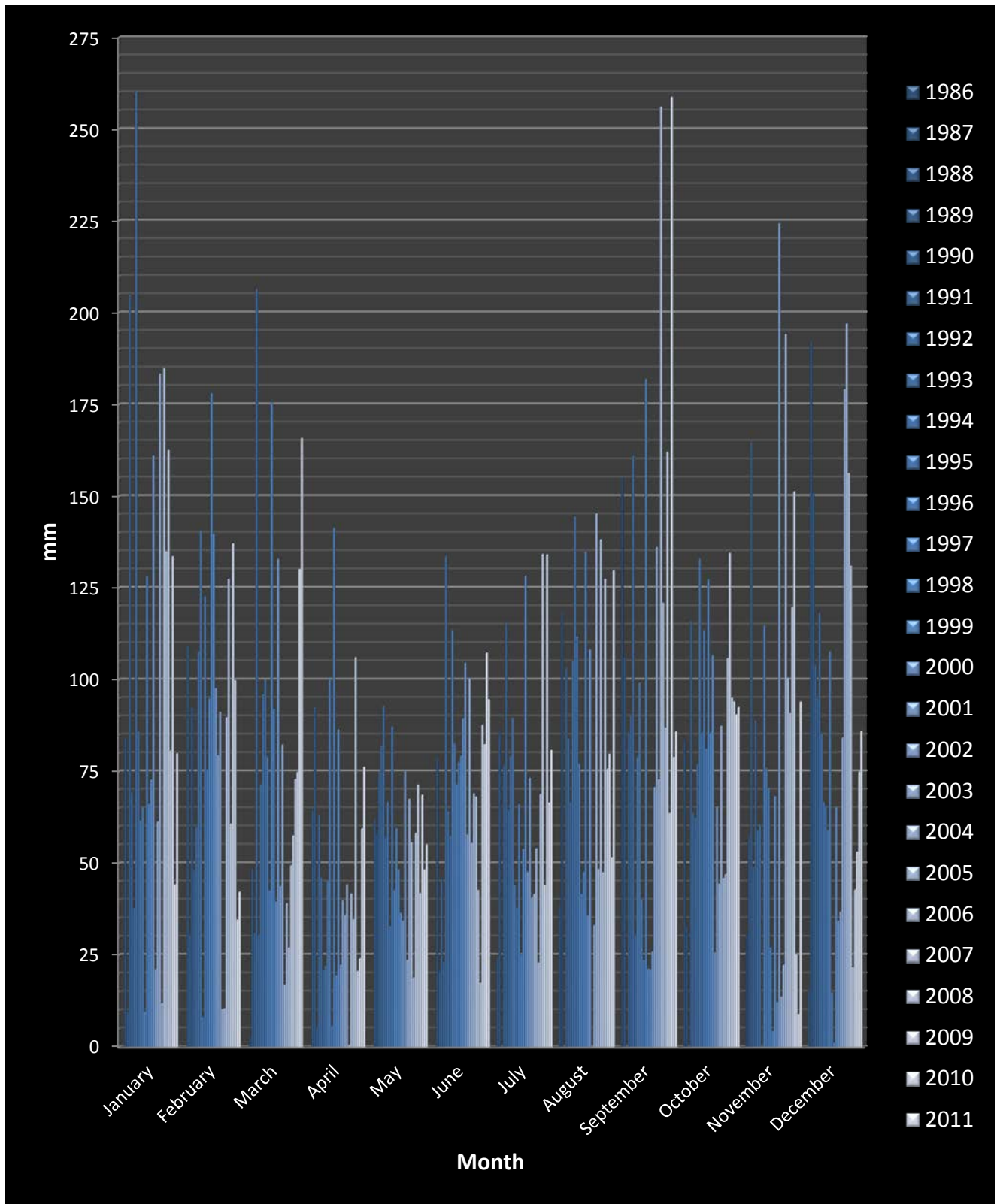


Figure 118: Monthly development in relation to the years

The annual average linear growth was estimated to be about 1.6% since the beginning of the RUHS measurement period. In addition, the actual average development indicated an increase of 2.7 %. These results could perhaps confirm the trends in precipitation due to climate change. However, these changes aren't necessarily based on monthly amounts.

Climate changes often lead to rainfall events that rapidly and intensely occur during a very short time. For that reason, further studies regarding individual events within the period should be performed.

4.3 Water balance

The water balance equation used for this thesis represented a limited edition of the general version:

$$Q = P - E - \text{Inf. (mm)}$$

See sub chapter 2.3 for more explanation about this.

As long as PCSWMM received the estimation of infiltration capacity and the evaporation potential, it could give accurate results to support the equation. For this operation the two chosen rainfall events were used, and after the calibrations the results were then available.

4.3.1 Water balance representing 02.June

***** Runoff Quantity Continuity *****	Volume hectare-m -----	Depth mm -----
Total Precipitation	0.022	1.040
Evaporation Loss	0.006	0.275
Infiltration Loss	0.009	0.436
Surface Runoff	0.007	0.330
Final Surface Storage	0.000	0.000
Continuity Error (‰)	-0.157	

Figure 119: Runoff quantity continuity (02.June) from the “Status” bar in PCSWMM after simulation

----- Outfall Node	Flow Freq. Pcnt.	Avg. Flow LPS	Max. Flow LPS	Total Volume 10^6 ltr
01	43.64	2.97	12.15	0.070
System	43.64	2.97	12.15	0.070

Figure 120: Outfall loadings (02.June) from the “Status” bar in PCSWMM after simulation

Table 24: Summary made of the runoff quantity continuity for 02.June

	SWMM Results			Calc. average	
Total precipitation mm	Surface runoff mm	Evaporation mm	Infiltration mm	Runoff coeff.	Response time min.
1.04	0.33	0.275	0.436	0.32	22

Table 24 includes an estimation of an average runoff coefficient that represents the entire field, by dividing the total surface runoff with the total precipitation. The result didn't differ too much from the percentage of the total amount of impervious surfaces estimated in sub chapter 3.3.1 on page 59 (25.4 %). However, the difference may indicate a degree of inaccuracy regarding the use of runoff coefficients.

Estimated water balance representing 02.June:

$$0.330 = 1.040 - 0.436 - 0.275 \text{ (mm)} \rightarrow Q = P - (0.419 * P) - (0.264 * P) \text{ (mm)}$$

Where:

Infiltration = 0.436 * P (mm)

Evaporation = 0.264 * P (mm)

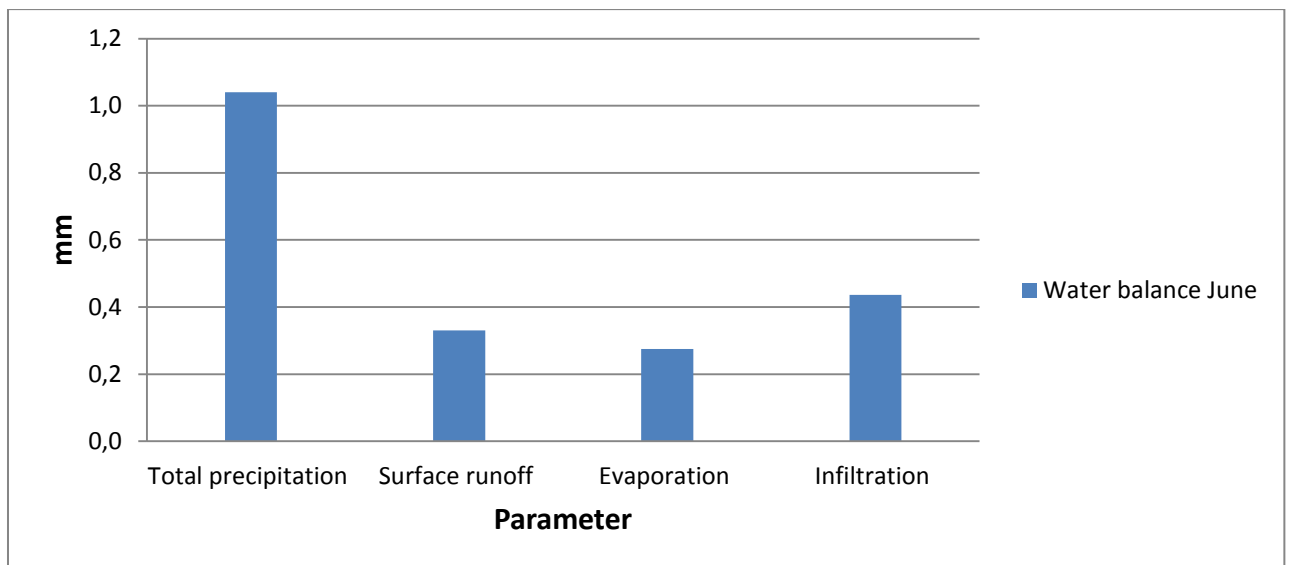


Figure 121: The water balance distribution representing 02.June

4.3.2 Water balance representing 16.Aug.

	Volume	Depth
Runoff Quantity Continuity	hectare-m	mm
Total Precipitation	0.449	21.100
Evaporation Loss	0.008	0.394
Infiltration Loss	0.298	14.011
Surface Runoff	0.144	6.773
Final Surface Storage	0.000	0.000
Continuity Error (%)	-0.373	

Figure 122: Runoff quantity continuity (16.Aug.) from the "Status" bar in PCSWMM after simulation

Outfall Node	Flow Freq. Pcnt.	Avg. Flow LPS	Max. Flow LPS	Total Volume 10 ⁶ ltr
01	88.25	18.91	58.52	1.442
System	88.25	18.91	58.52	1.442

Figure 123: Outfall loadings (16.Aug.) from the “Status” bar in PCSWMM after simulation

Table 25: Summary made of the runoff quantity continuity for 16.Aug.

	SWMM Results			Calc. average	
Total precipitation	Surface runoff	Evaporation	Infiltration	Runoff coeff.	Response time min.
21.10	6.77	0.394	14.011	0.32	15

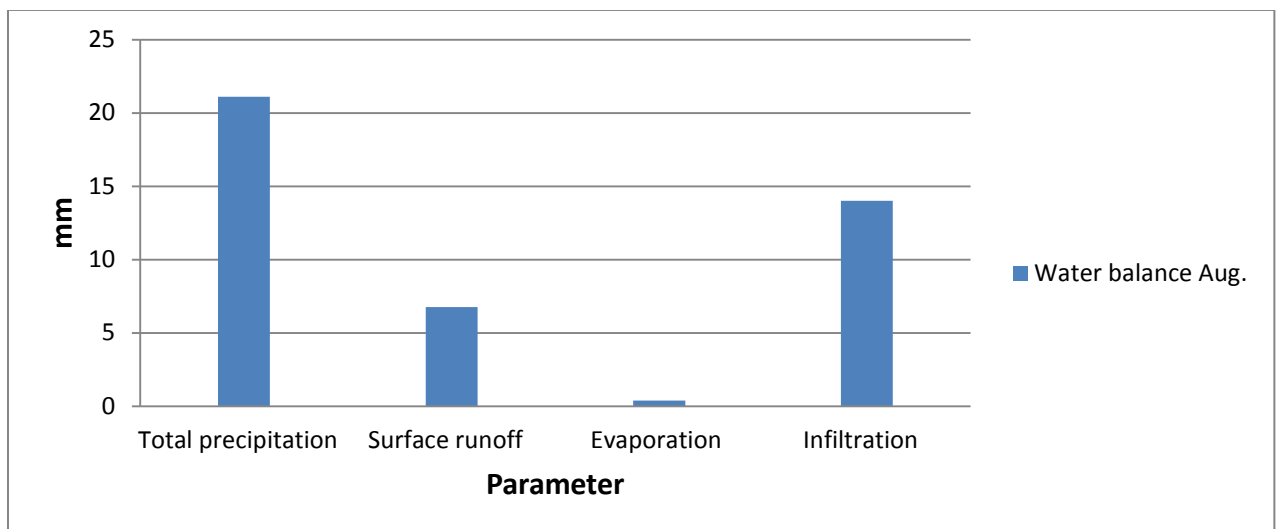


Figure 124: The water balance distribution representing 16.Aug.

Estimated water balance representing 16.August:

$$6.77 = 21.100 - 14.011 - 0.394 \text{ (mm)} \rightarrow Q = P - (0.664 * P) - (0.019 * P) \text{ (mm)}$$

Where:

Infiltration = 0.664 * P (mm)

Evaporation = 0.019 * P (mm)

The water balance equation given for 16.August, include a large amount of both precipitation and infiltration. This will further be discussed in the next main chapter. The relationship between the precipitation and the infiltration for both events seemed to be partially similar. However, what must be taken into account is that the increased amount of infiltration had to compensate for the larger total amount of precipitation. Perhaps the true amount of total infiltration was 5.3 mm (12 – 6.7 mm). The amount of evaporation seemed to deviate naturally between the events.

5. Runoff model

5.1 Model appearance

This sub chapter will present the runoff model's final appearance. How the model was developed is described in chapter 2. Tables containing its properties before calibration will also be presented.

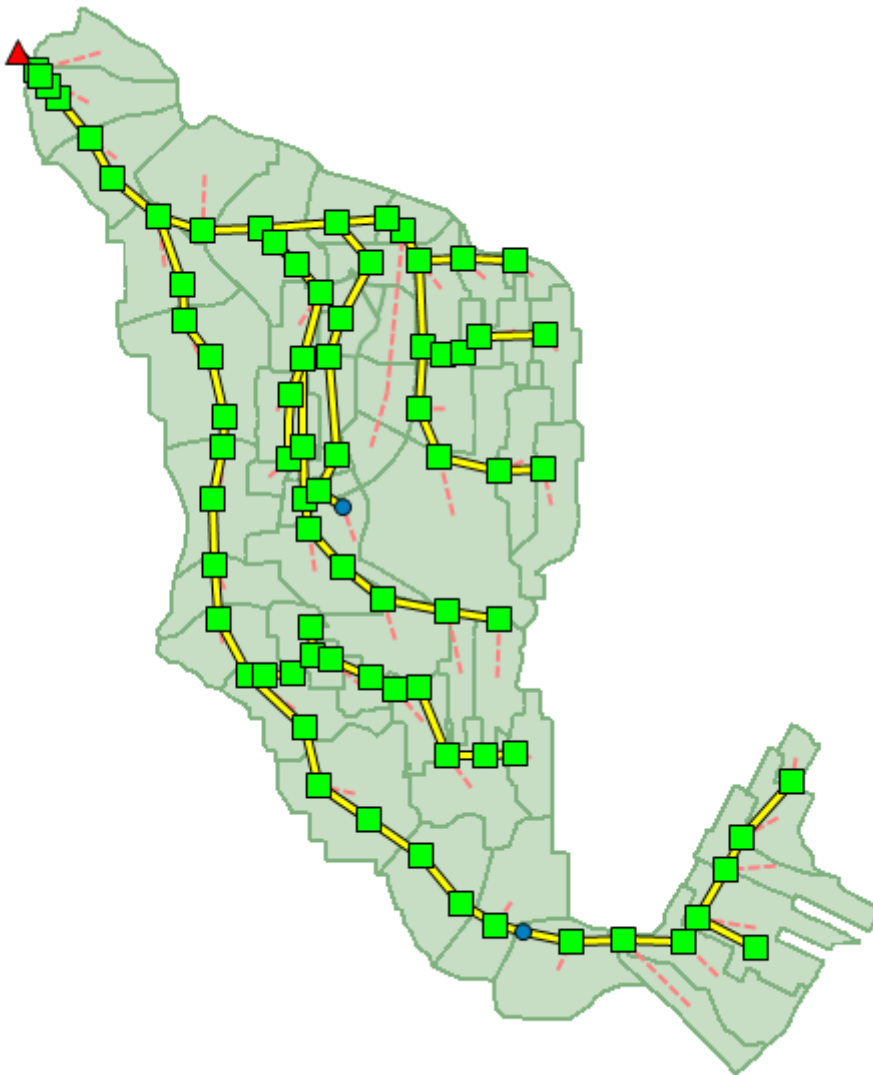


Figure 125: Initial plan overview of the runoff model (un-scaled)

The same coordinate system was used when the sub catchments and the pipe network were imported into PCSWMM. This was controlled by checking a few manhole coordinates and some catchment boundary coordinates. In addition, the model was able to be displayed on satellite pictures by using the added support from Google Earth. The model had the exact same properties as the one developed in ArcMap.



Figure 126: Model displayed on satellite pictures via Google Earth.

Table 26: Surface properties before calibration

ArcMap ID	PCSWMM ID	Area (ha)	Impervious %	Zero-impervious %	Slope %	Flow length (m)	Width (m)
42	Sub171	0.084	30	28	0.5	30	28
45	Sub176	0.098	51	10	4.0	25	39
54	Sub15	0.102	36	25	3.8	20	51
35	Sub148	0.108	42	1	7.1	35	31
46	Sub1	0.133	47	30	0.8	30	44
41	Sub175	0.144	66	3	4.3	20	72
39	Sub39	0.160	31	21	4.4	45	36
37	Sub146	0.168	41	22	15.5	45	37
38	Sub83	0.168	41	0	26.4	30	56
30	Sub30	0.173	35	0	4.1	40	43
34	Sub142	0.176	39	19	9.2	30	59
33	Sub145	0.185	19	46	5.3	40	46
21	Sub206	0.203	30	35	8.7	60	34
47	Sub84	0.210	33	0	9.3	55	38
44	Sub136	0.210	25	1	5.0	50	42
43	Sub135	0.221	27	33	1.8	50	44
36	Sub138	0.221	32	0	18.8	35	63
30	Sub31	0.226	34	0	4.9	30	75
48	Sub133	0.228	38	32	3.6	40	57
7	Sub137	0.238	25	0	4.8	30	80
40	Sub38	0.256	29	30	2.2	35	73
28	Sub790	0.264	37	0	10.3	50	53
20	Sub4000	0.265	34	31	1.8	60	44
27	Sub46	0.278	25	38	1.5	40	70
32	Sub150	0.291	25	38	10.6	45	65
13	Sub87	0.306	35	17	2.1	100	31
4	Sub82	0.310	21	17	11.5	30	103
10	Sub17	0.322	30	32	3.7	55	59
5	Sub139	0.324	40	14	17.1	60	54
31	Sub177	0.332	44	16	17.6	30	111
1	Sub40	0.333	29	12	17.8	80	42
22	Sub207	0.337	36	25	3.4	60	56
25	Sub186	0.347	28	29	9.9	45	77
51	Sub197	0.370	25	0	25.9	40	92
50	Sub196	0.403	25	0	22.7	40	101
24	Sub199	0.427	35	22	13.6	45	95
15	Sub18	0.433	34	25	3.0	75	58
26	Sub188	0.437	27	21	7.4	50	87
23	Sub205	0.487	41	19	9.1	65	75
55	Sub8	0.493	25	0	25.9	56	88
3	Sub2200	0.496	25	0	25.3	75	66
49	Sub33	0.498	25	0	11.7	60	83
18	Sub44	0.527	38	20	2.5	60	88
14	Sub89	0.578	24	18	2.5	65	89
53	Sub71	0.579	25	0	8.6	75	77
52	Sub166	0.614	36	0	8.7	65	94
2	Sub72	0.615	25	9	23.4	75	82
19	Sub78	0.632	27	0	10.0	60	105
16	Sub86	0.660	26	11	3.9	50	132
17	Sub80	0.681	29	20	7.2	75	91
12	Sub91	0.682	35	20	2.2	75	91
6	Sub79	0.775	26	3	17.1	75	103
11	Sub29	0.891	25	0	13.1	50	178
9	Sub127	1.015	26	0	10.2	90	113
8	Sub180	1.548	33	12	7.8	100	155

Table 27: Infiltration properties before calibration

		Max Inf. Rate	Min Inf. Rate	Decay Constant	Drying time	Max volume
ArcMap ID	PCSWMM ID	mm/h	mm/h	1/h	Days	mm
42	Sub171	1	0.1	3	7	2
45	Sub176	1	0.1	3	7	2
54	Sub15	1	0.1	3	7	2
35	Sub148	1	0.1	3	7	2
46	Sub1	1	0.1	3	7	2
41	Sub175	1	0.1	3	7	2
39	Sub39	1	0.1	3	7	2
37	Sub146	1	0.1	3	7	2
38	Sub83	1	0.1	3	7	2
30	Sub30	1	0.1	3	7	2
34	Sub142	1	0.1	3	7	2
33	Sub145	1	0.1	3	7	2
21	Sub206	1	0.1	3	7	2
47	Sub84	1	0.1	3	7	2
44	Sub136	1	0.1	3	7	2
43	Sub135	1	0.1	3	7	2
36	Sub138	1	0.1	3	7	2
30	Sub31	1	0.1	3	7	2
48	Sub133	1	0.1	3	7	2
7	Sub137	1	0.1	3	7	2
40	Sub38	1	0.1	3	7	2
28	Sub790	1	0.1	3	7	2
20	Sub4000	1	0.1	3	7	2
27	Sub46	1	0.1	3	7	2
32	Sub150	1	0.1	3	7	2
13	Sub87	1	0.1	3	7	2
4	Sub82	1	0.1	3	7	2
10	Sub17	1	0.1	3	7	2
5	Sub139	1	0.1	3	7	2
31	Sub177	1	0.1	3	7	2
1	Sub40	1	0.1	3	7	2
22	Sub207	1	0.1	3	7	2
25	Sub186	1	0.1	3	7	2
51	Sub197	1	0.1	3	7	2
50	Sub196	1	0.1	3	7	2
24	Sub199	1	0.1	3	7	2
15	Sub18	1	0.1	3	7	2
26	Sub188	1	0.1	3	7	2
23	Sub205	1	0.1	3	7	2
55	Sub8	1	0.1	3	7	2
3	Sub2200	1	0.1	3	7	2
49	Sub33	1	0.1	3	7	2
18	Sub44	1	0.1	3	7	2
14	Sub89	1	0.1	3	7	2
53	Sub71	1	0.1	3	7	2
52	Sub166	1	0.1	3	7	2
2	Sub72	1	0.1	3	7	2
19	Sub78	1	0.1	3	7	2
16	Sub86	1	0.1	3	7	2
17	Sub80	1	0.1	3	7	2
12	Sub91	1	0.1	3	7	2
6	Sub79	1	0.1	3	7	2
11	Sub29	1	0.1	3	7	2
9	Sub127	1	0.1	3	7	2
8	Sub180	1	0.1	3	7	2

See pipe network properties in Appendix CD.8

5.2 Calibration results

This sub chapter will present the simulation results before- and after calibration. In addition, change of parameters will be explained and presented. Finally, profiles illustrating the peak flow by the end of the system will be presented.

5.2.1 Calibration of 02. June rain event

The event extracted from June was relatively easy to calibrate. However, which combination of parameters to be changed had to be determined in advance along with the type of rain event input.

By systematically changing individual parameters to investigate the degree of impact on the system outflow, a combination of at least two parameters were chosen for the final calibration. This was necessary since the change of one parameter alone didn't provide satisfactory results. As mentioned earlier in chapter 2, the calibration was to take into account both the maximum flow rate (l/s) and the total volume (m³) from the entire system. To view the system outflow before calibration, see figures 127 and 128 below. From Figure 127 it was clear that the flow rate had to be increased, along with the decrease of response time. From Figure 128 the total volume from the model was almost the same as the measured one by NVE. However, the total volume accumulated too late, which also underlined that the response time should be shortened. During the changing of individual properties, it seemed that two parameters had a crucial impact on the system outflow. These parameters were the pipe roughness (mm), and the percentage amount of surface imperviousness (%).

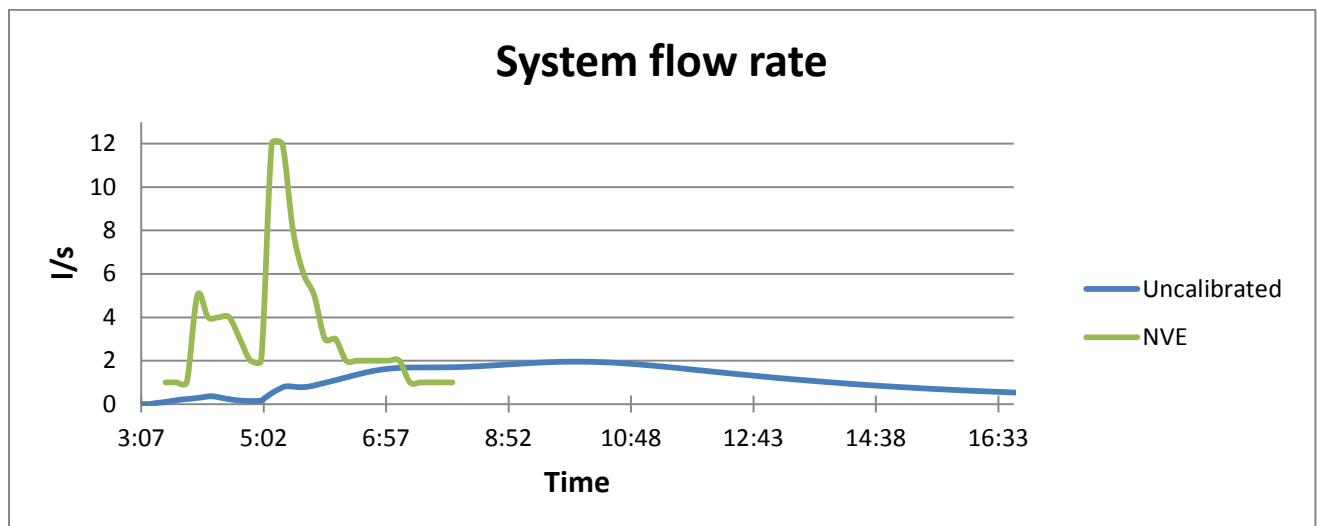


Figure 127: System flow rate before calibration, 02. June

The green curve represents the measured flow rate (l/s), the data set was obtained from NVE. The blue curve represents the simulated outflow from the model before calibration.

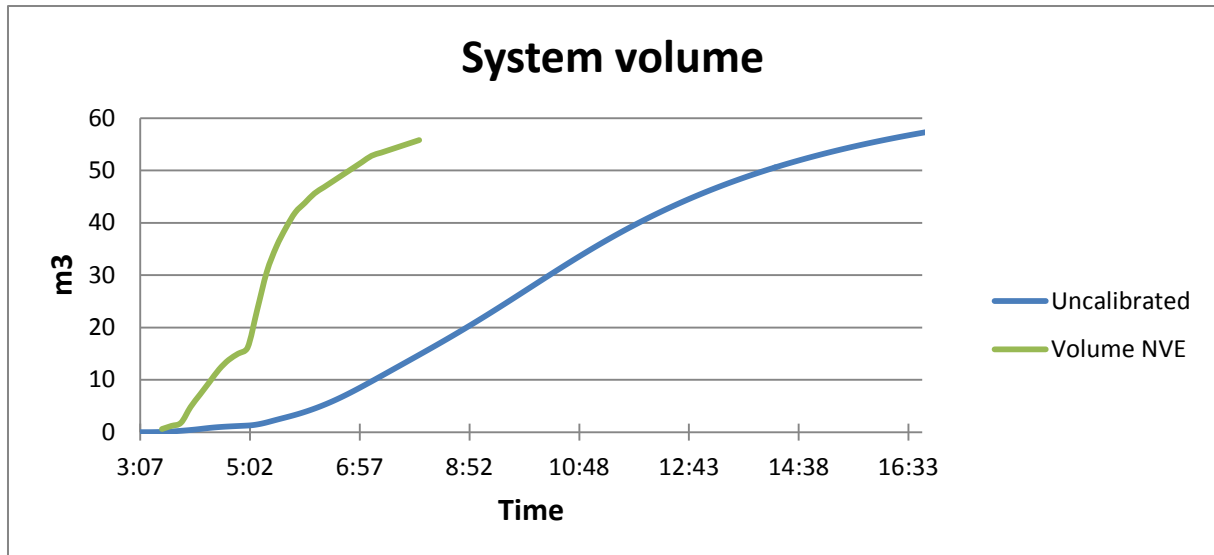


Figure 128: System volume before calibration, 02. June

By decreasing the pipe roughness, both the flow rate- and the response time changed considerably. At first the roughness was reduced from 1.0 to 0.04 mm to increase the flow rate up to the same level as the measured one (12 l/s). Especially for a 30 – 40 years old concrete pipe network, a roughness equal to 0.04 mm seemed very unrealistic. This raised questions to whether some of the network has been changed in later years after the original installation, or if some of the pipe diameter inputs were incorrectly stated. It was actually discovered that some of the diameters given by the municipality wasn't completely identical with the diameters given by the documentation written by Aasnes. Some of the diameters given by the municipality were slightly larger than the ones given by Aasnes.

The difference between the calibrated maximum flow rate and the measured one now only differed with 1.23 %. However, the calibrated volume still differed with 25.8 %. To decrease it, the degree of imperviousness was reduced with 30 %. The calibrated volume then only differed with 3.7 %. As a consequence the flow rate decreased a little bit. The roughness was then further reduced from 0.04 to 0.02 mm. Both the maximum flow rate and the total volume differed with 3.1% and 3.7%. To overview the results step by step, see figures next pages.

Calibration part 1:

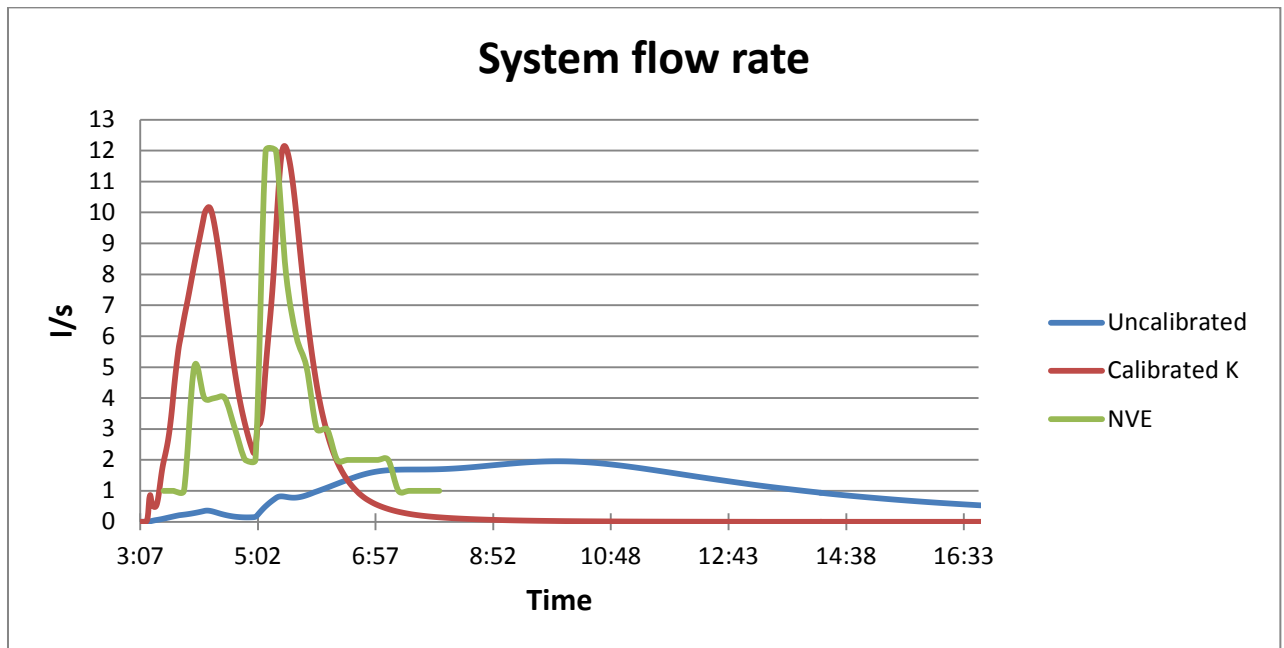


Figure 129: Flow rate results after first calibration of pipe roughness (K), 02. June

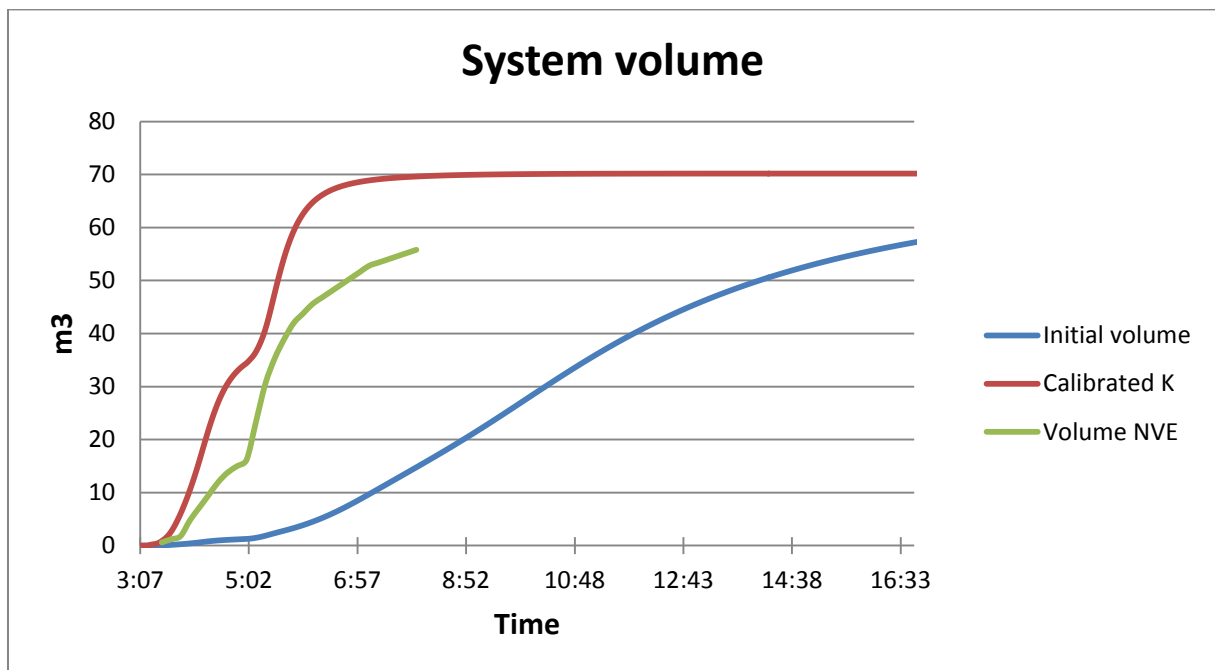


Figure 130: Total volume results after first calibration of pipe roughness (K), 02. June

Table 28: Calibration results after first reduction of pipe roughness, 02. June

	Max flow l/s	Max volume m3
NVE	12.0	55.8
SWMM	12.1	70
Difference %	1.23	25.8

Calibration part 2:

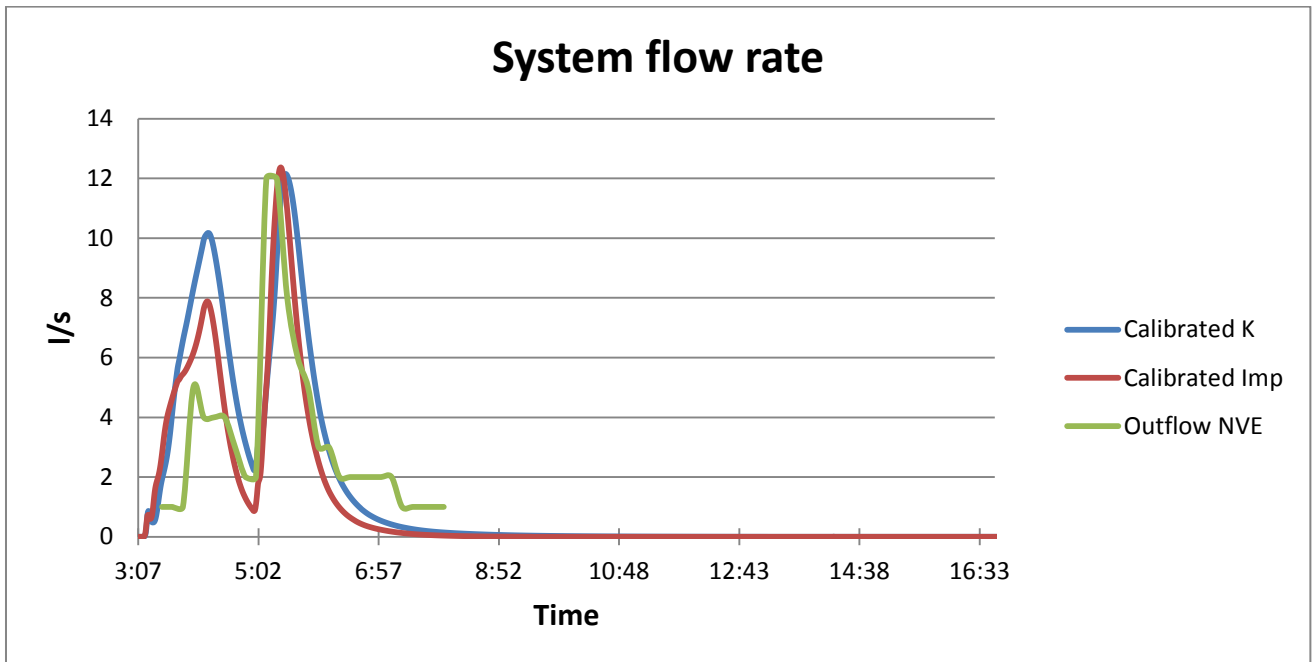


Figure 131: Flow rate results after final calibration of both pipe roughness (K) and imperviousness (%), 02. June

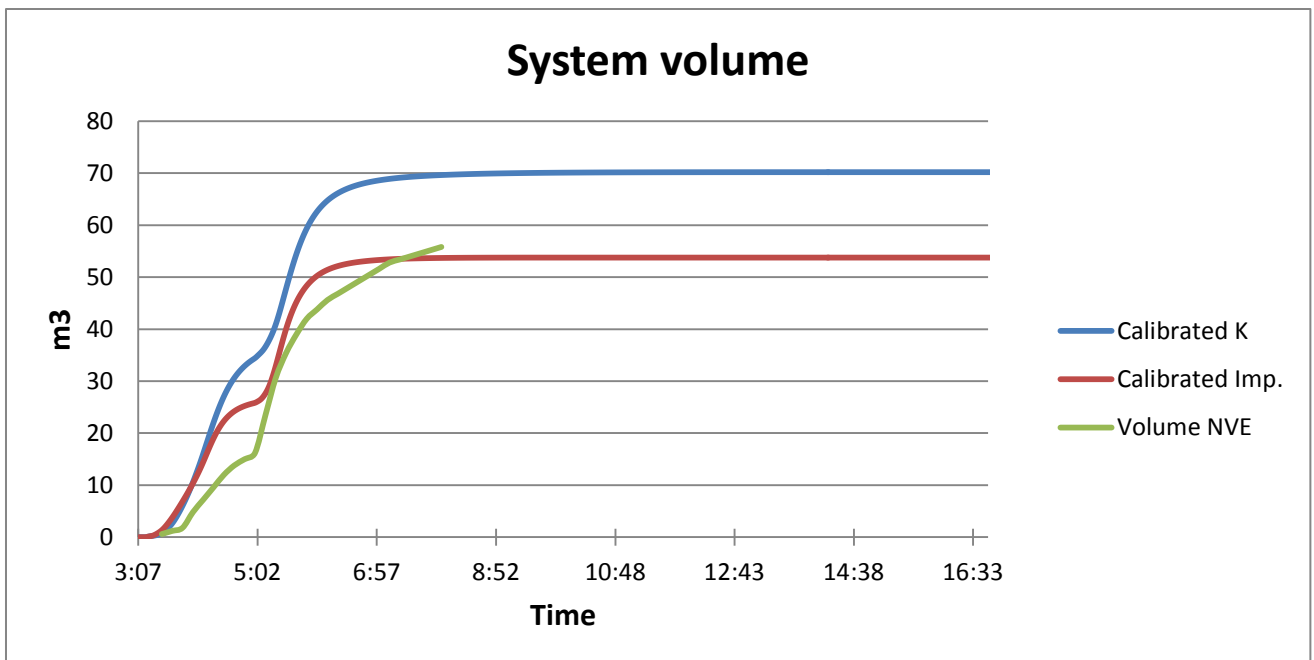


Figure 132: Volume results after final calibration of pipe roughness (K) and imperviousness (%), 02. June

Table 29: Final calibration results, 02. June

	Max flow l/s	Max volume m3
NVE	12.0	55.8
SWMM	12.4	54
Difference %	3.1	3.7

Table 30: Change of parameters during the calibration, 02. June

	K (mm)	Change Imp. %
Uncalibrated	1.00	0
Calibration 1	0.04	0
Calibration 2	0.02	-30

During the first part of the calibration, a change of rainfall input data was made. As earlier discussed in chapter 2 on page 35, there are three ways of importing rainfall data:

1. Importing the rainfall event into PCSWMM directly after conversion into 1 minute intervals.
2. Importing the rainfall event into PCSWMM after linear interpolation between the 1 minute intervals.
3. Importing the rainfall into PCSWMM after calculating the increase of precipitation by every minute.

In this case, input data was changed from principle 1 to principle 3 after comparison with each other. To view the flow rate generated from each input principle compared with the NVE's measurement, see figure 133 below.

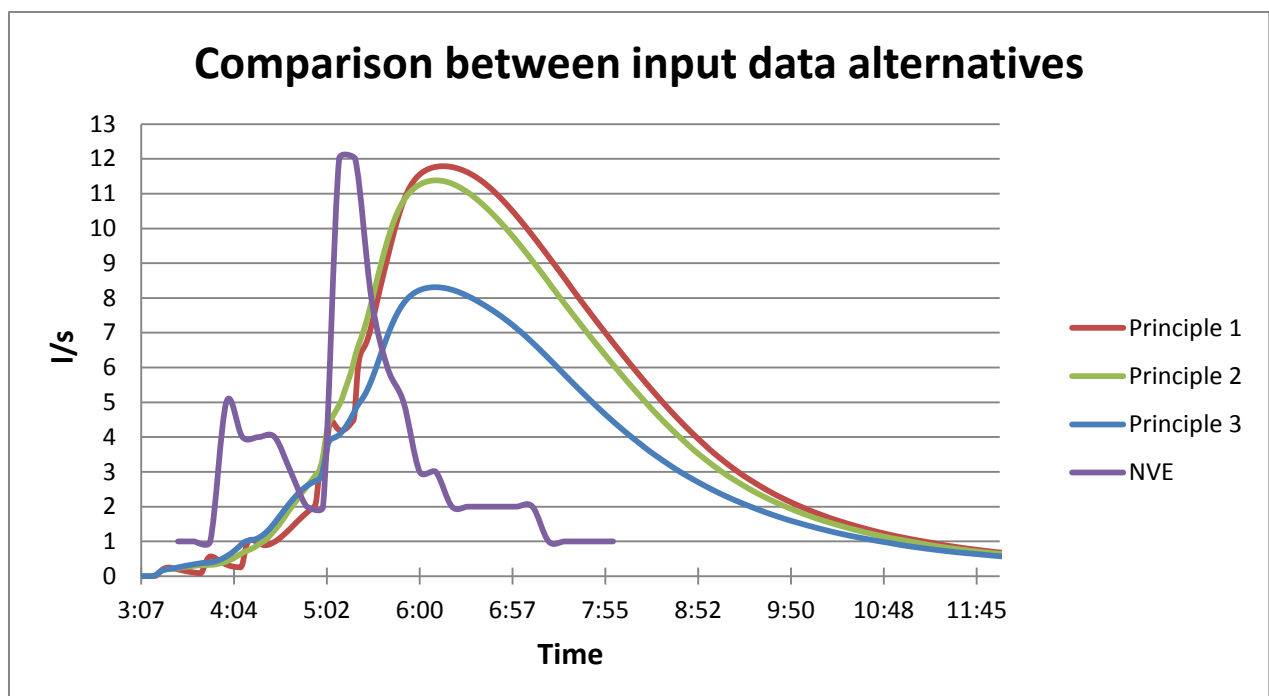


Figure 133: Comparison between flow rates, made from rainfall inputs following principle 1, 2 and 3

The rainfall input following principle 3 was chosen because it generated less volume from the system. It was easier to calibrate the maximum flow rate by reduction of pipe roughness.

The most important parameter to consider while performing calibrations depends on the purpose behind the operations. Here both maximum flow rate and total volume were taken into account. If by example the amount of storm water pollution was essential to investigate, perhaps the total volume should be prioritized. If a pipe network system was to be renovated or rebuilt, then the maximum flow rate should be prioritized.

5.2.2 Calibration of 16. August rain event

The event extracted from August was a bit complex to calibrate. The results from the status bar in PCSWMM showed that the total rainfall was equal to 21.1 mm, which was almost the double of the original amount given by the rainfall input. In this case, the rainfall input was based on principle 1 (directly imported into PCSWMM after conversion into 1 minute intervals). In addition, calibration of the total volume seemed to be more difficult than predicted.

The same procedure was performed here as for the event extracted from June, by changing individual parameters before picking out the ones with greatest impact on the results. The drawback was that it seemed that only one parameter was able to inflict larger changes; the pipe roughness. As for the event extracted from June, it was easy to increase the maximum flow rate to the required level. However, the total volume was almost 75 % higher than the measured one. As listed in chapter 2, the relevant parameters given for calibration were:

- Pipe roughness (mm)
- Imperviousness (%)
- Zero imperviousness (%)
- Flow length (m)
- Terrain slope (%)

All parameters except roughness were changed to both upper and lower extremities in the attempt to reduce the volume to the proper level. This didn't give any satisfactory results, and other parameters had to be looked upon.

The remaining two parameters available for change except the rainfall input were:

- Evaporation (mm)
- Infiltration (max and min infil. Rate, decay constant, drying time, and max volume)

By changing the evaporation, it was discovered that as much as 50 mm/h had to be added to satisfy the amount of total volume. This measure seemed to be both drastic and unrealistic to perform. This left only one option, by increasing the infiltration capacity.

The User's guide to SWMM5 defined several types of soil properties. The infiltration properties were described by five parameters based on Horton's equation. By changing the soil properties from moist soil to dry soil (partly vegetated), these parameters could be changed based on a realistic point of view. See Figure 18 chapter 2. The maximum infiltration rate was increased from 1 to 7 mm/h, and the minimum rate from 0.1 to 4 mm/h. The decay constant was decreased from 1/3 to 1/7 hour, and the drying time was shortened with 5 days. In addition, the maximum infiltration volume was increased by estimation from 2.0 to 100 mm. See figures below to view the results before, during and after the calibration steps.

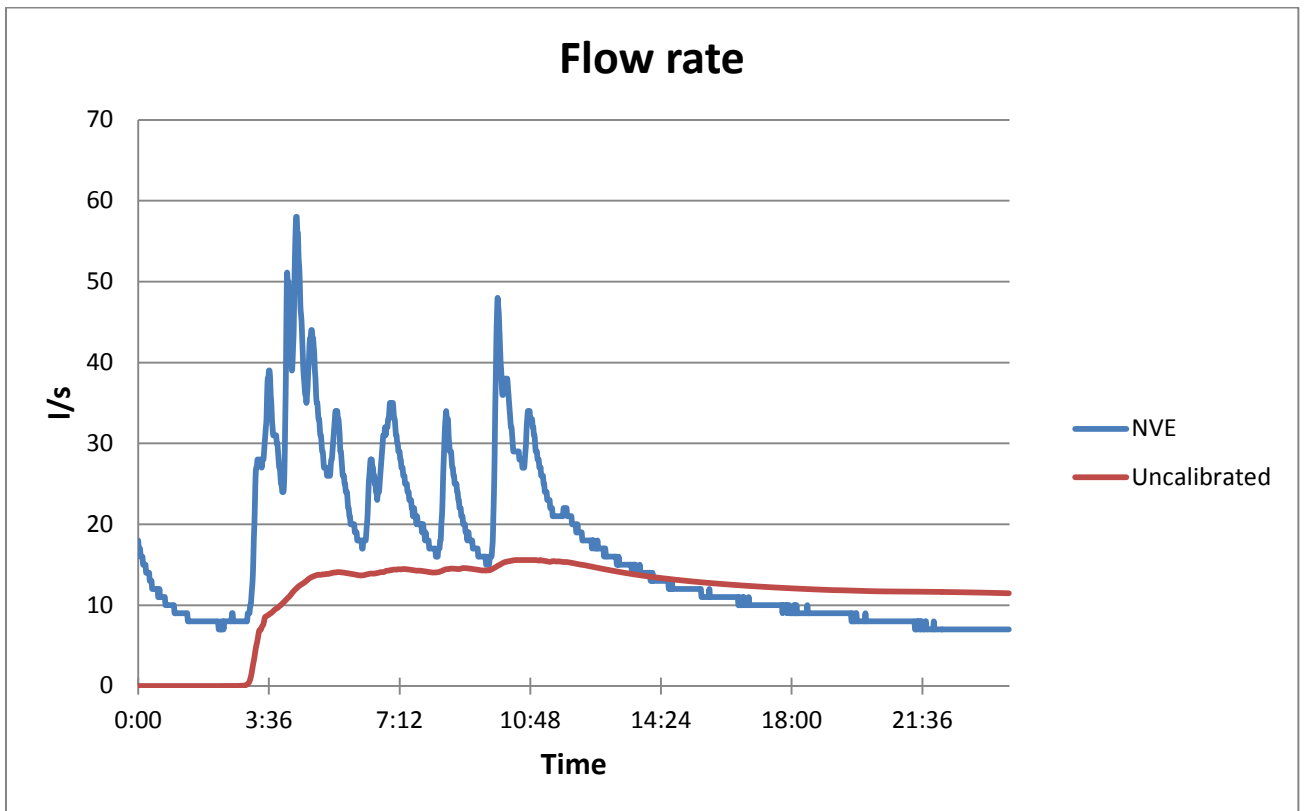


Figure 134: System flow rate before calibration, 16. August

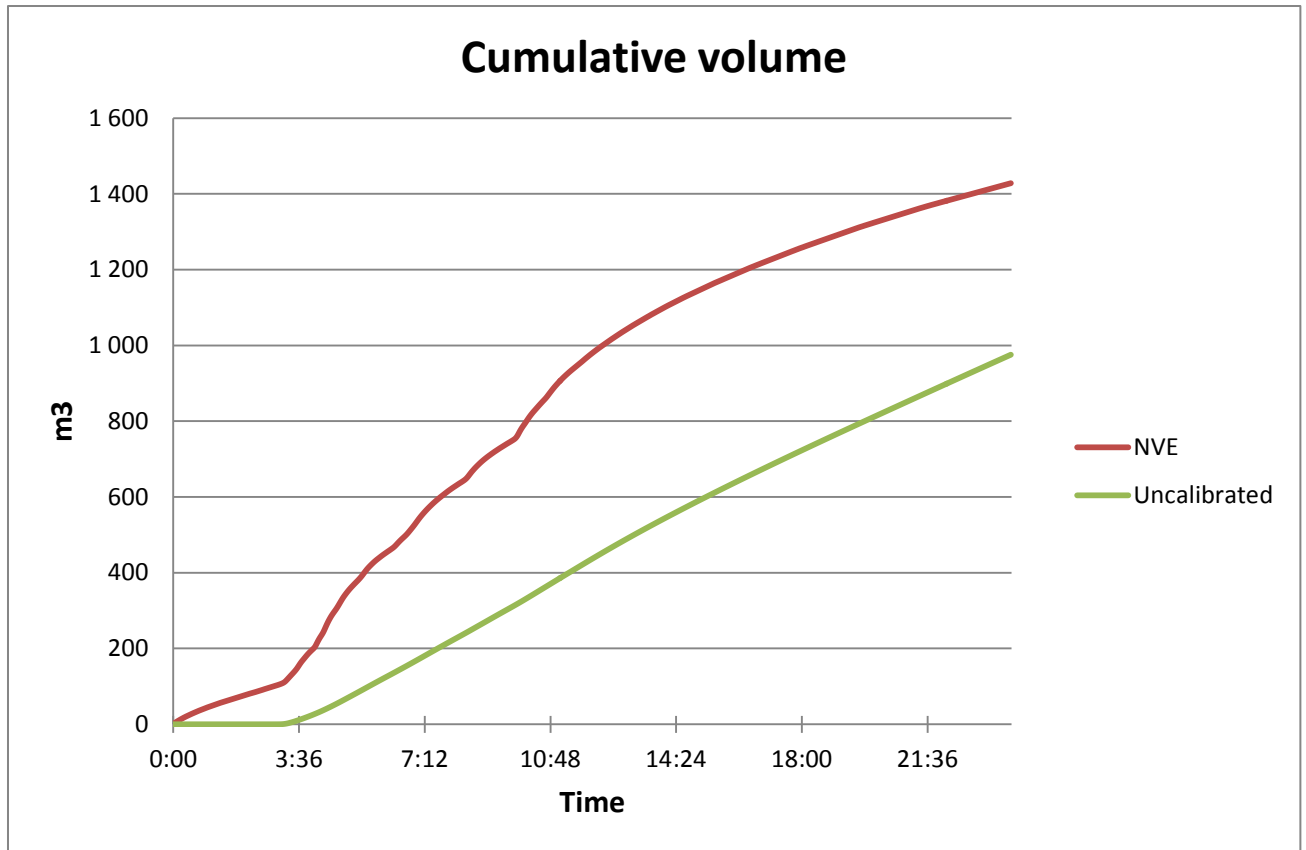


Figure 135: System volume before calibration, 16. August

Table 31: Initial conditions before calibration, 16. Aug

	Max flow l/s	Max volume m3
NVE	58.0	1428.2
SWMM	15.6	975.5
Difference %	73.1	31.7

Calibration part 1:

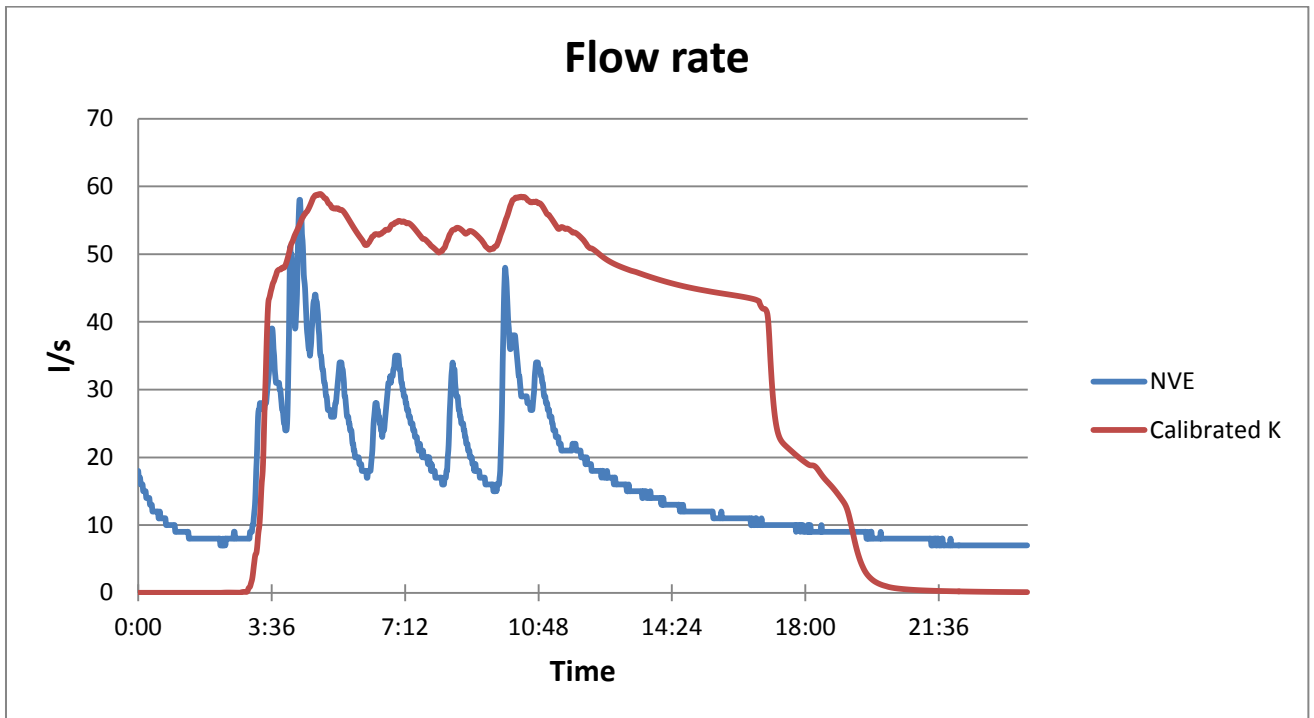


Figure 136: Flow rate after first calibration of pipe roughness (K), 16. August

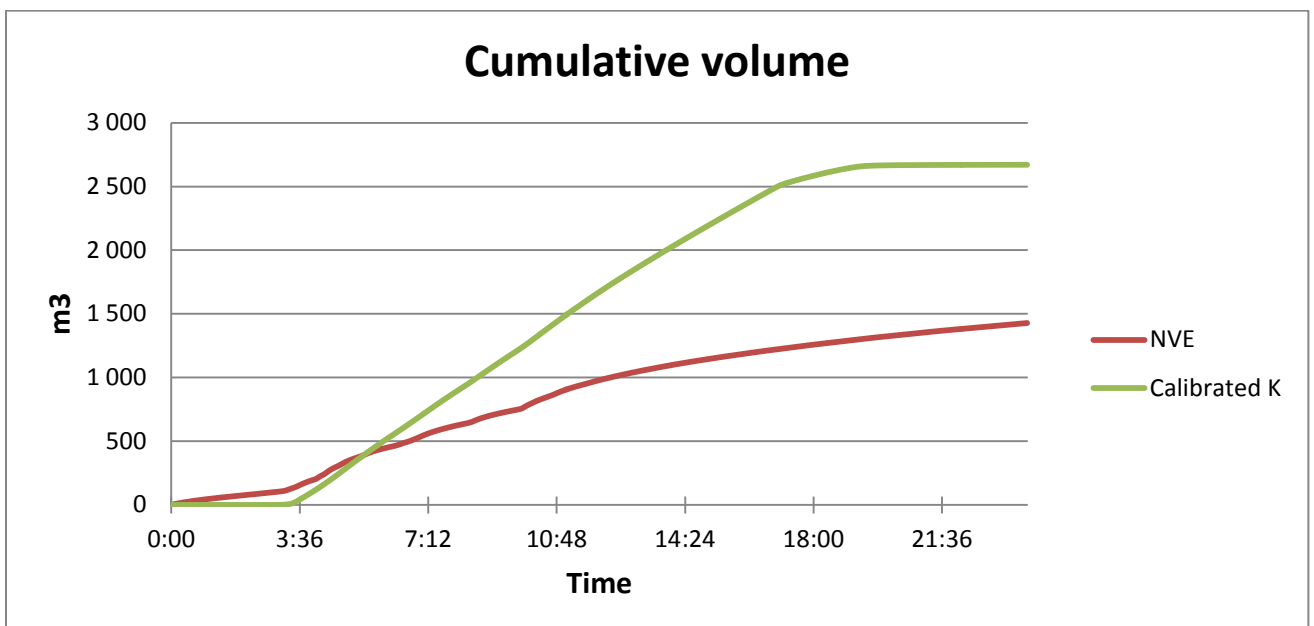


Figure 137: Total volume after first calibration, pipe roughness (K), 16. August

Table 32: Results from calibration part 1, 16. August

	Max flow l/s	Max volume m3
NVE	58.0	1428.2
SWMM	58.9	2670.8
Difference %	1.5	87.0

Table 33: Parameters changed during calibration part 1, 16. August

	K (mm)	Infiltration change
Uncalibrated	1	NO
Calibration 1	0.235	NO

Calibration part 2:

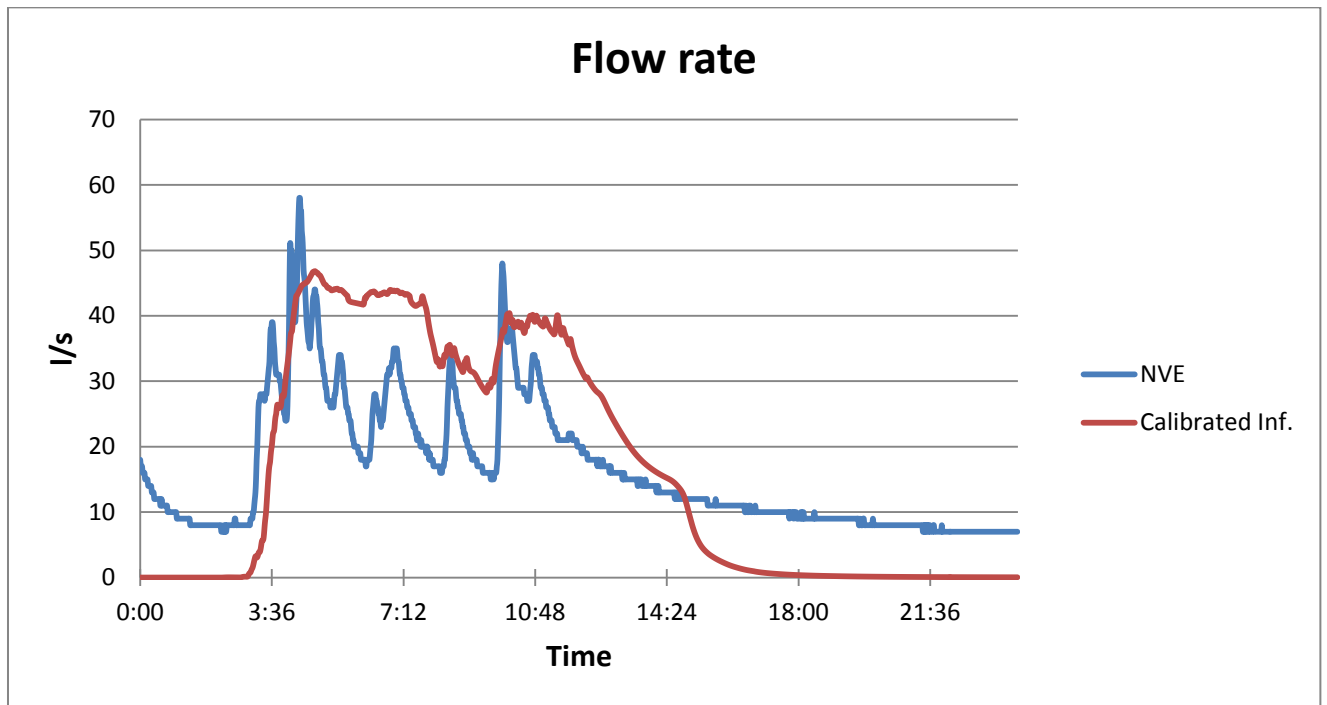


Figure 138: Flow rate after calibration part 2, infiltration changed, 16. August

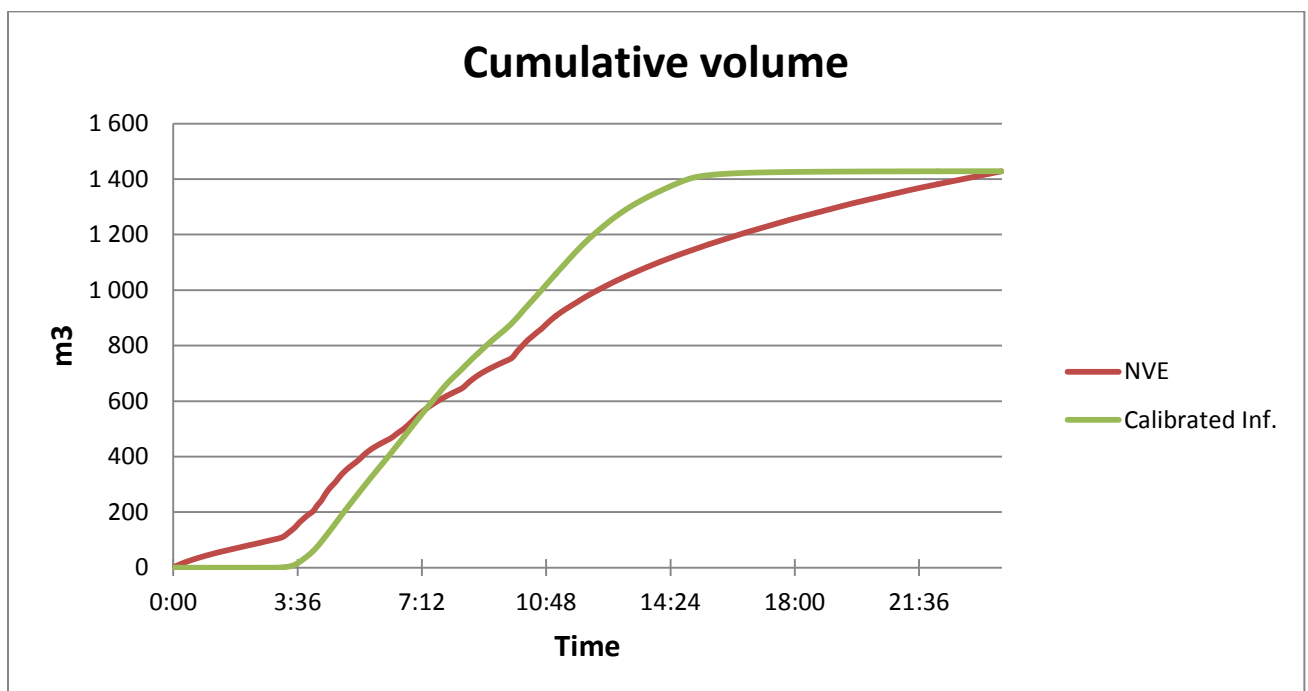


Figure 139: Total volume after calibration part 2, infiltration changed, 16. August

Table 34: Results from calibration part 2, 16. August

	Max flow l/s	Max volume m3
NVE	58.0	1428.2
SWMM	46.8	1428.5
Difference %	19.3	0.0

Table 35: Parameters changed during calibration part 2, 16. August

	K (mm)	Infiltration change
Uncalibrated	1	NO
Calibration 1	0.235	NO
Calibration 2	0.235	YES

Calibration part 3:

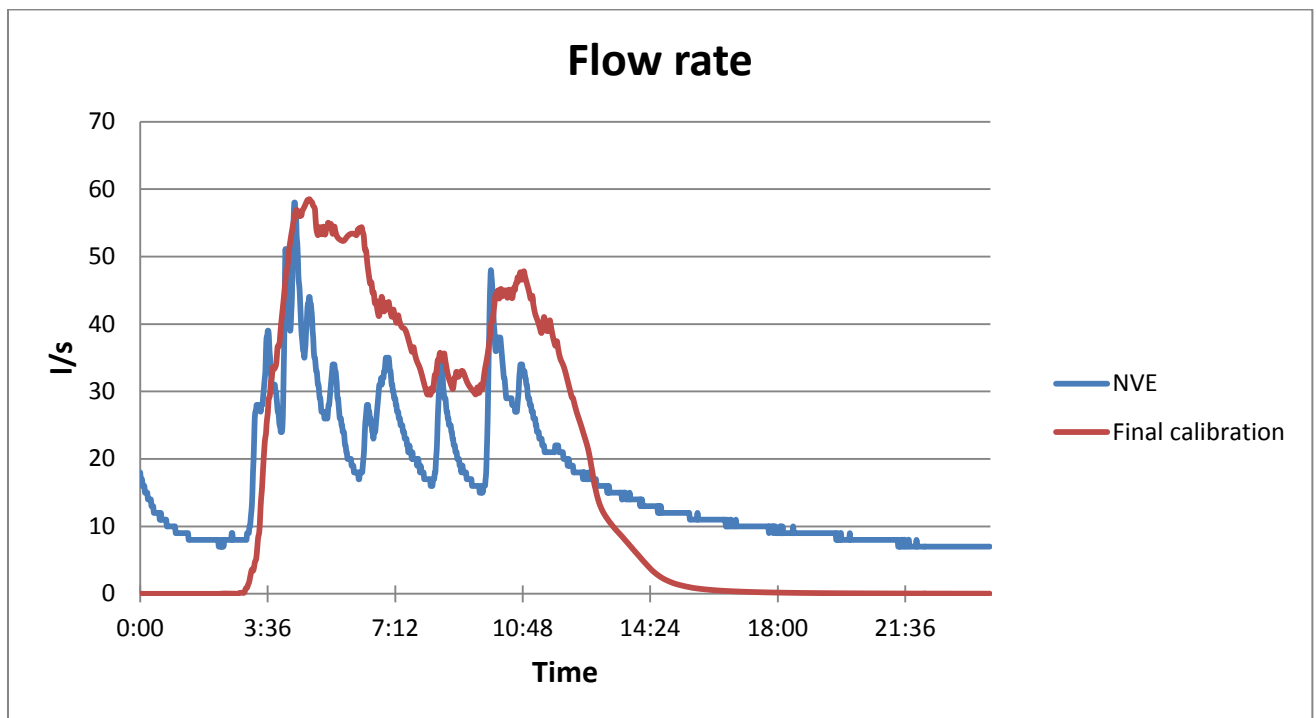


Figure 140: Flow rate after final calibration, 16. August

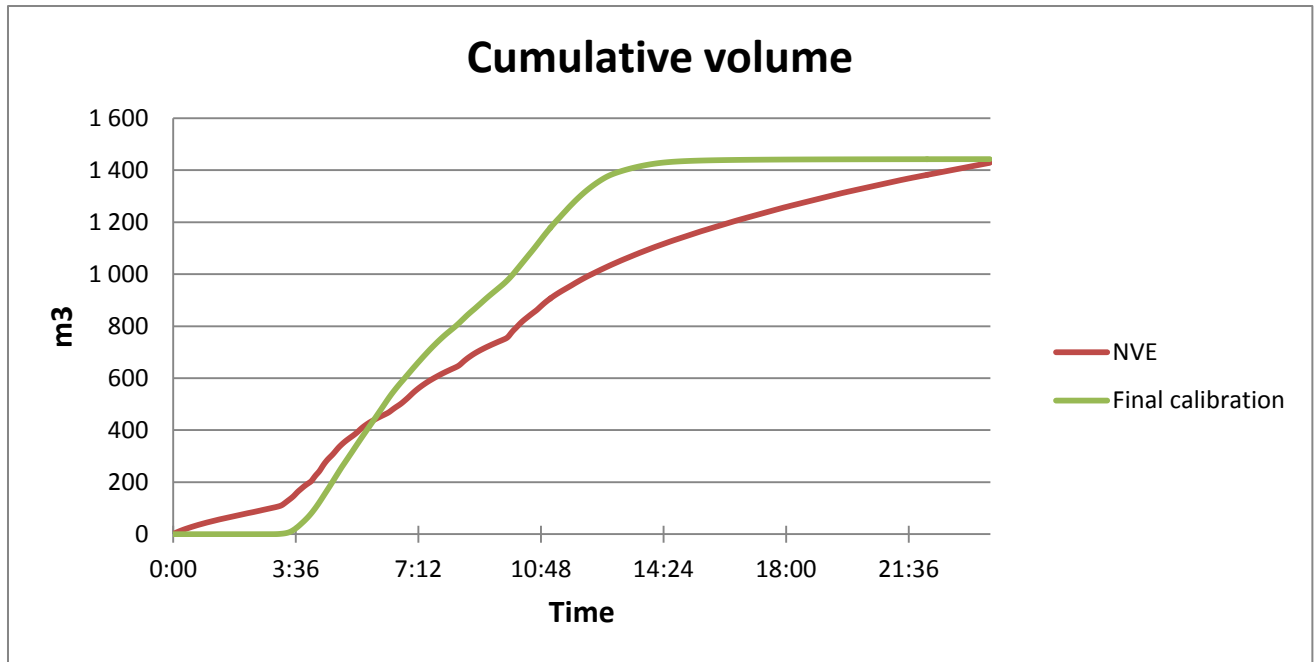


Figure 141: Total volume after final calibration, 16. August

Table 36: Results after final calibration, 16. August

	Max flow l/s	Max volume m3
NVE	58.0	1428.2
SWMM	58.5	1442.3
Difference %	0.9	1.0

Table 37: Parameters changed during the calibration steps, 16. August

	K (mm)	Infiltration change
Uncalibrated	1	NO
Calibration 1	0.235	NO
Calibration 2	0.235	YES
Calibration 3	0.185	YES

As mentioned in chapter 2, the SWMM routine was based on the box principle. This meant that as soon as the rainfall overloaded the infiltration capacity, the additional contribution of surface water was included into the hydraulic part of the simulation. This may be the explanation why the total system volume changed very little even when the entire field was made almost 0 % impervious. In other words, that meant that the predefined infiltration capacity was way too small.

Something that is difficult to explain is why the total rainfall result was stated to be 21.1 mm in total. Basically, that wouldn't even be physically possible considering the rainfall input itself gave a total of 12 mm. However, a rainfall input following principle 3 (calculation of the increase of precipitation every minute) should be tested for this event. See Figure 142 to overview the runoff quantity continuity for 16. August.

*****	Volume	Depth
Runoff Quantity Continuity	hectare-m	mm
*****	-----	-----
Total Precipitation	0.449	21.100
Evaporation Loss	0.008	0.394
Infiltration Loss	0.298	14.011
Surface Runoff	0.144	6.773
Final Surface Storage	0.000	0.000
Continuity Error (%)	-0.373	

Figure 142: Runoff quantity continuity for 16.August

5.2.3 Peak flow profiles

02. June 2011

Before calibration:

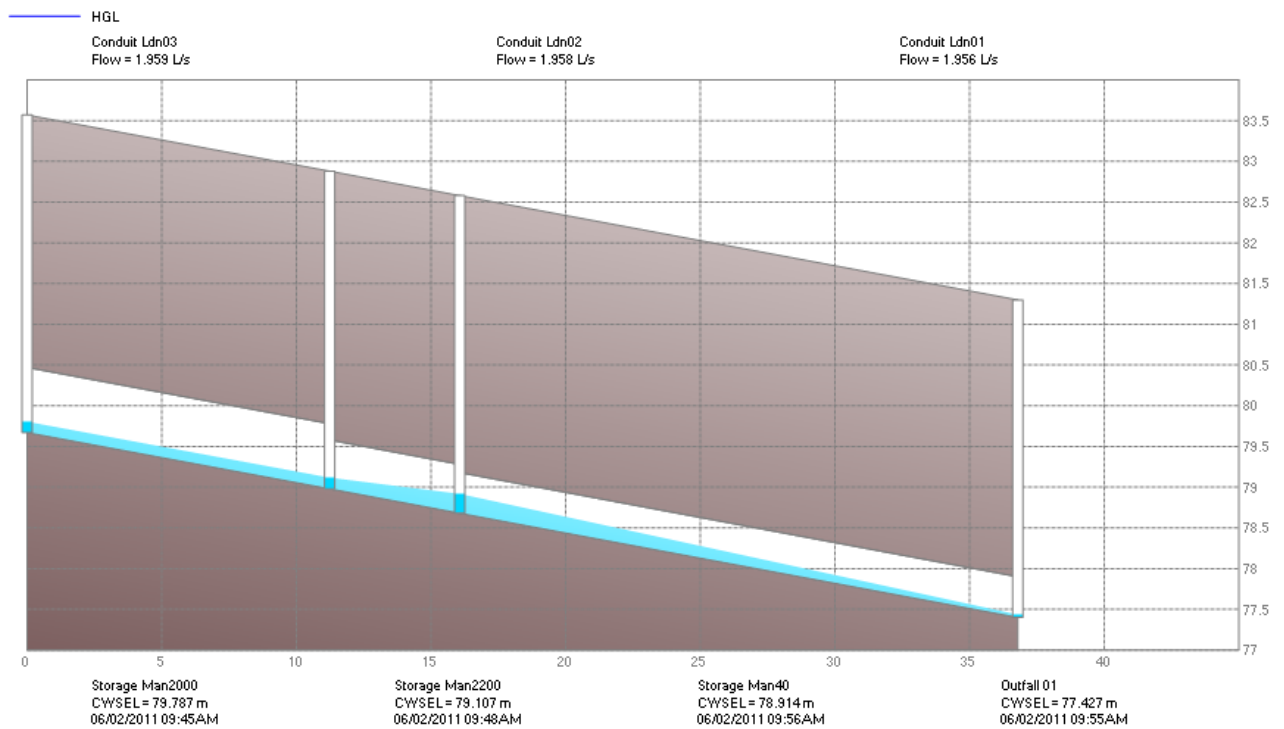


Figure 143: Maximum flow rate by the end of the system before calibration of 02. June

After calibration:

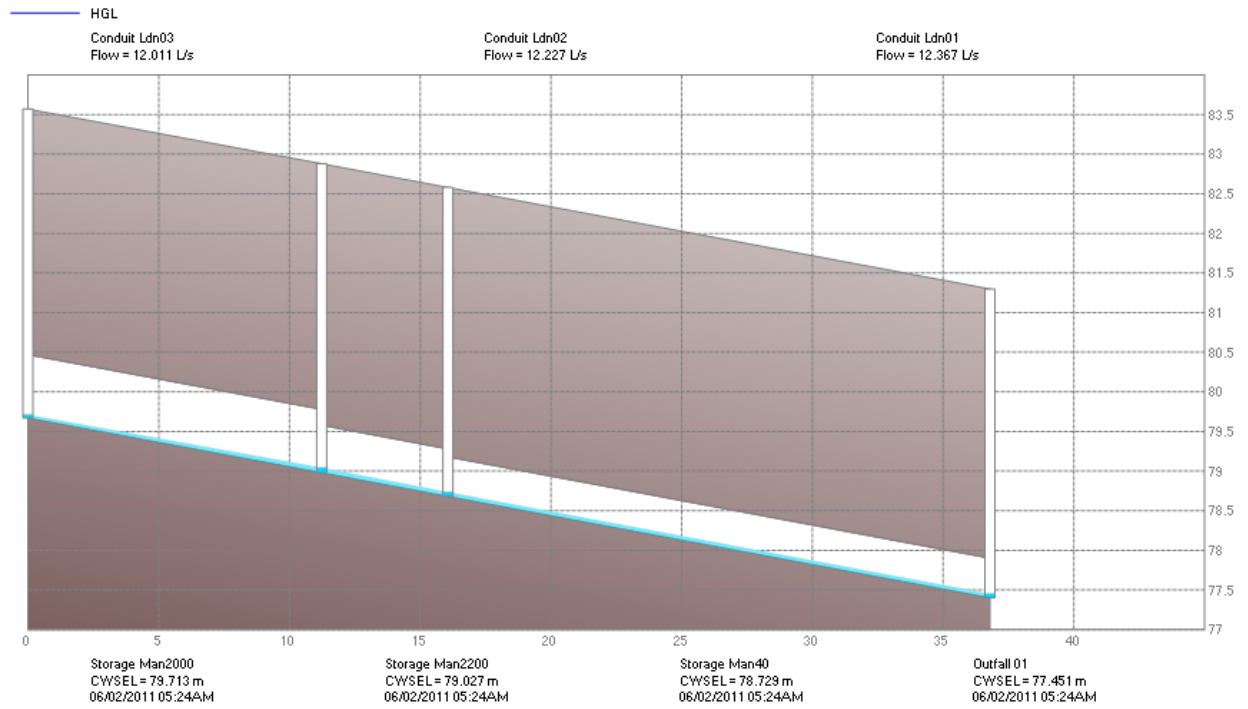


Figure 144: Maximum flow rate by the end of the system after calibration of 02. June

16. August 2011

Before calibration:

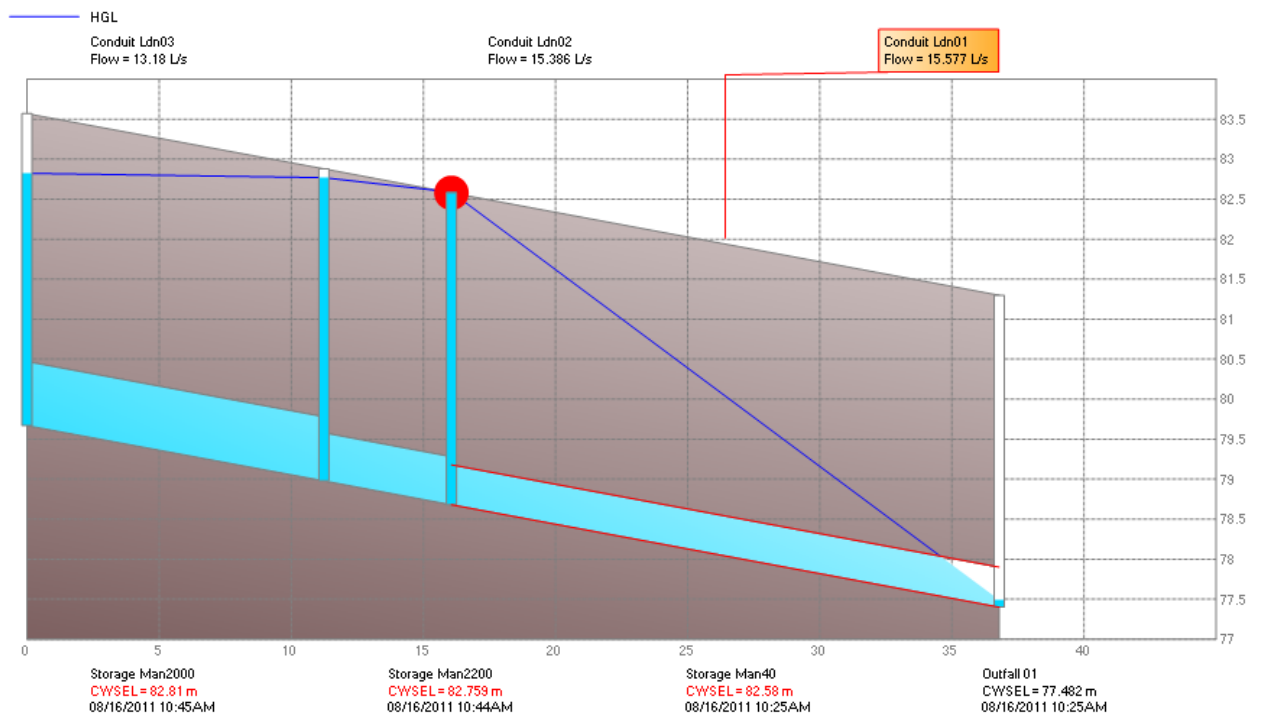


Figure 145: Maximum flow rate by the end of the system before calibration of 16. August

The blue line represents the hydraulic gradient line, and the circular red symbol represents surface flooding.

After calibration:

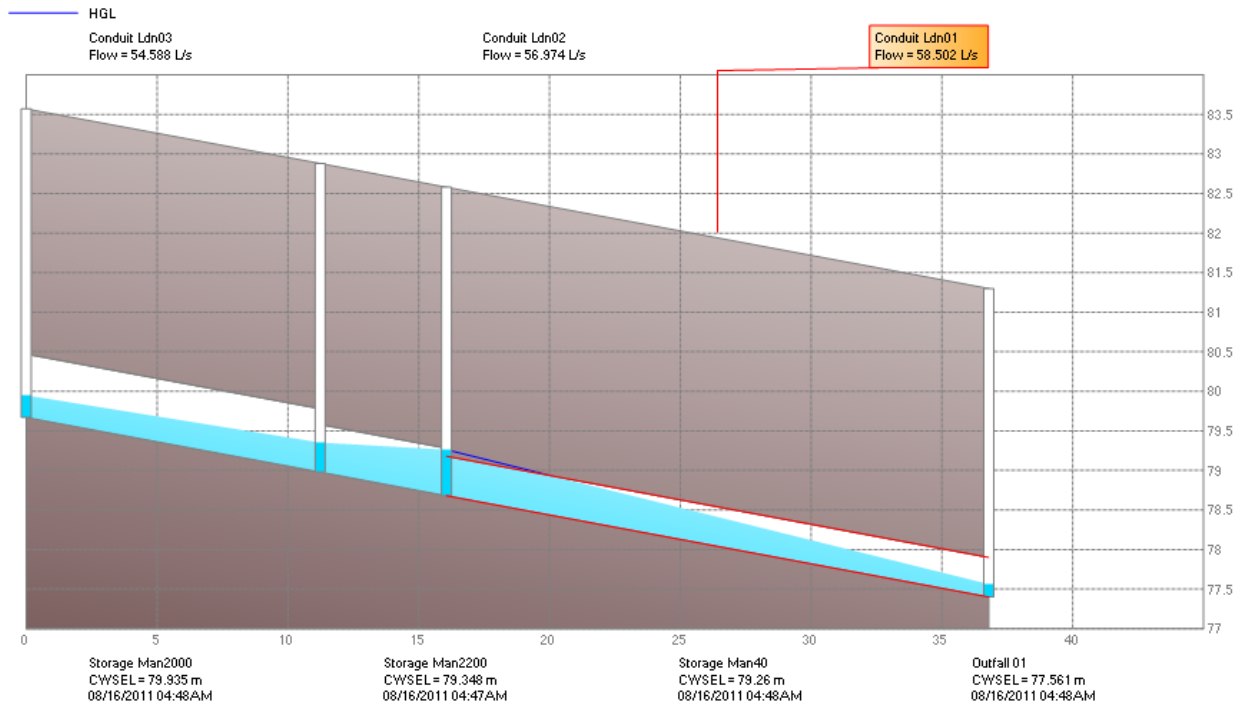


Figure 146: Maximum flow rate by the end of the system after calibration of 16. August

The PCSWMM files along with the rainfall events are available in Appendix CD.9.

6. Conclusions

The thesis provided a clear overview of the current conditions at the RUHRF. However, it also revealed how uncertain some of the catchment properties could be, and the degree of validity for some of the instruments at RUHS. The same goes for the available information about the pipe network.

The following findings of this thesis will be listed and explained below.

- The outer field boundary drawn during field inspections was considered to be partially valid. The watershed analyses generated catchments that were similar to it. However, the runoff contribution from the terrain surface (0.86 ha) located at the southeast area remains to be fully clarified. The thesis definition of the main catchment's total size is estimated to be between 20.84 to 21.70 hectares (21.27 +/- 0.86 ha).
- The topographic analyses of the main catchment performed in ArcMap and ArcScene were considered to be valid. The TIN – model, DEM, slope map and the spatial model gave very accurate representations of the main catchment and its contents.
- Changes have recently been made inside the main catchment (construction of new apartments, and installation of new storm water manhole). However, thus far these changes are too small to cause any significant effects.
- Most of the pipe network data were accounted for. A combination of obtaining data from both Trondheim Municipality and the earlier documentation written by E. Aasnes seemed to provide enough information for modeling purposes.
- The determination of surface characteristics was considered to be valid, since the creations of polygons were based on geo referred satellite images. However, the runoff coefficients used for these surfaces may be inaccurate.
- The number of sub catchments exceeded the expected amount. However, the count was almost identical to the runoff model developed by DHI. In addition, the model wasn't too difficult to calibrate after the real conditions. The runoff model is therefore considered to be realistic.
- The comparison between the precipitation gauges showed that the newly installed Geonor gauge didn't provide realistic precipitation data. Whether the equipment is malfunctioning, or the CR1000 logger contains mathematical errors, or the failure is partially affected of human activity, is difficult to determine at this time. The precipitation data from the Lambrecht gauge seemed to be very similar for both NVE's Sutron logger and NTNU's CR1000 logger.
- The statistical calculations of historical precipitation data showed that the annual amount of precipitation had slightly increased since 1986 (1.6 – 2.7 %). This development could perhaps confirm the trends in precipitation due to climate change. However, further studies regarding individual rainfall events should be performed as well.
- Both rainfall events used for runoff model calibration developed two independent water balance equations. These showed that the relationship between the precipitation and the infiltration for both events seemed to be partially similar. However, what must be taken into account is that the increased amount of infiltration had to compensate for the larger total

amount of precipitation (21.1 mm >> 12 mm). The amount of evaporation deviated naturally between the events.

- The formidable reduction of pipe roughness coefficients during the calibration could perhaps be a sign of pipe network changes in later years, which have not been accounted for. It was discovered that some of the diameters given by the municipality wasn't completely identical with the diameters given by the documentation written by Aasnes. Some of the diameters given by the municipality were slightly larger than the ones given by Aasnes.
- Thus far, it seemed that the best rainfall input to use regarding runoff model calibration was the input that followed principle 3: Importing the rainfall into the model after calculating the amount of increased precipitation every minute.
- The infiltration properties underwent major changes from the calibration of 02. June event to the calibration of the 16. August event. To determine the true infiltration capacity of the field could be complex. Because of the large deviation between the rainfall input and the simulated rainfall for the 16. August event, the main catchments true infiltration capacity could be approximately 5 mm. This must be further studied.

- In this thesis, the overall conclusion about Risvollan urban hydrological research field is that it is considered to be very representative for analysis regarding surface runoff in urban districts. By carefully using sophisticated softwares, it is easy to create physical models and perform runoff simulations. It is important however, to understand the local conditions in great detail in advance before performing such operations. Yet, a model is supposed to simplify the reality by producing satisfactory results adapted to the local environment. There is a close relationship between the time consumed for model development, the detailed quality of properties within the model, and the final results it actually produces.

6.2 Future studies

As mentioned earlier in the previous sub chapter, the thesis provided a clear overview of the current conditions at the RUHRF. It also revealed how uncertain the conditions could be as well. Below are listed suggestions that may help further studies.

- Check long-term plans for development in the field (Planning and Building Services / Trondheim Municipality), any possibilities for additional connections to the storm water system?
- Connect the storm water- and the wastewater measurement to NTNU's CR1000 logger.
- Closer examination of the field evaporation- and infiltration properties (take soil samples, find out more exact the amount of vegetation/trees)
- Test the runoff model in winter conditions, is it appropriate to extend / modify the water balance equation? Maybe also use the model to investigate the possibilities of LID solutions or surface water contamination.
- Test the runoff model by simulating flooding situations inside RUHS.

- Contact Geonor manufacturer for modification/calibration of the gauge. Further studies by comparison with Lambrecht and Plumatic gauges.
- Empty the V – notch weir basin frequently for sediments.
- Check with CHI if they are planning to develop import options for 3D – terrain.
- Measure flow rate generated from the southeastern area of the main catchment during heavy rainfall situations. Record the amount of rainfall as well.
- Reconsider the use of runoff coefficients.
- Clarify the actual pipe dimensions of the entire storm water system of RUHRF.
- Gather historical precipitation data from Voll station and the earlier station Tyholt, for comparison with precipitation data from Risvollan. Any local differences revealed?
- Check if any of the manholes are filled during heavy rainfall, especially manholes downstream pipes with steep slopes.
- Compare the results generated from this thesis model in PCSWMM with the DHI's model in Mike Urban.
- Expand the current pipe network inside the SWMM model (maybe include all pipe dimensions less than to 200 mm?)

References

MSc student Torstein Dalen, 2011, IVM NTNU

Thorolfsson, S.T., & Høgeli, S.A. 1994. Risvollan – Trondheim urban hydrologic research field. Trondheim: Department of Hydraulic and Environmental Engineering. *Norwegian: Thorolfsson, S.T., & Høgeli, S.A. 1994. Risvollan – Trondheim Urbanhydrologiske Forskningsfelt. Trondheim: Institutt for Vassbygging*

The great norwegian lexicon, 2011. Norwegian: Store norske leksikon, 2011. From: <http://snl.no/Sor-Trondelag/fylke>

IVM RUHS, 2011. From: <http://www.ivt.ntnu.no/ivm/risvollan/>

ESRI Website, 2011. From <http://www.esri.com/>

Ranveig Høseggen, 2010. FKB – data, Trondheim Municipality

Professor Karl Yngve Frøyen, 2011. Department of Urban Design and Planning.

WMS, 2011. ESRI. From: http://help.arcgis.com/en/arcgisserver/10.0/help/arcgis_server_java_help/index.html#/009200000051000000

Watershed Delineation Tools, 2011. ESRI. From: <http://arcscripts.esri.com/details.asp?dbid=15148>

Professor Karl Yngve Frøyen, 2011. Terrain- and raster analysis. Department of Urban Design and Planning.

Exploring digital elevation models, 2011. ESRI. From: <http://help.arcgis.com/en/arcgisdesktop/10.0/help/index.html#/009z0000005n000000.htm>

How watershed works, 2011. ESRI. From: http://help.arcgis.com/en/arcgisdesktop/10.0/help/index.html#/How_Watershed_works/009z00000000000680/

Hydraulic Design Manual, 2009. From: http://onlinemanuals.txdot.gov/txdotmanuals/hyd/the_rational_method.htm

E. Aasnes, 1985. Urban fields Blakli and Risvollan Field Documentation and data control with subsequent simulation.

Senior engineer Olav Nilssen, 2011. Trondheim municipality

Trondheim Municipality website, 2011. From: http://webhotel2.gisline.no/GISLINEWebInnsyn_Trondheim/

Documentation of Risvollan Urban Hydrological Research Field, 2011

Trondheim Municipality, 2005. FKB – data received from Professor Karl Yngve Frøyen autumn 2011, Department of Urban Design and Planning, NTNU.

Wiel Wauben, 2004. Precipitation amount and intensity measurements with the Ott Pluvio.

The Metrological Institute of Norway (DNMI), 2011. From:
http://sharki.oslo.dnmi.no/portal/page?_pageid=73,39035,73_39049&_dad=portal&_schema=PORTAL

The Metrological Institute of Norway (DNMI), 2011. From:
<http://www.yr.no/>

Norwegian water resources and energy directorate (NVE), 2011. From:
<http://www.nve.no/>

Norsk Vann Report 162, 2008.

S.Lawrence Dingman, 2008. Physical Hydrology

Norwegian Climate Center, 2009.

The Norwegian Geological Research Institute (NGU), 2011. From:
<http://www.ngu.no/kart/losmasse/>

Senior engineer Harald Sveian, 2011. NGU

William James, Lewis E. Rossman et.al, 2008. User's guide to SWMM5

Hans Vebjørn Kristoffersen, 2010. Master thesis Analysis of stormwater system

CHI, 2011. From:
<http://www.chiwater.com/Software/PCSWMM.NET/index.asp>

David Butler and John Davies, 2010. Urban drainage 3rd edition

Lewis E. Rossman, 2009. Storm water management model, User's manual version 5.0

PH – Consults, 2001. Lecture notes from Professor Sveinung Sægrov

Senior engineer Harald Viken, 2011. NVE

Senior engineer Svein Taksdal, 2011. NVE
Norsk Vann Report 172, 2008. L. S. Hafskjold

Documentation of Risvollan Urban Hydrological Research Field, 2011

Basal, 2011. From:

<http://www.basal.no/admin/kategorier/bilder/Basal%20prod.katalog%20s14.pdf>

Post Doc. Tone Muthanna and engineer Helge Aarøen (ITAS), 2011. CR1000 Manual

PhD student Teklu Tesfaye Hailegeorgis, 2010. IVM

Senior engineer Birgitte Johannessen, 2011. Trondheim Municipality

Professor Sveinung Sægrov, 2011. IVM

IVM Thorolfsson, S.T, 08.09 2010. Folder: Uhdata- Risvollan.pdf

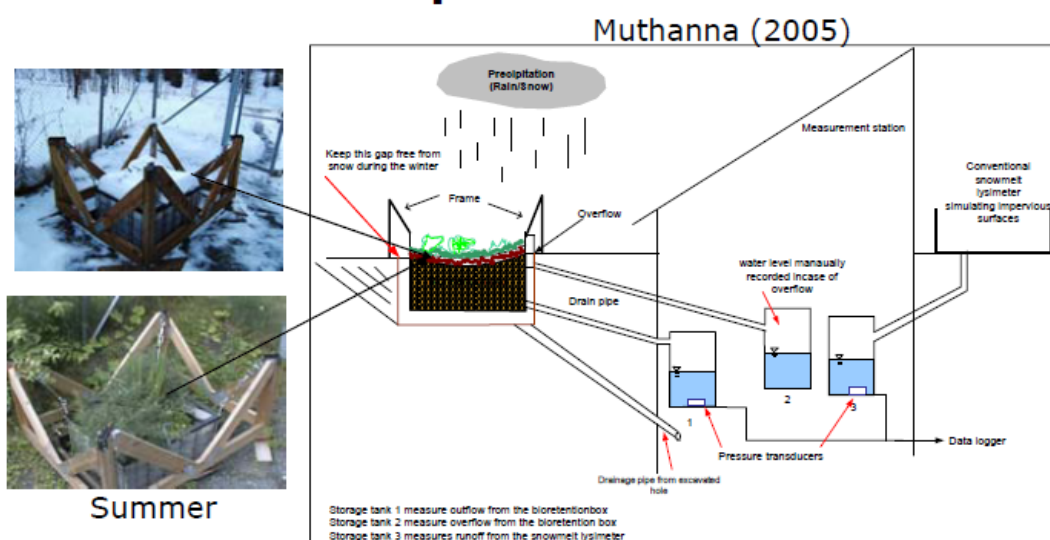
Appendices

Appendix A: Some RUHRF/RUHS thesis

Later storm water projects:

- 2011, Torstein Dalen (Semester thesis: Hydrologic performance of rain bed in cold climate conditions).
- 2010, Christian Sveen (Semester thesis: Surface analysis of RUHRF, pervious and impervious areas, runoff coefficients).
- 2008, Jan Inge Claudius (Master thesis: Former, present and future storm water management).
- 2007, Jan Inge Claudius (Semester thesis: Detention pond, LID – solutions).
- 2006, Espen Artzen (Semester thesis: Green roofs, ponds, closed detention, LID – solutions).
- 2005, Jostein Meyer (Semester thesis: Open storm water management, reduction of flooding downstream the catchment)
- 2005, Tone Muthanna (PhD thesis: bioretention box with different plant species, compared with normal runoff by using the snowmelt lysimeter)

Research setup at Risvollan



Plant species used in the bioretention box:

Common Norwegian name	Latin name	Type of plant
Strandkattehale	Lythrum salicaria	Flower
Sverd Iris	Iris pseuacorus	Flower
Gravmyrt (evergreen)	Vinca Minor	Small ground cover shrub
Tinved	Hippophae rahmnoides	Shrub

Sveinn T. Thorolfsson

21

Figure: Bio retention project, PhD thesis by Tone Muthanna in 2005 From IVM Thorolfsson, S.T, 08.09 2010. Folder: Uldata- Risvollan.pdf (Appendix B)

Earlier projects from IVM RUHS, 2011

Literature

Data from the RUHS has been used in many Ph.D., M.Sc. theses and scientific/engineering articles/reports throughout the years.

Ph.D. theses.	Year
Matheussen, B.V. Effect of anthropogenic activities on snow distribution, and melt in an urban environment. Norwegian University of Science and Technology (NTNU). Faculty of Engineering Science and Technology. Department of hydraulic and Environmental Engineering. ISBN 82-471-6347-0	2004
Linmei, Nie Flooding analysis of urban drainage systems. Norwegian University of Science and Technology (NTNU). Faculty of Engineering Science and Technology. Department of hydraulic and Environmental Engineering. ISBN 82-471-6240-7	2004
Risholt, L.P. Pollution based real time control of urban drainage systems. Norwegian University of Science and Technology (NTNU). Department of hydraulic and Environmental Engineering. ISBN 82-7984-062-1	2000
Lei, J. H. Uncertainty analysis of urban rainfall - runoff modelling. Norwegian University of Science and Technology (NTNU). Department of hydraulic and Environmental Engineering. ISBN 82-7119-966-8	1996

Documentation of Risvollan Urban Hydrological Research Field, 2011

M.Sc. theses (In Norwegian)

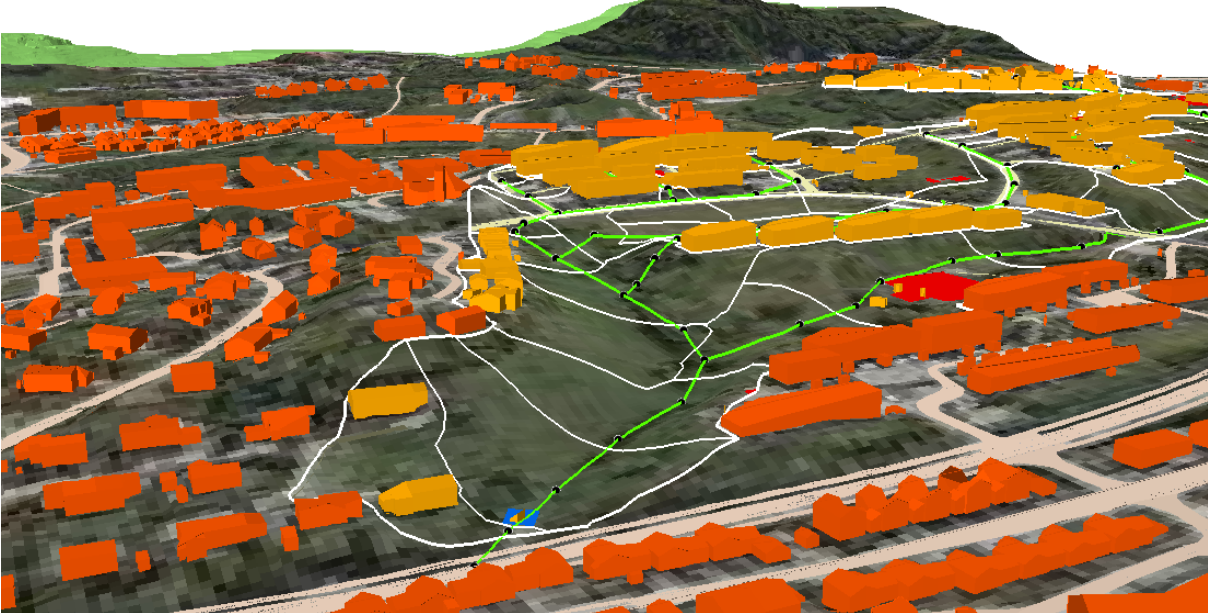
Garder, O.E. Belastningskontroll og tiltaksvurdering for overvannssystemer. Studieområde: Flatåsen i Trondheim	2004
Sætern A.I. Tiltaksanalyse vha urbane avrenningsmodeller Studieområde: Fredlybekken feltet med delfeltet Risvollan i Trondheim	2002
Brunvoll E. Analyse av flommen i Fredlybekken i Trondheim i månedskiftet mars/april 1997 basert på informasjon fra Risvollan feltlaboratorium.	2000
Matheussen B.V. Studier av snøsmelting og vinteravrenning i Risvollan forskningsfelt	1996
Oveland T.A PINE som urbanhydrologisk simuleringsverktøy	1995
Brandt J. Urban avrenning i vintersituasjon sammenlignet med sommersituasjon. En studie basert på Risvollan urbanhydrologiske feltlaboratorium	1994
Pettersen R. Urbanhydrologisk datafangst og datakontroll for avrenningsstudier i Trondheim med spesiell vekt på korttidsnedbør	1993
Høgeli S. A. Avrenning fra langtidsnedbør og punktstudie av snøsmelting med modelltilpassninger. Studieområde: Risvollan - Trondheim	1991

Documentation of Risvollan Urban Hydrological Research Field, 2011

Solstad I.H. Urban avrenning i Trondheim by. Eksempel: Risvollan og Ladebekken	1990
Saga L. Risvollan urbanhydrologiske forskningsfelt. Databearbeidelse og kalibrering.	1989
Olsen B.Ø. Datafangst og datakontroll i Risvollan målestasjon. Uttesting av VALOG og modellanvendelse	1988
Silseth H. Risvollan urbanhydrologisk feltlaboratorium. Feltdokumentasjon og kalibrering.	1987
Åsnes E. Urbanfeltene Blakli og Risvollan Feltdokumentasjon og datakontroll med etterfølgende simulering.	1985
Guldbrandsen T. Urbanhydrologisk studie i Ladebekkens nedslagsfelt med boligområdet Angeltrøa som studieområde (En forstudie for å finne hensiktsmessig felt i Trondheim).	1980

Appendix B

Geo referred satellite picture on TIN - model



Appendix C: Presentation V – notch weir

V – notch weir

A way to measure stormwater discharge

Christian Sveen, MSc student NTNU


26.10.2010 TVM4127 VA - Systemer Høst 2010

Presentation V – notch weir.

Program:


1. Purpose and function.
2. Calculation formulas.
3. Risvollan Urban Hydrological Station.
4. Agenda.
5. Analysis/results.
6. Advantages and disadvantages.
7. Conclusions.

➤ References.



[1]

26.10.2010 Christian Sveen TVM4127 VA - Systemer Høst 2010 1



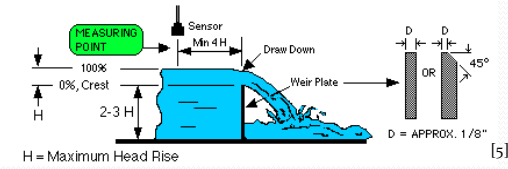
Det skapende universitet

1. Purpose and function:

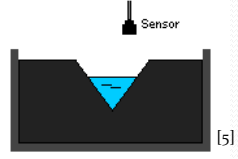
> Purpose:
 Measure the stormwater discharge by creating a relationship between the watersurface level and the flow: $Q = f(H)$. [2]

> Function:
 A rectangular channel/basin which function is to establish stable flow conditions : Critical flow by the crest (Fr nr. = 1,0), and to ensure that the waterlevel is measured within stable subcritical conditions ($Fr < 1,0$ and "horizontal" surface). [3][4]

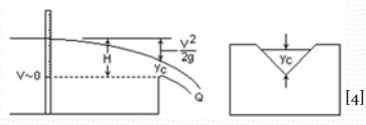
V-notch weir:




H = Maximum Head Rise [5]



V-Notch Weir [5]




[4]



[11]

26.10.2010 Christian Sveen TVM4127 VA - Systemer Høst 2010 2



Det skapende universitet

How to measure Q and H?

Q:

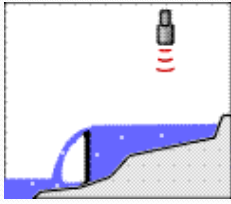
- > Electronic equipments, i.e. an ultra sonic sensor. [6]
- > Use a bucket with a known volume and use time series. [7]

H:


- > Float device/stillingwell: detects level. [8]
- > Stakepipe: detects pressure. [9]
- > Meterstick attached to the weirchannel wall. [7][10][11]

How to find the relationship between both:

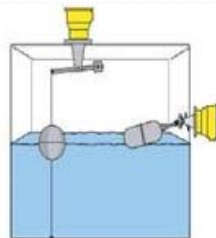
- > Perform labtests (known dimensions and discharges). [12]
- > Use software to perform 3D hydraulic modeling. [12]



[6]



[13]



[8]

26.10.2010 Christian Sveen TVM4127 VA - Systemer Høst 2010 3

NTNU
Det skapende universitet

2. Calculation formulas:

- Kindsvater - Shen formula (ISO 1438/1 - 1980). [14]
- Kindsvater - Shen formula (USB 1997). [15]

$$Q = \frac{8}{15} * C_e * \tan \frac{\phi}{2} * \sqrt{2g} * H^{\frac{5}{2}}$$

$$Q = 4,28 * C_e * \tan \frac{\phi}{2} * (H + k)^{\frac{5}{2}}$$

↓

C and k vs. Notch Angle

Ce = Contraction coefficient (discharge coefficient)
 Φ = Notch angle (degree)
 H = Head (m)
 k = Head correction factor (-)

26.10.2010 Christian Sveen TVM4127 VA - Systemer Høst 2010 4

NTNU
Det skapende universitet

3. Risvollan urban hydrological station:

- Location, shape and size of the station's catchment area.

Excursion tuesday 19.10.2010:

- Measured V-notch depth (H) and critical depth (Hc).

[11] [16] [17]

26.10.2010 Christian Sveen TVM4127 VA - Systemer Høst 2010 5

NTNU
Det skapende universitet

Dimensions:
➤ Prinsipal sketches Risvollan station

26.10.2010 Christian Sveen TVM4127 VA - Systemer Høst 2010 6

NTNU
Det skapende universitet

Hydraulic data collection:

Time 10:00:25
Meterstick weirchannel wall and manual meterstick:

- V – notch depth $H = 19,0$ cm
- Critical depth $H_c = 17,5$ cm

NVE runoff data at 10:00:30
➤ $Q = 0,0246$ m³/s = 24,6 l/s

eKlima precipitation data 09:00 – 10:00
➤ Lambrecht: 19 tip * 0,1 mm = 1,9 mm
(for surface runoff calculation, rational method).

26.10.2010 Christian Sveen TVM4127 VA - Systemer Høst 2010 7



Det skapende universitet


4. Agenda:

- Compare the KS formula ISO 1980 with the KS formula USBR 1997.
- Check what happens with the calculated discharge if angle and contraction coefficient are changed.
- Calculate the stormwater discharge at Risvollan by using the KS formulas and the rational method.
- Compare the calculated discharges with the NVE's registered discharge (stillingwell).
- Check if it's a critical point above the crest (Froude number = 1,0).
- Check the theoretical channel length with the real length.
- Calculate the amount of sediments at the bottom of the channel (earlier checked, 12.10.2010).



[11]

26.10.2010
Christian Sveen
TVM4127 VA - Systemer Høst 2010
8



Det skapende universitet

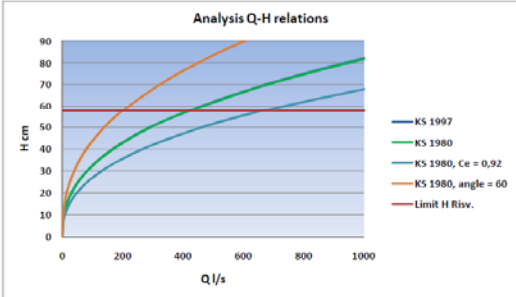
5. Analysis/results:

- Calculation formulas compared, with some variations (changed C_e and angle).
- Capacity limit Risvollan.

Rational method:
 $1,9 \text{ mm/h} = 5,3 \text{ l/s*ha}$

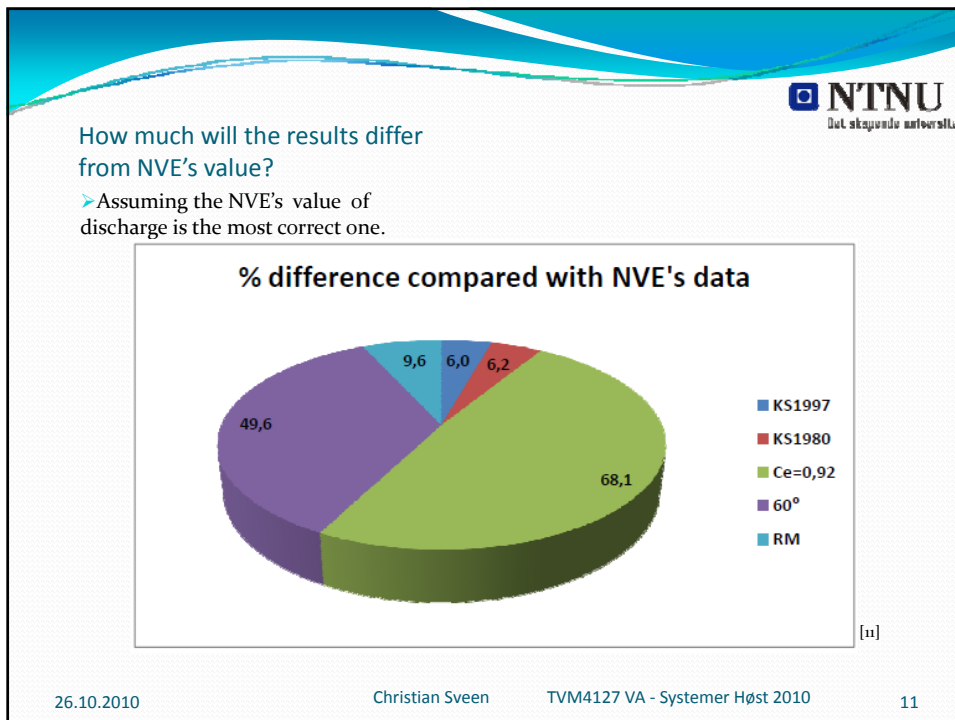
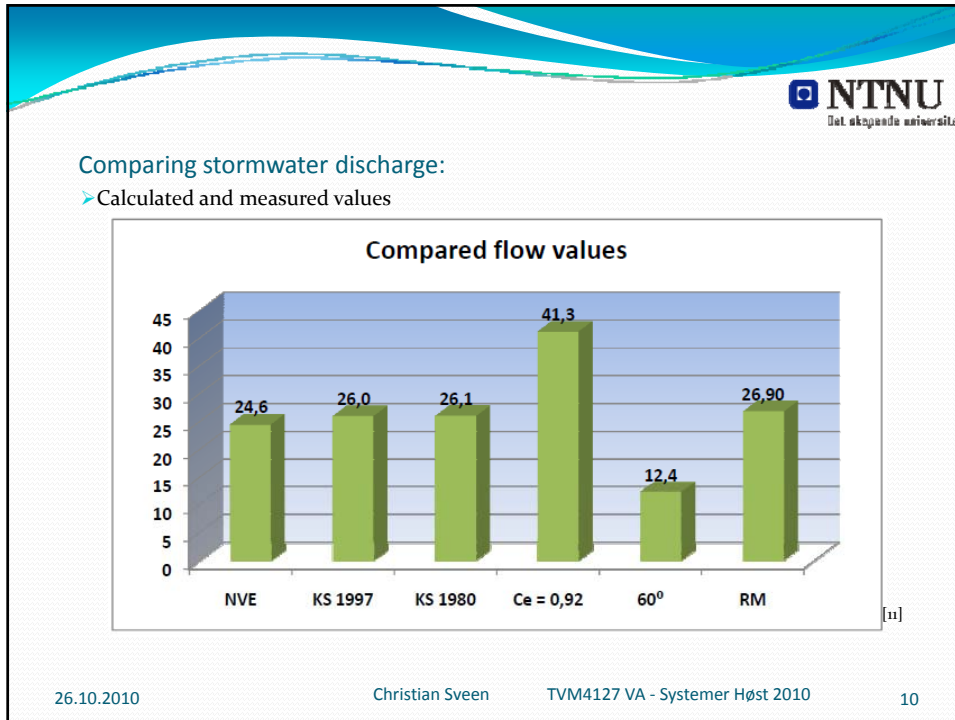
$Q = C * I * A$
 $Q = 0,26 * 5,28 * 19,6 = 26,9 \text{ l/s}$


Angle 100°	$C_e = 0,58$		$C_e = 0,58$		$C_e = 0,92$		$C_e = 0,92$	
	KS USBR 1997	KS ISO 1438/1-1980	KS ISO 1438/1-1980	KS ISO 1438/1-1980	KS ISO 1438/1-1980	KS ISO 1438/1-1980	KS ISO 1438/1-1980	KS ISO 1438/1-1980
H cm	Q l/s	Q l/s	Q l/s	Q l/s	Q l/s	Q l/s	Q l/s	Q l/s
0	0,00	0	0,00	0	0,00	0	0,00	0
10	0,01	5	0,01	5	0,01	8	0,00	2
20	0,03	30	0,03	30	0,05	47	0,01	14
30	0,08	81	0,08	82	0,13	129	0,04	39
40	0,17	166	0,17	168	0,27	265	0,08	88
50	0,29	290	0,29	293	0,46	484	0,14	139
60	0,42	421	0,42	417	0,66	660	0,20	198
70	0,46	458	0,46	462	0,73	731	0,22	219
80	0,67	673	0,68	679	1,08	1075	0,32	322
90	0,94	939	0,95	948	1,50	1501	0,45	454
95	1,26	1260	1,27	1273	2,02	2015	0,60	604
100	1,64	1639	1,66	1656	2,62	2623	0,79	787
19	0,03	26,0	0,03	26,1	0,04	41,3	0,01	12,4
NVE	0,025	24,6						



[11]

26.10.2010
Christian Sveen
TVM4127 VA - Systemer Høst 2010
9



 NTNU
Det skapende universitet

Other results:


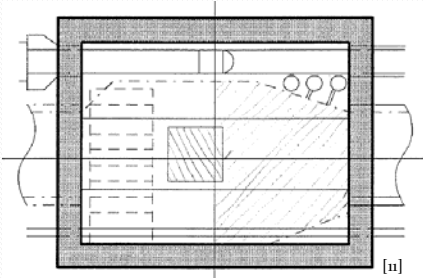
➤ **Froude number calculation:**

Formula used: $Fr^2 = \frac{Q^2 B}{g A^3}$ [3]


Hc = 17,5 cm → Fr = 0,73
Fr = 1,0 → Hc = 15,4 cm

➤ **Theoretical channel length:**
= 4*H – 5*H = 2,3 – 2,9 meters. [10]

➤ **Sediments:**
Bottom weirchannel: 5,0 – 7,0 cm.
Sediment catcher: 7,0 – 10 cm .
Volume: 0,079 – 0,111 m³.
Density wet clay: 1,826 ton/m³
Assume density sandy wet clay: 2,0 ton/m³.
Weight sediments: 158 – 222 kilos.

 [11]
 [11]

26.10.2010 Christian Sveen TVM4127 VA - Systemer Høst 2010 12

 NTNU
Det skapende universitet

6. Advantages and disadvantages:


➤ **Advantages:**

1. V -notch weir are able to operate during all seasons. [7]
2. It gives reliable and good data, especially in ideal conditions (secured against frostevents , normal discharges and no sediements). [18]
3. Usually cheap to construct and install. [7]

➤ **Disadvantages:**

1. The amount of sediments (floating and sinking) will over time increase inside the channel (disturbing the discharge by the crest and eventually plug the connection pipe into the stillingwell). [18]
2. Biofilm growth at the bottom of the V – crest. [7]
3. Cannot handle extreme rain events, large discharges can easy create flooding. [19]


26.10.2010 Christian Sveen TVM4127 VA - Systemer Høst 2010 13



7. Conclusions:

- It's a slight difference between the two KS formulas. The calculated discharges are almost identical with each other, the difference is therefore neglectable. Reason: KS formula USBR1997 is a rewritten version of the KS formula ISO 1980, so that american units can be used. [15]
- If the V - notch angle is decreased, the discharge capacity will decrease. If the contraction coefficient is increased, the discharge capacity will increase.
- All the calculated values (KS formulas and the rational method) gives a slightly larger discharge than the NVE's registered discharge. However, the difference in percentage between the calculated values and the registered value is within the acceptable limit of operational failure (8%). [17] There are many reasons behind such differences:
 1. Calculation formulas assume perfect operational conditions, also maybe a wrong contractioncoefficient is used (each installed V - notch weir may have their own unique contraction coefficient or modified calculation formulas).
 2. Human failure (by measuring H).
 3. Sediments at the bottom of the channel that partly could plug the connection pipe into the stillingwell (cannot registrate rapid changes of discharges) [7].
 4. Perhaps because the length of the channel is to short (compared with the theoretical calculated length).
- Froude number above the crest were lower than 1,0 as expected (subcritical conditions). This because the meterstick were 3-4 cm inside the channel, not directly above the crest.

26.10.2010 Christian Sveen TVM4127 VA - Systemer Høst 2010 14



References:

- [1] Heidra. (<http://www.heidra.co.uk/>)
- [2] VA - teknikk book, Sveinn T. Thorolfsson, page 4 - 71.
- [3] Kompendium TVM4175 Hydraulikk 2008, Yngve Robertsen, page 63 - 70.
- [4] Open channel flow, Dr. James B. Calvert, 6th of june 2007
- [5] Control Electronics inc, 1999-2008. (<http://www.controlelectronics.com/360PrimDev.html>)
- [6] Greyline instruments inc., Ultrasonic Technologies. (<http://www.greyline.com/howitwk.htm>)
- [7] Conversation Sveinn Thorolfsson.
- [8] Sigum leverandør. (<http://www.sigum.no/no/produkter/instrumentering/nivavakter/flottor-nivavakter>)
- [9] Insitu - Inc., Innovations in water monitoring. (<http://www.in-situ.com/>)
- [10] Risvollan - Trondheim urbanhydrologiske forskningsfelt Del 1, dokumentasjon 1994.
- [11] Christian Sveen (documentation, observations, pictures and calculations).
- [12] Conversation Nils Reidar B. Olsen.
- [13] Hydrogeology slides, V - notch weir experiment. (<http://hercules.gcsu.edu/~sdatta/home/teaching/hydro/slides/index.html>)
- [14] Statens forurensningstilsyn, program for VAR - Teknikk, h n bok i vannf ringsm linger.
- [15] LMNO Engineering. (<http://www.lmnoeng.com/Weirs/vweir.htm>)
- [16] Kart.gulesider.no
- [17] Sveinn Thorolfsson lecture document, Risvollan general.
- [18] HydraTeam, veileder for m ling av minstevannf ringer 2008, page 4 -5.
- [19] Thomas Eidsmo.

26.10.2010 Christian Sveen TVM4127 VA - Systemer H st 2010

